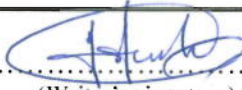




University of  
Stavanger

Faculty of Science and Technology

**MASTER'S THESIS**

|                                                                                                                                    |                                                                                                                      |
|------------------------------------------------------------------------------------------------------------------------------------|----------------------------------------------------------------------------------------------------------------------|
| Study program/ Specialization:<br><br><b>Master of Science in Petroleum<br/>Engineering</b><br><br><b>Reservoir Engineering</b>    | Spring semester, 2014<br><br><b>Open</b>                                                                             |
| Writer: <b>Héctor Silva González</b>                                                                                               | <br>.....<br>(Writer's signature) |
| Faculty supervisor: <b>Steinar Evje</b>                                                                                            |                                                                                                                      |
| External supervisor(s):                                                                                                            |                                                                                                                      |
| Thesis title:<br><br><b>"Investigations of a drilling operation by using a simplified gas-liquid mathematical model"</b>           |                                                                                                                      |
| Credits (ECTS): 30                                                                                                                 |                                                                                                                      |
| Key words:<br><br><b>Gas-liquid drift flux model</b><br><b>Gas injection</b><br><b>ECD modeling</b><br><b>Drilling application</b> | Pages: 54<br><br>+ enclosure: 28<br><br>Stavanger, <b>May 23rd, 2014</b><br>Date/year                                |

# Investigations of a drilling operation by using a simplified gas-liquid mathematical model

## ABSTRACT

There was a strong wish to investigate the physics of fluid flow involved in drilling operations where nitrogen injection is used to lower the hydrostatic pressure. This work is based on a reduced version of the full drift-flux model first presented to the academic community by Zuber and Findlay [1] that Dr. Steinar Evje developed and programmed numerically in MATLAB. The mathematical model implemented to predict the behavior of the system is a simplification of the full "transient gas-liquid drift flux model" [2], where a system of two strongly coupled "advection-diffusion" equations is obtained [2]. The model allows exploring relevant phenomena for drilling operations including the effect of liquid and gas expansion on pressure distribution along the wellbore.

Two methods of gas injection are studied:

- 1) **Direct nitrogen injection:** Nitrogen is injected directly through the drill string from the surface to the bottom of the well and out through the annulus, see figure 1.1. This process will create a reduction in pressure at the bottom of the well and hence a reduction of the equivalent circulating density (ECD), the method is particularly used in depleted reservoirs and underbalanced drilling, however the disadvantages of this method relay on tools functionality due to excessive gas flowing through the drill string affecting mainly positive displacement drilling motors (PDM) and measurement while drilling tools (MWD) [3, 4] and some issues related to transmission of surveying parameters such as inclination and azimuth (maximum 20% gas cut to allow proper communication of such parameters [5]).
- 2) **Concentric nitrogen injection:** In this method nitrogen is injected through the annulus space between casings, (e.g. 9 5/8" and 7 5/8") using a complement perforated at the bottom and connected to the top of a liner, see figure 1.2. We will demonstrate in this work that the injection point (top of the liner) along with wellbore inclination and liquid-gas injection rate play an important role on pressure distribution; we also want to gain insight into the understanding of forces intervening in this operations (e.g. friction and gravity). The main advantage of this method relays on the existence of proper communication of surveying parameters (inclination and azimuth) because the pressure pulses are not disturbed by gas and they can travel along a continuous liquid phase since the drill string is filled with mud.

Two different scenarios with concentric nitrogen injection are investigated:

- 1) The first set up, models the injection of nitrogen in a vertical well, where the natural phenomena of slippage between phases liquid-gas coexists due to the natural tendency of gas to flow faster than liquid in vertical pipes because of buoyancy and lower frictional effects in the gas phase [2, 6], gas expansion is observed close to the surface due to pressure reduction [2, 5] as well as downward liquid flow once the gas injection has been stopped or the mixture velocity is sufficiently small [2, 7], followed by a transition from multiphase system to a state where single phase of liquid and gas is archived [2].
- 2) The second set up simulates a more realistic scenario for our purposes, where a horizontal well flow is studied and nitrogen is introduced in the system at different positions given by the injection point, the phenomena explored include different phase flow velocities of liquid and gas and friction effects [2], strong gas expansion close to surface is observed [2, 5] and a reduction of gravitational effects due to the inclination of the well.

## DEDICATION

¡To **God** who is always taking care of me!

To my lovely parents Magdalena González Castillo and Héctor Silva Durán for believing in me and for respecting my decisions , I'm also grateful to my brother Carlos and my sister Karina for looking after our parents while I have been away.

I would like to express my gratitude and love to my girlfriend Nely Ramirez who has been always with me, thank you for your incomparable support, affection and love.

To my Grandmother Cristina, thanks for all your praying; and to my Grandmother Ignacia, *rest in peace*.

¡I miss you!

## ACKNOWLEDGMENTS

I want to thank my friends in Norway, Hilda Choque, Elsa Mehari, Diana Pavón and Alireza Roostaei ; Guys  
without you I wouldn't have made it.

I want thank Mr. Aadnøy for encouraging me to apply to Stavanger University, I wouldn't have taken the plunge if I  
hadn't met you, ¡Thanks professor!

To my thesis supervisor, Dr. Steinar Evje for his invaluable time and for accepting me for this project

## TABLE OF CONTENTS

|                                                                  |    |
|------------------------------------------------------------------|----|
| ABSTRACT.....                                                    | 2  |
| DEDICATION .....                                                 | 3  |
| ACKNOWLEDGMENTS.....                                             | 4  |
| TABLE OF CONTENTS .....                                          | 5  |
| NOMENCLATURE.....                                                | 7  |
| LIST OF FIGURES.....                                             | 9  |
| LIST OF TABLES.....                                              | 12 |
| 1. - INTRODUCTION.....                                           | 13 |
| 1.1. - Back Ground.....                                          | 13 |
| 1.2. - Motivation .....                                          | 15 |
| 1.3. - Scope of Study.....                                       | 15 |
| 2. - DEVELOPMENT OF THE MODEL.....                               | 16 |
| 2.1. - Introduction.....                                         | 16 |
| 2.2. - Basic definitions.....                                    | 16 |
| 2.3. - Drift-flux model .....                                    | 18 |
| 2.4. - Boundary conditions.....                                  | 22 |
| 2.5. - Initial state .....                                       | 22 |
| 2.6. - Discretization of the model.....                          | 23 |
| 3. - NUMERICAL SIMULATIONS (VERTICAL GEOMETRY).....              | 26 |
| 3.1. - Specification of parameters .....                         | 26 |
| 3.2. - Variation of Injection point. ....                        | 26 |
| 3.3. - Flow regimes for different injection points.....          | 31 |
| 3.4. - Variation of Injection rate .....                         | 33 |
| 3.5. - Flow regimes for different injection rates.....           | 36 |
| 4. - CALIBRATION OF THE MODEL.....                               | 38 |
| 4.1. - Parameters used to calibrate the model.....               | 38 |
| 4.2. - Results .....                                             | 40 |
| 5. - NUMERICAL SIMULATIONS (DIRECTIONAL GEOMETRY).....           | 41 |
| 5.1. - Directional well path.....                                | 41 |
| 5.2. - Wellbore architecture .....                               | 42 |
| 5.3. - Specification of parameters.....                          | 43 |
| 5.4. - Variation of Injection point .....                        | 43 |
| 5.5. - Flow regimes for different injection points.....          | 48 |
| 5.6. - Variation of Injection rate.....                          | 50 |
| 5.7. - Flow regimes for different injection rates.....           | 52 |
| APPENDIX 1 – SENSITIVITY OF LIQUID-GAS RATE AT BOTTOM HOLE ..... | 55 |
| A1. – Analysis of pressures and ECDs at bottom hole .....        | 55 |
| A1.1 Vertical Well.....                                          | 55 |

|                                                                     |           |
|---------------------------------------------------------------------|-----------|
| – Direct nitrogen injection.....                                    | 55        |
| – Injection point x1 = 500 (m).....                                 | 57        |
| – Injection point x2 = 1000 (m).....                                | 58        |
| – Injection point x3 = 1500 (m).....                                | 59        |
| – Injection point x4 = 2000 (m).....                                | 60        |
| A1.2 Directional well.....                                          | 61        |
| – Direct nitrogen injection.....                                    | 61        |
| – Injection point x1 = 500 (m).....                                 | 62        |
| – Injection point x2 = 1000 (m).....                                | 63        |
| – Injection point x3 = 1500 (m).....                                | 64        |
| – Injection point x4 = 2000 (m).....                                | 65        |
| <b>APPENDIX 2 – SENSITIVITY OF LIQUID-GAS RATE AT THE SHOE.....</b> | <b>66</b> |
| A. 2. – Analysis of pressures and ECDs at shoe.....                 | 66        |
| A2.1 Vertical well.....                                             | 66        |
| – Direct nitrogen injection.....                                    | 66        |
| – Injection point x1 = 500 (m).....                                 | 67        |
| – Injection point x2 = 1000 (m).....                                | 68        |
| – Injection point x3 = 1500 (m).....                                | 69        |
| – Injection point x4 = 2000 (m).....                                | 70        |
| A.2.2 Directional well.....                                         | 71        |
| – Direct nitrogen injection.....                                    | 71        |
| – Injection point x1 = 500 (m).....                                 | 72        |
| – Injection point x2 = 1000 (m).....                                | 73        |
| – Injection point x3 = 1500 (m).....                                | 74        |
| – Injection point x4 = 2000 (m).....                                | 75        |
| <b>APPENDIX 3 – COMPARISON DIRECTIONAL VS VERTICAL.....</b>         | <b>76</b> |
| – Direct injection.....                                             | 76        |
| – Injection point x1 = 500 (m).....                                 | 77        |
| – Injection point x2 = 1000 (m).....                                | 78        |
| – Injection point x3 = 1500 (m).....                                | 79        |
| – Injection point x4 = 2000 (m).....                                | 80        |
| <b>REFERENCES.....</b>                                              | <b>82</b> |

## NOMENCLATURE

- ECD: Equivalent circulating density
- PDM: Positive displacement motors
- MWD: Measurement while drilling
- EM MWD: Electromagnetic measurement while drilling
- UBD: Underbalanced drilling
- EOS: Equation of state
- PWD: Pressure while drilling
- LOT: Leak off test
- FIT: Formation Integrity test
- KOP: Kick off point
- BUR: Build up rate ( $^{\circ}/30\text{m}$ )
- Re: Reynolds number
- S: Slip ratio
- $q_L$ : Volumetric liquid rate ( $\text{m}^3/\text{s}$ )
- $q_G$ : Volumetric gas rate ( $\text{m}^3/\text{s}$ )
- A: Cross section area ( $\text{m}^2$ )
- $q_T$ : Total volumetric rate ( $\text{m}^3/\text{s}$ )
- $W_L$ : Mass liquid rate ( $\text{kg}/\text{s}$ )
- $W_G$ : Mass gas rate ( $\text{kg}/\text{s}$ )
- $W_T$ : Total mass rate ( $\text{kg}/\text{s}$ )
- $u_{GS}$ : Superficial gas velocity ( $\text{m}/\text{s}$ )
- $u_{LS}$ : Superficial liquid velocity ( $\text{m}/\text{s}$ )
- $u_G$ : Gas phase velocity ( $\text{m}/\text{s}$ )
- $u_L$ : Liquid phase velocity ( $\text{m}/\text{s}$ )
- $\rho_f$ : Actual fluid density ( $\text{kg}/\text{m}^3$ )
- $\Delta p_f$ : Pressure drop in the annulus
- $g$ : Gravity force ( $\text{m}/\text{s}^2$ )
- $tv_d$ : True vertical depth (m)
- $p_{system}$ : Pressure in the system at a the point of interest (Pa)
- $\alpha_l$ : Liquid fraction [ ]

## Nomenclature

---

- $\alpha_g$  : Gas fraction [ ]
- $\rho_g$  : Gas density (kg/m<sup>3</sup>)
- $\rho_l$  : Liquid density (kg/m<sup>3</sup>)
- $q_g$  : Gas flow rate (kg/m<sup>2</sup> s)
- $q$  : External forces (friction / gravity)
- $P$  : Reference pressure for both liquid and gas (Pa)
- $\rho_l^0$  : Reference density of liquid (kg/m<sup>3</sup>)
- $p_0$  : Initial pressure (bar)
- $a_l$  : Speed of sound in the liquid phase (m/s)
- $a_g$  : Speed of sound in the gas phase (m/s)
- $c_0$  : Distribution parameter
- $c_1$  : Drift velocity (m/s)
- $n, m$  : Mass variables (kg/m<sup>3</sup>)
- $u_M$  : Mixture velocity (m/s)
- $\mu_M$  : Mixture viscosity (pa s)
- $f$  : Friction factor
- $D$  : External pipe diameter (m)
- $d$  : Internal pipe diameter (m)
- $\rho_M$  : Mixture density (kg/m<sup>3</sup>)
- $\phi$  : Wellbore inclination (°)
- $\rho_l^*$  : Density at surface conditions (kg/m<sup>3</sup>)
- $\rho_{l,0}$  : Density distribution along the wellbore (kg/m<sup>3</sup>)
- $\Delta_x$  : Grid/space increments (m)
- $\alpha, \beta$  : Constants resulting from the discretization process
- $\Delta t$  : Time increment (s)
- $O(\Delta x)$  : First order approximation
- $O(\Delta x^2)$  : Second order approximation



## LIST OF FIGURES

|                                                                                                                                                                                                                                                               |    |
|---------------------------------------------------------------------------------------------------------------------------------------------------------------------------------------------------------------------------------------------------------------|----|
| – Figure 1.1 Schematic representation of direct nitrogen injection .....                                                                                                                                                                                      | 13 |
| – Figure 1.2 Schematic representation of concentric nitrogen injection.....                                                                                                                                                                                   | 14 |
| – Figure 2.0 Multiphase flow variables .....                                                                                                                                                                                                                  | 16 |
| – Figure 2.1 Schematic representation of the system, divided into N number of grid cells. ....                                                                                                                                                                | 23 |
| – Figure 2.2 Schematic representation of “chord approximations” [23] .....                                                                                                                                                                                    | 24 |
| – Figure 3.0 Pressure profile for $T= 0$ (s) and $T=100$ (s).....                                                                                                                                                                                             | 27 |
| – Figure 3.1 Pressure “left”, superficial liquid and gas velocities “middle” and liquid mass rate “right” of the system at 100 (s) and 200(s) after gas injection, $x_1= 500$ (m) and injection rate $q_G= 0.5$ (kg/m <sup>2</sup> s).....                    | 28 |
| – Figure 3.2 Final superficial liquid and gas velocity at the end of the simulation, $T= 10000$ (s) for $x_1= 500$ (m) “left” and $x_2= 3000$ (m) “right”. ....                                                                                               | 28 |
| – Figure 3.3 Gas fraction, pressure and ECD at $T= 10000$ (s) for $x_1= 500$ (m) “top” and $x_2= 3000$ (m) “bottom”.....                                                                                                                                      | 29 |
| – Figure 3.4 Gas fraction, pressure and ECD at $T= 10000$ (s) for $x_1= 500$ (m) “top” and $x_2= 3000$ (m) “bottom”, after modification of the friction factor $f$ .....                                                                                      | 30 |
| – Figure 3.5 Superficial liquid and gas velocities at three different positions; <i>left figure</i> corresponds to an injection point $x_1= 500$ (m) whereas <i>right figure</i> corresponds to an injection point $x_2= 3000$ (m). $T = 10000$ (s).....      | 31 |
| – Figure 3.6 Flow regimes maps for two-phase vertical annular flow. ....                                                                                                                                                                                      | 32 |
| – Figure 3.7 Gas fraction and pressure at $q_G= 0.5$ (kg/m <sup>2</sup> s), $T= 2700$ (s) left, $x=500$ (m), $T= 10000$ (s) right. ....                                                                                                                       | 34 |
| – Figure 3.8 Pressure at the bottom of the well for different gas rates, “left”, ECD for two different position (bottom of the well and previous casing shoe) “right”. ....                                                                                   | 35 |
| – Figure 3.9 Final pressure distribution for three different gas injection rates, $q_G= 0.5$ (kg/m <sup>2</sup> s) “left”, $q_G= 1.0$ (kg/m <sup>2</sup> s) “middle”, $q_G= 2.0$ (kg/m <sup>2</sup> s) “right”, $x= 500$ (m), $T= 10000$ (s).....             | 35 |
| – Figure 3.10 Final ECD distribution for three different gas injection rates, $q_G= 0.5$ (kg/m <sup>2</sup> s) “left”, $q_G= 1.0$ (kg/m <sup>2</sup> s) “middle”, $q_G= 2.0$ (kg/m <sup>2</sup> s) “right”, $x= 500$ (m), $T= 10000$ (s).....                 | 35 |
| – Figure 3.11 Final superficial velocities $UL_s$ , $UG_s$ for three different positions along the wellbore, $x= 500$ (m), $q_G= 0.5$ (kg/m <sup>2</sup> s) “left”, $q_G= 1.0$ (kg/m <sup>2</sup> s) “middle”, $q_G= 2.0$ (kg/m <sup>2</sup> s) “right” ..... | 36 |
| – Figure 4.1 Schematic configuration of the well used to calibrate the model.....                                                                                                                                                                             | 38 |
| – Figure 4.2 Schematic configuration of the well used to calibrate the model. ....                                                                                                                                                                            | 39 |
| – Figure 4.3 Sensitivity analysis to determine the calibrated value of friction factor to be used in further simulation, “blue” points represent actual ECD readings, “red” points represent results given by simulations. ....                               | 40 |
| – Figure 5.0 Directional well path, well inclination (°) “left”, well displacement (m) “middle”, BUR (°/30m) “right”. ....                                                                                                                                    | 41 |
| – Figure 5.1 Well architecture; concentric nitrogen injection “left”, direct nitrogen Injection “right” .....                                                                                                                                                 | 42 |
| – Figure 5.2 Initial pressure profile for a horizontal well.....                                                                                                                                                                                              | 44 |
| – Figure 5.3 Pressure profile for $T= 0$ (s) and $T= 80$ (s).....                                                                                                                                                                                             | 44 |
| – Figure 5.4 Superficial liquid velocity profile for $T= 80$ (s).....                                                                                                                                                                                         | 45 |
| – Figure 5.5 Pressure “left”, superficial liquid and gas velocities “middle” and liquid mass rate “right” at 140 (s) and 220(s) after gas injection, $x_1= 500$ (m) and $q_G= 0.5$ (kg/m <sup>2</sup> s). ....                                                | 45 |
| – Figure 5.6 Pressure “left”, superficial liquid and gas velocities “middle” and liquid mass rate “right” at 140 (s) and 220(s) after gas injection, $x_2= 3000$ (m) and $q_G= 0.5$ (kg/m <sup>2</sup> s). ....                                               | 46 |

- Figure 5.7 Final superficial liquid and gas velocity at the end of the simulation, for  $x_1= 500$  (m) “left”, for  $x_2= 3000$  (m) “right”.  $T= 8000$  (s) ..... 47
- Figure 5.8 Gas fraction “left”, pressure “middle” and ECD “right” at  $T= 8000$  (s) for  $x_1= 500$ (m) “top” and  $x_2= 3000$ (m) “bottom”. ..... 48
- Figure 5.9 Superficial liquid and gas velocities at three different positions; *left figure* corresponds to an injection point  $x_1= 500$  (m) whereas *right figure* corresponds to an injection point  $x_2= 3000$  (m). Final time,  $T = 8000$  (s)..... 49
- Figure 5.10 Final pressure distribution for three different gas injection rates,  $q_G= 0.5$  (kg/m<sup>2</sup> s) “left”,  $q_G= 1.0$  (kg/m<sup>2</sup> s) “middle”,  $q_G= 2.0$  (kg/m<sup>2</sup> s) “right”,  $x= 500$  (m),  $T= 8000$ (s). ..... 51
- Figure 5.11 Final ECD distribution for three different gas injection rates,  $q_G= 0.5$  (kg/m<sup>2</sup> s) “left”,  $q_G= 1.0$  (kg/m<sup>2</sup> s) “middle”,  $q_G= 2.0$  (kg/m<sup>2</sup> s) “right”,  $x= 500$  (m),  $T= 8000$ (s). ..... 51
- Figure A1.1.6 Sensitivity analysis of gas-liquid injection rate for a vertical well @ bottom, “Injection point  $x= 1000$  (m)”,  $f = 6000$  ..... 52
- Figure 5.12 Final superficial velocities  $UL_s, UG_s$  for three different positions along the wellbore,  $x= 500$  (m),  $q_G= 0.5$  (kg/m<sup>2</sup>s) “left”,  $q_G= 1.0$  (kg/m<sup>2</sup> s) “middle”,  $q_G= 2.0$  (kg/m<sup>2</sup> s) “right” ..... 53
- Figure A.1.1 Sensitivity analysis of gas-liquid injection rate for a vertical well @ bottom, “Direct Nitrogen Injection”,  $f = 600$  ..... 56
- Figure A1.1.2 Sensitivity analysis of gas-liquid injection rate for a vertical well @ bottom, “Direct Nitrogen Injection”,  $f = 6000$  ..... 56
- Figure A1.1.3 Sensitivity analysis of gas-liquid injection rate for a vertical well @ bottom, “Injection point  $x_1= 500$  (m)”,  $f = 600$  ..... 57
- Figure A1.1.4 Sensitivity analysis of gas-liquid injection rate for a vertical well @ bottom, “Injection point  $x_1= 500$  (m)”,  $f = 6000$  ..... 57
- Figure A1.1.5 Sensitivity analysis of gas-liquid injection rate for a vertical well @ bottom, “Injection point  $x_2= 1000$  (m)”,  $f = 600$  ..... 58
- Figure A1.1.6 Sensitivity analysis of gas-liquid injection rate for a vertical well @ bottom, “Injection point  $x_2= 1000$  (m)”,  $f = 6000$  ..... 58
- Figure A1.1.7 Sensitivity analysis of gas-liquid injection rate for a vertical well @ bottom, “Injection point  $x_3= 1500$  (m)”,  $f = 600$  ..... 59
- Figure A1.1.8 Sensitivity analysis of gas-liquid injection rate for a vertical well @ bottom, “Injection point  $x_3= 1500$  (m)”,  $f = 6000$  ..... 59
- Figure A1.1.9 Sensitivity analysis of gas-liquid injection rate for a vertical well @ bottom, “Injection point  $x_4= 2000$  (m)”,  $f = 600$  ..... 60
- Figure A1.1.10 Sensitivity analysis of gas-liquid injection rate for a vertical well @ bottom, “Injection point  $x_4= 2000$  (m)”,  $f = 6000$  ..... 60
- Figure A1.2.1 Sensitivity analysis of gas-liquid injection rate for a horizontal well @ bottom, “Direct Nitrogen Injection”,  $f = 600$  ..... 61
- Figure A1.2.2 Sensitivity analysis of gas-liquid injection rate for a horizontal well @ bottom, “Direct Nitrogen Injection”,  $f = 6000$  ..... 61
- Figure A1.2.3 Sensitivity analysis of gas-liquid injection rate for a horizontal well @ bottom, “Injection point  $x_1= 500$  (m)”,  $f = 600$  ..... 62

- Figure A1.2.4 Sensitivity analysis of gas-liquid injection rate for a horizontal well @ bottom, "Injection point  $x_1= 500$  (m)",  $f = 6000$  ..... 62
- Figure A1.2.5 Sensitivity analysis of gas-liquid injection rate for a horizontal well @ bottom, "Injection point  $x_2= 1000$  (m)",  $f = 600$  ..... 63
- Figure A1.2.6 Sensitivity analysis of gas-liquid injection rate for a horizontal well @ bottom, "Injection point  $x_2= 1000$  (m)",  $f = 6000$  ..... 63
- Figure A1.2.7 Sensitivity analysis of gas-liquid injection rate for a horizontal well @ bottom, "Injection point  $x_3= 1500$  (m)",  $f = 600$  ..... 64
- Figure A1.2.8 Sensitivity analysis of gas-liquid injection rate for a horizontal well @ bottom, "Injection point  $x_3= 1500$  (m)",  $f = 6000$  ..... 64
- Figure A1.2.9 Sensitivity analysis of gas-liquid injection rate for a horizontal well @ bottom, "Injection point  $x_4= 2000$  (m)",  $f = 600$  ..... 65
- Figure A1.2.10 Sensitivity analysis of gas-liquid injection rate for a horizontal well @ bottom, "Injection point  $x_4= 2000$  (m)",  $f = 6000$  ..... 65
- Figure A2.1.1 Sensitivity analysis of gas-liquid injection rate for a vertical well @ shoe, "Direct Nitrogen Injection",  $f = 600$  ..... 66
- Figure A2.1.2 Sensitivity analysis of gas-liquid injection rate for a vertical well @ shoe, "Direct Nitrogen Injection",  $f = 6000$  ..... 67
- Figure A2.1.3 Sensitivity analysis of gas-liquid injection rate for a vertical well @ shoe, "Injection point  $x_1= 500$  (m)",  $f = 600$  ..... 67
- Figure A2.1.4 Sensitivity analysis of gas-liquid injection rate for a vertical well @ shoe, "Injection point  $x_1= 500$  (m)",  $f = 6000$  ..... 68
- Figure A2.1.5 Sensitivity analysis of gas-liquid injection rate for a vertical well @ shoe, "Injection point  $x_2= 1000$  (m)",  $f = 600$  ..... 68
- Figure A2.1.6 Sensitivity analysis of gas-liquid injection rate for a vertical well @ shoe, "Injection point  $x_2= 1000$  (m)",  $f = 6000$  ..... 69
- Figure A2.1.7 Sensitivity analysis of gas-liquid injection rate for a vertical well @ shoe, "Injection point  $x_3= 1500$  (m)",  $f = 600$  ..... 69
- Figure A2.1.8 Sensitivity analysis of gas-liquid injection rate for a vertical well @ shoe, "Injection point  $x_3= 1500$  (m)",  $f = 6000$  ..... 70
- Figure A2.1.9 Sensitivity analysis of gas-liquid injection rate for a vertical well @ shoe, "Injection point  $x_4= 2000$  (m)",  $f = 600$  ..... 70
- Figure A2.1.10 Sensitivity analysis of gas-liquid injection rate for a vertical well @ shoe, "Injection point  $x_4= 2000$  (m)",  $f = 6000$  ..... 71
- Figure A2.2.1 Sensitivity analysis of gas-liquid injection rate for a horizontal well @ shoe, "Direct Nitrogen Injection",  $f = 600$  ..... 71
- Figure A2.2.2 Sensitivity analysis of gas-liquid injection rate for a horizontal well @ shoe, "Direct Nitrogen Injection",  $f = 6000$  ..... 72
- Figure A2.2.3 Sensitivity analysis of gas-liquid injection rate for a vertical well @ shoe, "Injection point  $x_1= 500$  (m)",  $f = 600$  ..... 72
- Figure A2.2.4 Sensitivity analysis of gas-liquid injection rate for a vertical well @ shoe, "Injection point  $x_1= 500$  (m)",  $f = 6000$  ..... 73

- Figure A2.2.5 Sensitivity analysis of gas-liquid injection rate for a horizontal well @ shoe, “Injection point  $x_2= 1000$  (m)”,  $f = 600$  ..... 73
- Figure A2.2.6 Sensitivity analysis of gas-liquid injection rate for a horizontal well @ shoe, “Injection point  $x_2= 1000$  (m)”,  $f = 6000$  ..... 74
- Figure A2.2.7 Sensitivity analysis of gas-liquid injection rate for a horizontal well @ shoe, “Injection point  $x_3= 1500$  (m)”,  $f = 600$  ..... 74
- Figure A2.2.8 Sensitivity analysis of gas-liquid injection rate for a horizontal well @ shoe, “Injection point  $x_3= 1500$  (m)”,  $f = 6000$  ..... 75
- Figure A2.2.9 Sensitivity analysis of gas-liquid injection rate for a horizontal well @ shoe, “Injection point  $x_4= 2000$  (m)”,  $f = 600$  ..... 75
- Figure A2.2.10 Sensitivity analysis of gas-liquid injection rate for a horizontal well @ shoe, “Injection point  $x_4= 2000$  (m)”,  $f = 6000$  ..... 76
- Figure A3.1 Sensitivity analysis of gas-liquid injection rate for a horizontal well @ bottom, “Injection point  $x_1= 0$  (m)”,  $f = 6000$ , Horizontal “solid line”, Vertical “dashed line” ..... 76
- Figure A3.2 Sensitivity analysis of gas-liquid injection rate for a horizontal well @ shoe, “Injection point  $x_1= 0$  (m)”, Horizontal “solid line”, Vertical “dashed line” ..... 77
- Figure A3.3 Sensitivity analysis of gas-liquid injection rate for a horizontal well @ bottom, “Injection point  $x_1= 500$  (m)”,  $f = 6000$ , Horizontal “solid line”, Vertical “dashed line” ..... 77
- Figure A3.4 Sensitivity analysis of gas-liquid injection rate for a horizontal well @ shoe, “Injection point  $x_1= 500$  (m)”,  $f = 6000$ , Horizontal “solid line”, Vertical “dashed line” ..... 78
- Figure A3.5 Sensitivity analysis of gas-liquid injection rate for a horizontal well @ bottom, “Injection point  $x_1= 1000$  (m)”,  $f = 6000$ , Horizontal “solid line”, Vertical “dashed line” ..... 78
- Figure A3.6 Sensitivity analysis of gas-liquid injection rate for a horizontal well @ shoe, “Injection point  $x_1= 1000$  (m)”,  $f = 6000$ , Horizontal “solid line”, Vertical “dashed line” ..... 79
- Figure A3.7 Sensitivity analysis of gas-liquid injection rate for a horizontal well @ bottom, “Injection point  $x_1= 1500$  (m)”,  $f = 6000$ , Horizontal “solid line”, Vertical “dashed line” ..... 79
- Figure A3.8 Sensitivity analysis of gas-liquid injection rate for a horizontal well @ shoe, “Injection point  $x_1= 1500$  (m)”,  $f = 6000$ , Horizontal “solid line”, Vertical “dashed line” ..... 80
- Figure A3.9 Sensitivity analysis of gas-liquid injection rate for a horizontal well @ bottom “Injection point  $x_4= 2000$  (m)”,  $f = 6000$ , Horizontal “solid line”, Vertical “dashed line” ..... 80
- Figure A3.10 Sensitivity analysis of gas-liquid injection rate for a horizontal well @ shoe, “Injection point  $x_4= 2000$  (m)”,  $f = 6000$ , Horizontal “solid line”, Vertical “dashed line”..... 81

#### LIST OF TABLES

- Table 2.1 Friction factor constants. .... 20
- Table 3.1 Parameters used for the numerical examples (Vertical Well) ..... 26
- Table 4.1 Parameters used for model calibration..... 39
- Table 5.1 Parameters used for the numerical examples (Directional Well) ..... 43

## 1. - Introduction

### 1.1. - Back Ground

We aim on this work to give a practical application of the reduced drift flux model proposed by Dr. Steinar Evje, it is important to mention that due confidential rights it has been decided to keep anonymous the names of the wells, but the sources of information have been taken from real data.

It is well known that pressure depletion in the reservoir creates fluid loss and particle plugging during common overbalanced drilling operations, leading to a significant damage do to fluid invasion and particle plugging, therefore some strategies are normally implemented to diminish the amount of fluid lost, among them the injection of nitrogen, which aims to reduce the hydrostatic column of mud and therefore reduce the amount of fluid lost in the pay zone.

Two different ways of injecting nitrogen into the system will be explore in this work; the first technique is called **direct injection** which consists of injecting nitrogen through the drill string from the surface down to the bottom of the well and out of the system through the annulus space, as show schematically in figure 1.1

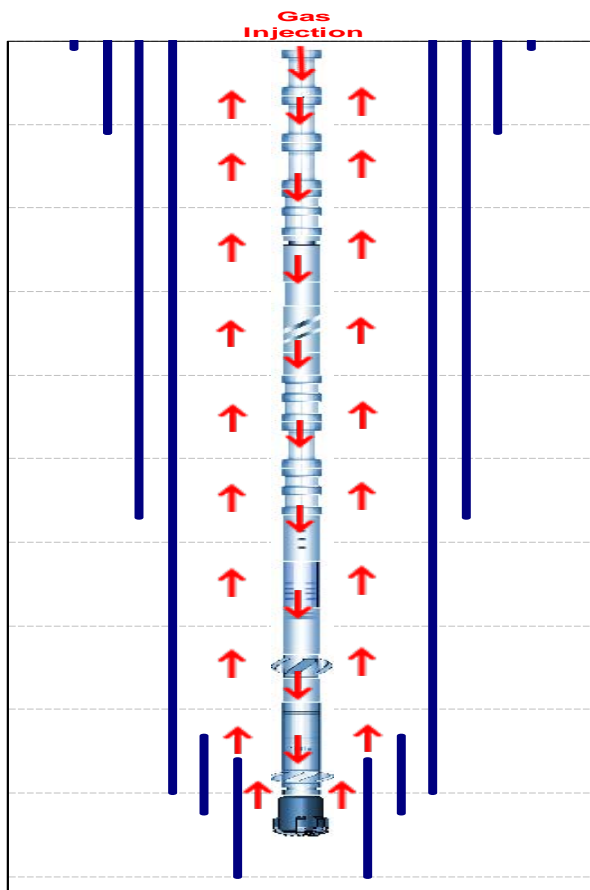


Figure 1.1 Schematic representation of direct nitrogen injection

Direct nitrogen injection method has been rapidly accepted among the drilling crew simply because it is relatively easy to handle in field operations and because it saves time due to the fact that there is no need to lower an additional casing (complement) into the wellbore to be able to inject nitrogen, as it is the case for concentric nitrogen injection; however its application is limited to the rate of gas that can be injected without interfering the communication with the MWD tool (i.e. surveying parameters such as inclination and azimuth are not properly transmitted), and the influence of the tools on the ECD (e.g. the increment on annular pressure due to tool joints see [8] or the reduction of equivalent circulating density by using tools designed to archive this purpose, e.g. ECD RT tool, see [9]).

Other methods have been proposed to overcome this issue for example, electromagnetic measurement while drilling (EM MWD), giving in some cases good results, see [10] but in some others not, see [3].

The second method that we will explore in this work to reduce the fluid loss in the reservoir is called **concentric injection**, which consists of injecting nitrogen through the annulus space between casings (e.g. 9 5/8" and 7 5/8"); liquid is pumped directly through the drill pipe and gas is introduced at the injection point, a multiphase mixture is created at the injection point and the return to surface takes place in the annular space created between the previous casings and the drill string; This method has the advantage to handle relatively large amounts of nitrogen without interfering the signal transmission from the down hole tools, however its limitation relies on the pressure generated by friction when gas is injected. Two main effects are observed in this scenario; first, a hydrostatic pressure reduction and second and an increment in pressure due to friction, both happens simultaneously but in most cases one dominates the other, therefore controlling the behavior of the system. The concentric nitrogen injection is shown schematically in figure 1.2.

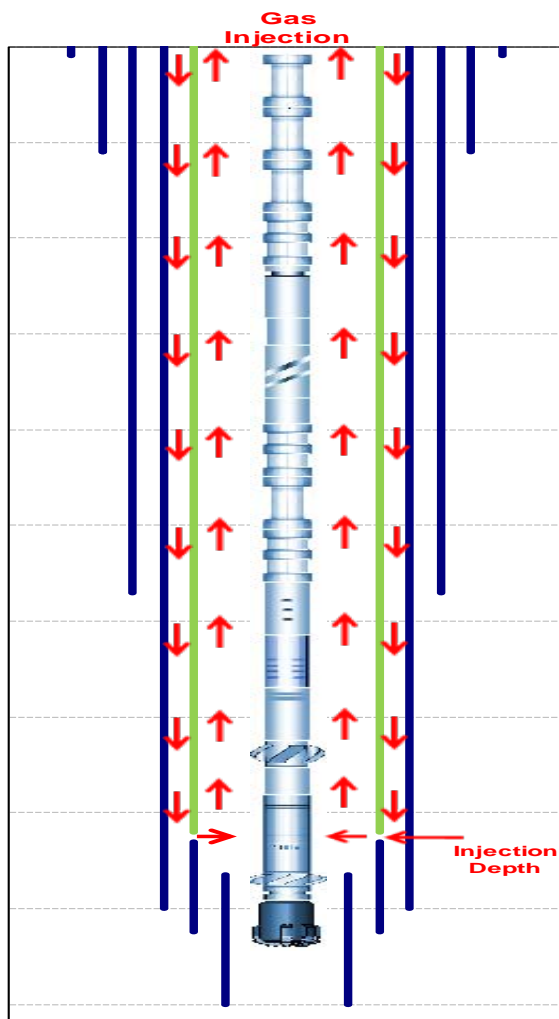


Figure 1.2 Schematic representation of concentric nitrogen injection

After drilling several wells in the field, based on practical experience, concentric nitrogen injection has given better results in terms of time reduction in drilling operations and surveying parameters transmission. Both methods (concentric and direct injection) address the issue of pressure reduction and therefore equivalent circulating density (ECD) reduction, but concentric injection allows introducing gas in the system without having problems with signal transmission from the MWD tool and therefore better directional control is obtained.

## 1.2. - Motivation

Nitrogen injection is extensively used to reduce the pressure at the bottom of the well in drilling operations; therefore, the main motivation of this work is based on the problems that drilling engineers experience when dealing with depleted reservoirs and the wish to understand the physics occurring in such operations (i.e. forces involved). Also it will be demonstrated that it is possible to use a relatively simple model to gain understanding of the basic mechanisms involved in the flow multiphase mixtures and the advantage that represents having a simple tool (mathematical model) that can be modified and adjusted to other well configurations and can also be used to speed up the process of well design and quality check the proposal given by service companies.

Therefore the results of this work will be applicable to the understanding of the forces involved (i.e. friction and gravity) in operations where gas is injected in a well to reduce the hydrostatic pressure at the bottom of the well, and will also give insight into the process of well design in terms of nitrogen injection. Furthermore it will allow the design engineers to make better decisions and discuss different configurations of well geometry and casing setting depths as well as injection rates of liquid and gas.

Among the relevant parameters than can be modified during the process of well design includes the *injection point depth and liquid-gas rates*; these two parameters will take our attention during this work.

## 1.3. - Scope of Study

The scope of this work will be limited to explore the forces (i.e. friction and gravity) interviewing in drilling operations where a gas is injected to reduce the hydrostatic pressure and to understand the physics of the fluid flow behavior of the system with particular emphasis on the role played by the liquid and gas injection rates and the injection point. It is not our intention to attempt to describe more complex configurations such as underbalanced drilling or dual gradient drilling, however drift-flux equations have been used to model such operations, for example Lage et al proposed a drift-flux formulation to model transient behavior in underbalanced drilling operations (UBD) by using full scale facility and comparing the observations with the simulation results, the model proposed gives good approximation to observations; the scenarios simulated included unloading of a well and single phase gas and mixture pulses, see Lage et al [11].

## 2. – Development of the model

### 2.1. – Introduction

Gas-liquid multiphase flow is of great importance not only in the oil industry; many other industries in different fields find multiphase processes in their everyday life, to mention some of them: chemical engineering , reactors in nuclear engineering, geothermal engineering and space industry engineering [6].

Different ways have been developed throughout the time in the oil industry to give a better understanding and practical application of fluid flow of complex mixtures, the following classification is expressed by (Shoham,2006) [6]: The *empirical* approach is based on experiments and which main aim is to develop correlations and finally make predictions (generally correlation are only valid for similar conditions to which the experiment were performed), the *mathematical* approach which tries to find a exact solution to a set of partial differential equations developed through rigorous mathematical analysis and which limitation relays on the complexity of such equations, the *numerical* approach dealing with numerical schemes and its discretization in space and time, the solution of these equations are given in either implicit or explicit form, therefore for the second method (explicit) stability restrictions are included, and the last approach called the *modeling* approach which is a combination of empirical and mathematical approaches with some simplifications making the models easier to handle mathematically without losing the physical essence of the phenomena (Shoham, 2006) [6].

In the subsequent, we will give a brief description of the so called *modeling* approach based on the concept of a drift flux model that was presented to the scientific community by Zuber and Finlay in 1965 [1].

### 2.2. – Basic definitions

To be able to describe multiphase flow processes some basic definitions must be first introduced:

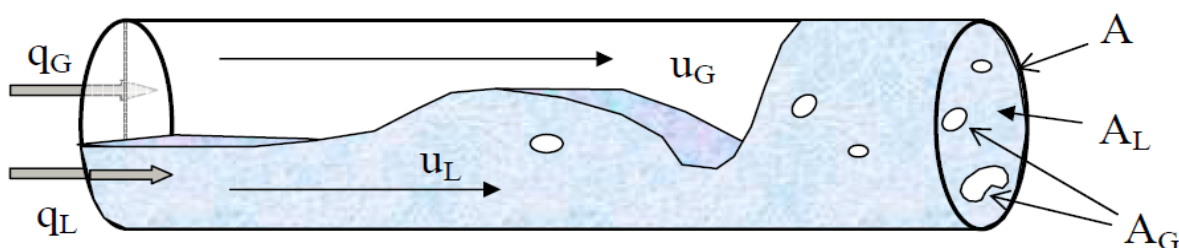


Figure 2.0 Multiphase flow variables, taken from Time, 2009 [12]

**Volumetric flow rates:** The volumetric rates of liquid and gas are defined as the amount of liquid and gas that flows through a pipe of a given cross section area  $A$  ( $m^2$ ), see figure 2.0.

- $q_L$ , volumetric liquid rate ( $m^3/s$ )
- $q_G$ , volumetric gas rate ( $m^3/s$ )
- $q_T$ , total volumetric rate ( $m^3/s$ )
- $q_T = q_L + q_G$ , ( $m^3/s$ )



**Mass flow rates:** The mass flow rates of liquid and gas is the amount of mass being transported through a pipe of a given cross section area  $A$  ( $m^2$ ) per unit of time.

- $W_L$ , mass liquid rate (kg/s)
- $W_G$ , mass gas rate (kg/s)
- $W_T$ , total mass rate (kg/s)
- $W_T = W_L + W_G$  (kg/s)

**Superficial flow velocities:** Superficial flow velocities of liquid and gas are defined as the flow velocity that liquid and gas would have as if they would be flowing as single phase, usually referred to 'apparent velocities' (Time, 2009 [12]). In other words:

$$u_{GS} = \frac{q_G}{A}, \quad u_{LS} = \frac{q_L}{A}$$

- $u_{GS}$ , superficial gas velocity
- $u_{LS}$ , superficial liquid velocity

**Phase velocities:** Phase velocities or actual velocities are the *real* flow phase velocities, which are calculated by dividing the volumetric rate of each phase by its own fluid fraction.

$$u_G = \frac{q_G}{A_G}, \quad u_L = \frac{q_L}{A_L}$$

- $u_G$ , gas phase velocity
- $u_L$ , liquid phase velocity

**Equivalent circulating density (ECD):** The equivalent circulating density (ECD) can be defined as a dynamic quantity generated by the actual fluid density in the system plus the contribution to friction (pressure) of fluids expressed in terms of density, in other words the ECD is meaningless when the system is stagnant, in such case the ECD simply corresponds to the density of the fluid at statics conditions.

One way to calculate the ECD is:

$$ECD = \rho_f + \frac{\Delta p_f}{g * tvd}$$

Where:

- $\rho_f$ , actual fluid density
- $\Delta p_f$ , pressure drop in the annulus from the depth of interest to the surface (usually called parasitic pressure)
- $g$ , gravity force
- $tvd$ , true vertical depth

Another way to calculate the ECD is:

$$ECD = \frac{P_{system}}{g * tvd}$$

Where:

- $P_{system}$ , Total pressure in the system at a the point of interest
- $g$ , gravity force
- $tvd$ , true vertical depth

### 2.3. – Drift-flux model

Two phase flow models analyze the system by considering two different phases (liquid and gas) separately and developing a set of equations describing the fluid behavior for each phase, on the other hand drift flux models treat the mixture as a whole [13], which enables to reduce the mathematical treatment from solving 6 partial differential equations (two flow model) to just 3 equations [13]; In addition drift flux models need to specify an slip relationship which enables to couple the phase velocities and represent relevant flow behavior like opposite flow direction of liquid and gas phase and different phase flow velocities (slip) [2, 6, 7, 14] .

It is my intention to acknowledge Dr. Steinar Evje for his contribution of the development of the model for which this thesis is based; the following derivations are based on the paper that Evje has internally used at the University of Stavanger, Norway. "A reduced Gas-Liquid drift-flux model"; The reader is encouraged to look at the paper [2] for more details; In the following a brief explanation of the mathematical development and assumptions is described.

A reduced drift-flux transient model proposed in [2] has the following form:

$$\begin{aligned} \partial_t[\alpha_g \rho_g] + \partial_x[\alpha_g \rho_g u_g] &= q_g, \\ \partial_t[\alpha_l \rho_l] + \partial_x[\alpha_l \rho_l u_l] &= 0, \\ \partial_t[\alpha_g \rho_g u_g + \alpha_l \rho_l u_l] + \partial_x[\alpha_g \rho_g u_g^2 + \alpha_l \rho_l u_l^2 + P] &= q, \end{aligned} \quad (1)$$

In order to solve system (1) the following variables need to be computed:

- $\rho_l(p), \rho_g(p)$ , densities of liquid and gas.
- $\alpha_l, \alpha_g$ , volumes fractions of liquid and gas.

The first two equations of (1) represents the mass conservation in space and time for liquid and gas phases,  $q_g$  accounts for gas injection at some point  $x$  at a time  $T$ ; the last equation takes into account the momentum balance and allows introducing external forces in the system (i.e. friction and gravity) [2, 11].

It's clear that the gas and liquid fractions satisfies the following constrain

$$\alpha_g + \alpha_l = 1, \quad (2)$$

And the rest of the variables are:

- $u_g, u_l$ , fluid velocities of gas and liquid respectively.
- $P$ , reference pressure for both liquid and gas.
- $q$ , accounts for friction and gravity forces.

The following pressure relationship has been adopted based on equations of state (EOS) [15-18].

$$\rho_l = \rho_l^0 + \frac{P - p_0}{a_l^2} \quad \text{With } \rho_g = \frac{P}{a_g^2} \quad (3)$$

And the corresponding parameters defined as:

- $\rho_l^0, p_0$ , reference density and initial pressure respectively.
- $a_l, a_g$ , represent the speed of sound for liquid and gas in its own phase.

We make use of the following relationship for slip [1, 2, 7, 13, 14]

$$u_g = c_0 u_M + c_1 \quad (4)$$

Where  $c_0$  accounts for the phase distribution of the gas, which tends to concentrate where the mixture velocity is the highest, normally corresponding to the pipe center for vertical flow; And  $c_1$  accounts for natural behavior of the gas to flow upwards through the liquid due to density difference as stated by Shi, H., et al in [14]. Furthermore Julia and Hibiki [19] suggested that  $c_0$  and  $c_1$  are flow pattern dependant which also agrees with Time et al [11] and Evje [2].

Where:

- $u_g$ , is the gas velocity.
- $c_0, c_1$ , represents the shape parameter and drift-flux velocity respectively.

Moreover Evje [2] considered the following reduced version of the drift-flux model presented in (1) by assuming that the convection term in the third equation of (1) goes to zero faster than the other terms, which is the case when the time tends to infinity, therefore (5) represents the “long time behavior” of (1), (Evje,2013) [20]

$$\begin{aligned} \partial_t [\alpha_g \rho_g] + \partial_x [\alpha_g \rho_g u_g] &= q_g \\ \partial_t [\alpha_l \rho_l] + \partial_x [\alpha_l \rho_l u_l] &= 0 \\ \partial_x [P] &= q \\ u_g &= c_0 + u_M + c_1, \end{aligned} \quad (5)$$

Where  $u_M$  is the mixture velocity given by the mixing rules (homogeneous model) as:  $u_M = \alpha_g u_g + \alpha_l u_l$ .

Evje [2] found useful to define the following variables:

$$n = \alpha_g \rho_g, \quad m = \alpha_l \rho_l, \quad (6)$$

The external forces are introduced in the following way:

$$q = -Fu_M - gm, \quad F = f\mu_M, \quad (7)$$

Where  $q$  allows introducing the forces in the system (i.e. friction and gravity) [2], and  $f$  is the friction factor that accounts for friction between the fluids and the wall pipe and  $g$  is the gravity acceleration.

The friction gradient usually takes the following form: [21]

$$q_f = \frac{2f}{D-d} \rho_M u_M |u_M| \quad (8)$$

Where:

- $f$ , friction factor
- $D$ , external pipe diameter.
- $d$ , internal pipe diameter.

And the gravity gradient takes the following form: [21]

$$q_H = \rho_M g \cos \phi \quad (9)$$

Where:

- $\rho_M = \alpha_g \rho_g + \alpha_l \rho_l$ , mixture density
- $g$ , gravity acceleration
- $\phi$ , wellbore inclination

It is convenient to recall that the friction factor ( $f$ ) vary depending on the flow regime, and it is related to the Reynolds number as follows:

$$f \equiv \frac{16}{\text{Re}} \text{ laminar flow (fanning)}, \quad f \equiv \frac{64}{\text{Re}} \text{ laminar flow (moody)} \quad [12].$$

$f = C \text{Re}^{-n}$  where  $C$  and  $n$  vary depending on the correlation used (Dukler, Blasius):

| Correlation | C     | n    |
|-------------|-------|------|
| Dukler      | 0.046 | 0.20 |
| Blasius     | 0.079 | 0.25 |

Table 2.1 Friction factor constants taken from Time 2009 lecture notes [12].

$$\frac{1}{\sqrt{f}} = 1.74 - 2 \log_{10} \left[ \frac{2\varepsilon}{D} + \frac{18.7}{\text{Re} \sqrt{f}} \right] \text{ Colebrook-White formulation for rough pipe [12].}$$

According to the mixing rules for the homogeneous model the mixture viscosity is given by  $\mu_M = \alpha_g \mu_g + \alpha_l \mu_l$ .

Based on the variables introduced by Evje [2] the drift-flux model presented in (5) can be written in the following way:

$$\begin{aligned}\partial_t n + \partial_x [n(C_0 + u_M + C_1)] &= q_g \\ \partial_t [m] + \partial_x [mu_l] &= 0 \\ \partial_x [P(n, m)] &= -Fu_M - gm,\end{aligned}\tag{10}$$

Which results in a consistent system in terms of the variables  $m$  and  $n$  introduced in (6)

The pressure distribution along the system is obtained from the combination of equations (2) and (3), which solution proposed by Evje in [2] is:

$$P(n, m) = \frac{-B(n, m) + \sqrt{B(n, m)^2 + 4AC(n)}}{2A}\tag{11}$$

Were:

$$A = \frac{1}{a_l^2} \quad B(n, m) = \left( \rho_l^0 - \frac{P_0}{a_l^2} \right) + n \frac{a_g^2}{a_l^2} - m \quad C(n) = -na_g^2 \left( \rho_l^0 - \frac{P_0}{a_l^2} \right)$$

The derivation of (7) is given below:

We know from (2) that:  $\alpha_g + \alpha_l = 1$ , and the mass variables  $n = \alpha_g \rho_g$ ,  $m = \alpha_l \rho_l$ ,

$$\text{We can write (2) in the following form: } \frac{n}{\rho_g} + \frac{m}{\rho_l} = 1,\tag{12}$$

Combining (12) with (3)

$$\frac{n}{\frac{P}{a_g^2}} + \frac{m}{\frac{\rho_l^0 a_l^2 + P - p_0}{a_l^2}} = 1 \quad \rightarrow \quad \frac{na_g^2}{P} + \frac{ma_l^2}{\rho_l^0 a_l^2 + P - p_0} = 1 \quad \rightarrow \quad \frac{ma_l^2}{\rho_l^0 a_l^2 + P - p_0} = \frac{P - na_g^2}{P}$$

$$Pma_l^2 = (P - na_g^2)(\rho_l^0 a_l^2 + P - p_0) \quad \rightarrow \quad Pma_l^2 - Pa_l^2 \rho_l^0 + Pp_0 + Pna_g^2 - P^2 = -na_g^2 a_l^2 \rho_l^0 + p_0 na_g^2$$

$$-P^2 + P(ma_l^2 - a_l^2 \rho_l^0 + p_0 + na_g^2) + na_g^2 a_l^2 \rho_l^0 - p_0 na_g^2 = 0$$

$$P^2 \frac{1}{a_l^2} + P \left[ \left( \rho_l^0 - \frac{P_0}{a_l^2} \right) + n \frac{a_g^2}{a_l^2} - m \right] - na_g^2 \left( \rho_l^0 - \frac{P_0}{a_l^2} \right) = 0$$

In other words a second order equation in  $P$  is obtained:

$$P^2 A + PB - C = 0, \text{ Where } A, B, C \text{ defined above are presented in (11).}$$

For the drift flux velocity  $c_1$  and the distribution parameter  $c_0$  it has been defined the following relationship [2]:

$$c_0 = K - [K - 1]\alpha_g^r, \quad c_1 = [1 - \alpha_g]S = \alpha_l S, \quad (13)$$

The parameters  $c_0$  and  $c_1$  have been chosen in such way that a "smooth transition" is achieved from a state where both liquid and gas coexists to a single gas phase, (Evje,2013) [2].

Where:

- $S$ , corresponds to slip ratio, defined as the ratio between the superficial gas velocity and superficial liquid velocity  $\left(\frac{u_{GS}}{u_{LS}}\right)$ , (in other words when both gas and liquid flows at the same velocity  $S$  becomes 1).
- $K$ , is defined as a parameter such that for relatively small values of gas fraction ( $\alpha_g$ ) the distribution parameter  $c_0$  is set to  $K \geq 1$ , and approaches the value of 1 as gas fraction ( $\alpha_g$ ) increases, similarly happens for small values of  $\alpha_g$  [2].

## 2.4. – Boundary conditions

The boundary conditions are specified by the input parameters (liquid and gas rates) and the surface pressure on the right side, since we are assuming the system is open to surface.

- The left boundary condition is found by assuming that liquid is injected in the system at the bottom of the well and gas is injected at a specific position called injection point [2].
- The right boundary condition is specified by assuming that a constant atmospheric pressure is archived at surface [2].

## 2.5. – Initial state

The initial state has been considered corresponding to a stagnant system with an entire mud column, starting from the bottom of the well and ending at the surface (i.e. the well is completely filled with mud and no circulation of any fluid is performed).

These gives rise to:

- The initial mixture velocity is zero.
- The initial gas distribution is zero.

Obtaining the following ordinary differential equation [2].

$$-\frac{g}{al^2} = \frac{1}{\rho_{l,0}} \frac{d\rho_{l,0}}{dx}$$

Which solution is expressed as [2]:

$$\rho_{l,0}(x) = \rho_l^* \exp\left[\frac{g}{al^2}(L-x)\right] \tag{14}$$

The derivation of (14) is given below:

$$-\int_x^L \frac{g}{al^2} dx = \int_{\rho_{l,0}}^{\rho_l^*} \frac{d\rho_{l,0}}{\rho_{l,0}} \rightarrow -\frac{g}{al^2} x \Big|_x^L = \ln(\rho_{l,0}) \Big|_{\rho_{l,0}}^{\rho_l^*} \rightarrow -\frac{g}{al^2} (L-x) = \ln \frac{\rho_l^*}{\rho_{l,0}} \rightarrow \exp\left[-\frac{g}{al^2} (L-x)\right] = \frac{\rho_l^*}{\rho_{l,0}}$$

Finally

$$\rho_{l,0}(x) = \rho_l^* \exp\left[\frac{g}{al^2}(L-x)\right]$$

Where

- $\rho_l^*$ , corresponds to the density at surface conditions.
- $\rho_{l,0}$ , corresponds to the initial density distribution along the wellbore.

## 2.6. – Discretization of the model

We have chosen to divide the system into  $N$  number of grid cells from  $[0, L]$  as shown schematically in Fig 2.1

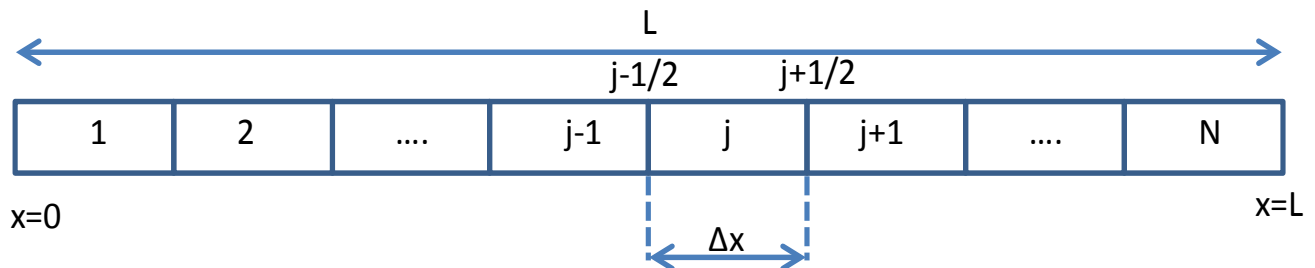


Figure 2.1 Schematic representation of the system, divided into  $N$  number of grid cells.

The discrete scheme proposed is based on an explicit formulation considering “up-wind flow” [2] (direction of flow is taken into account for calculations of subsequent steps), therefore restrictions (stability conditions) must be fulfilled in order to compute a stable solution.

Since the system (10) implies a partial derivative with respect to time and a second partial derivative with respect to space, therefore a first order derivative approximation in time is proposed and a second order derivative approximation in space is used, leading to restrictions (stability) of the following form:

- 1)  $\gamma \frac{\Delta t}{\Delta x} \leq 1.0$ , for the case of first order derivative approximation
- 2)  $\beta \frac{\Delta t}{\Delta x^2} \leq 0.5$ , for the case of second order derivative approximation

Where:

- $\gamma$  and  $\beta$  are constants resulting from the discretization process
- $\Delta t$ , corresponds to time increments  $\left( \frac{Total\_time}{Time\_Step} \right)$
- $\Delta x$ , corresponds to space increments (see figure 2.1)

Based on mathematical and numerical research and it has been found that the upper limit for the approximation of the first derivative 1) that makes the discretization stable corresponds to a value of 1.0 [22], whereas the upper limit for the approximation of the second derivative 2) that meets the stability constrain corresponds to a value of 0.5 [22].

For illustration purposes, the first and second order approximation will be explained in a general matter, based on ‘chord approximations’ [23] and making use of the definition of the derivate of a given function  $f(x)$  shown below:

$$f'(x) = \lim_{\Delta x \rightarrow 0} \frac{f(x + \Delta x) - f(x)}{\Delta x}$$

The derivatives can be approximated using Taylor expansion; the derivate of  $f(x)$  can be substituted by the following approximations

- i)  $f'(x) = \frac{f(x + \Delta x) - f(x)}{\Delta x}$
- ii)  $f'(x) = \frac{f(x) - f(x - \Delta x)}{\Delta x}$
- iii)  $f'(x) = \frac{f(x - \Delta x) + f(x + \Delta x) - 2f(x)}{2\Delta x}$

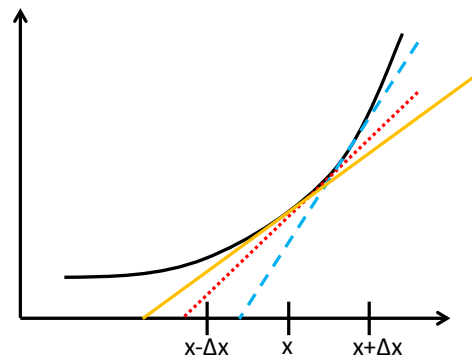


Figure 2.2 Schematic representation of “chord approximations” [23]



Derivative approximations i),ii) and iii) can be expressed in terms of Taylor expansion if the points  $x$ ,  $x + \Delta x$  and  $x - \Delta x$  belong to an interval  $[a,b]$  where the function  $f$  is also defined[23]

Therefore for the points  $x + \Delta x$  and  $x - \Delta x$  would have a Taylor expansion of the following form [23]:

$$\begin{aligned} \text{a) } f(x + \Delta x) &= f(x) + f'(x)\Delta x + \frac{1}{2}f''(x)\Delta x^2 + \frac{1}{3!}f'''(x)\Delta x^3 + \frac{1}{4!}f^{(4)}(\xi)\Delta x^4 + \dots \\ \text{b) } f(x - \Delta x) &= f(x) - f'(x)\Delta x + \frac{1}{2}f''(x)\Delta x^2 - \frac{1}{3!}f'''(x)\Delta x^3 + \frac{1}{4!}f^{(4)}(\xi)\Delta x^4 - \dots \end{aligned}$$

We will make use of Taylor expansion to calculate the first order approximation of the derivative of  $f(x)$ ; from a) we can solve for  $f'(x)$ , resulting in:

$$f'(x) = \frac{f(x + \Delta x) - f(x)}{\Delta x} - \frac{1}{2}f''(\xi)\Delta x$$

In other words:

$$f'(x) = \frac{f(x + \Delta x) - f(x)}{\Delta x} + O(\Delta x), \text{ where the term } O(\Delta x) \text{ is called first order approximation[23].}$$

Similarly from b) we can solve for  $f'(x)$ , resulting in:

$$f'(x) = \frac{f(x) - f(x - \Delta x)}{\Delta x} + O(\Delta x)$$

And finally

$$f'(x) = \frac{f(x + \Delta x) - f(x - \Delta x)}{2\Delta x} + O(\Delta x^2), \text{ where the term } O(\Delta x^2) \text{ is called second order approximation[23].}$$

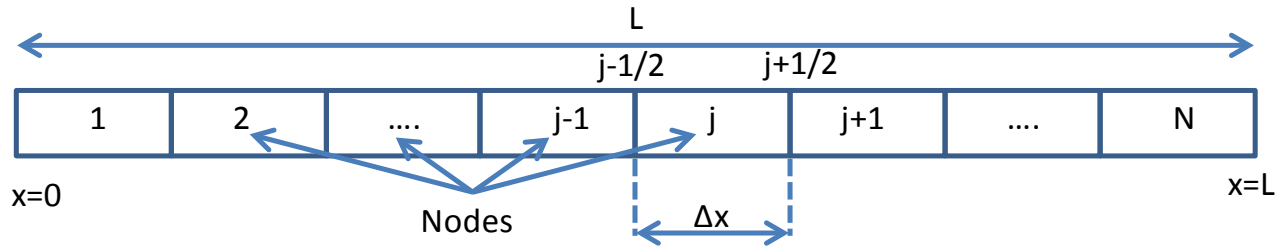
In the same way, for the second derivative of  $f(x)$  an approximation is given as follows:

$$f''(x) = \frac{f(x + \Delta x) + f(x - \Delta x) - 2f(x)}{\Delta x^2} + O(\Delta x^2), \text{ Second order approximation[23].}$$

The discretization of the model has been carried out using the same principles explained above, for further details related to the discretization of the numerical model used in this thesis the reader is encouraged to look at the original paper "A reduced Gas-Liquid drift-flux model" [2] and its own cited references.

### 3. – Numerical simulations (vertical geometry)

We consider the following representation for the wellbore.



Where

- $L$ , represents the total length of the well.
- $N$ , represents the number of grid cells.
- $x$ , gives the position of the injection point along the wellbore where  $x=0$  represents the bottom of the well and  $x=L$  represents the surface.

#### 3.1. - Specification of parameters

Table 3.1 gives the details of the parameters used in the numerical simulation for the vertical well.

|                                   |                 |
|-----------------------------------|-----------------|
| $\rho_{L,0}$ (kg/m <sup>3</sup> ) | 920             |
| $p_0$ (Pa)                        | $10^5$          |
| $a_L$ (m/s)                       | 1000            |
| $a_G$ (m/s)                       | 316.3           |
| $f$ ( )                           | $5 \times 10^4$ |
| $\mu_L$ (Pa-s)                    | 0.15            |
| $\mu_G$ (Pa-s)                    | 0.00005         |
| $L$ (m)                           | 5000            |
| $N$ ( )                           | 40              |

Table 3.1 Parameters used for the numerical examples (Vertical Well)

#### 3.2. - Variation of Injection point.

We would like to investigate the role played by the position of injection point “ $x$ ” by running different simulations within the period  $[0, T]$ , we set constant liquid and gas injection rate at the bottom of the well. In other words:

Constant parameters:

- $T = 10\,000$  (s), (Simulation time)
- $q_L = 400$  (kg/m<sup>2</sup> s), (Flow rate of liquid/mud)
- $q_G = 0.5$  (kg/m<sup>2</sup> s), (Flow rate of gas)

And we will vary the injection point considering two different positions

- $x_1 = 500$  (m)
- $x_2 = 3000$  (m)

General observations:

We consider the initial state corresponding to a stagnant system with the well completely filled with mud. Liquid is injected at the bottom of the well simulating only circulation through the drill string, there after gas injection begins at a position dictated by “x”.

**What would one expect when the circulation begins?**

- As we see in figure 3.0, an increment in pressure is observed due to pure friction between liquid and the wall pipe, but we can say that the pressure along the wellbore corresponds to a non linear profile; this is because the model considers a pressure dependence of the form  $p = p(\rho)$ .

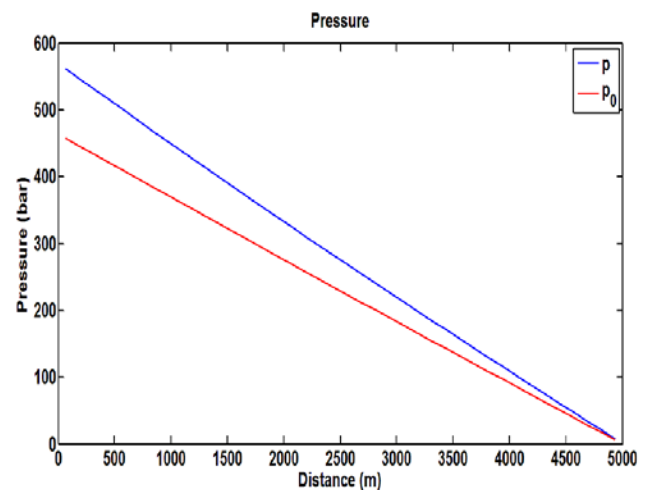


Figure 3.0 Pressure profile for  $T = 0$  (s) and  $T = 100$ (s).

**What about gravity?**

- Gravity is acting in the same way as before, when the system was stagnant. In real life, the pressure profile will be also affected by the change of fluid density as a result of cuttings being incorporated in the mud, with higher pressure gradient close to the bottom due to compressibility of cuttings and liquid.

**What happens when the gas comes into the system?**

Now we want to start injecting gas at  $x_1 = 500$  (m) at a time  $T = 500$  (s), we observe an **increment of:**

- Liquid phase velocity close to the injection point (liquid velocity is given a boost due to influx of gas), Fig 3.1 “middle” (dashed line).
- Friction caused by an increment of the mixture fluid velocity, Fig 3.1 “left” (dashed line).

- Liquid mass rate at the surface (liquid is being pushed out of the system), Fig 3.1 "right", followed by a decrement on surface liquid rate which happens around  $T = 2790$  (s) when the influx of gas breaks through at surface red line Fig 3.1 "right".

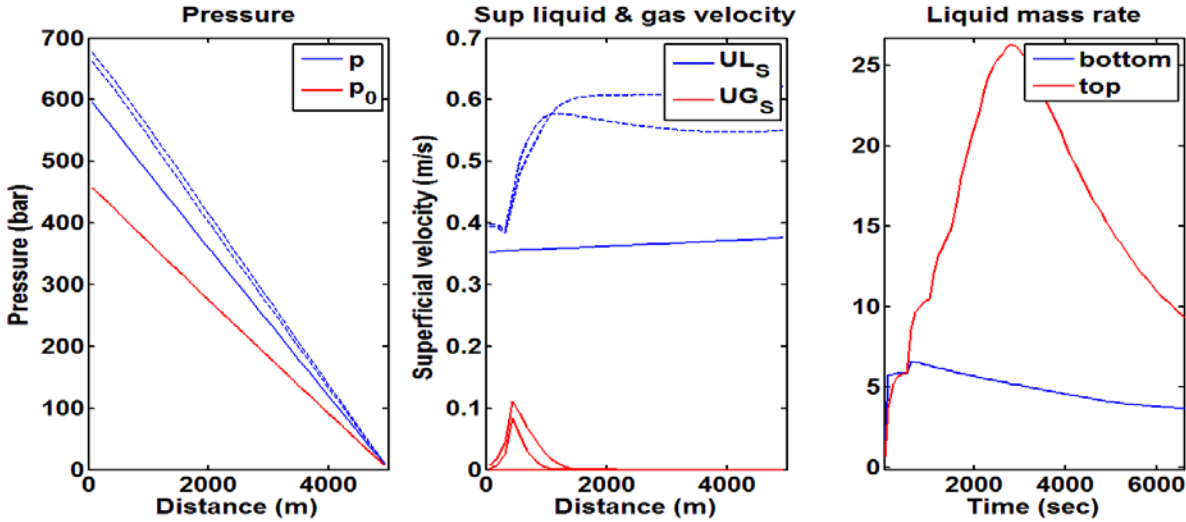


Figure 3.1 Pressure "left", superficial liquid and gas velocities "middle" and liquid mass rate "right" of the system at 100 (s) and 200(s) after gas injection,  $x_1 = 500$  (m) and injection rate  $q_G = 0.5$  (kg/m<sup>2</sup> s).

**What can we expect if more and more gas comes into the system?**

- There will be a point where the gas fraction begins to dominate the behavior of the system and a reduction on the pressure will be observed, this is observed on figure 3.8

**What do we know about the gas velocity profile along the wellbore?**

- We observe zero gas velocity below the injection point and gas is expanding close to the surface (since pressure is lower at surface) resulting in high gas velocity profile (see Fig 3.2)

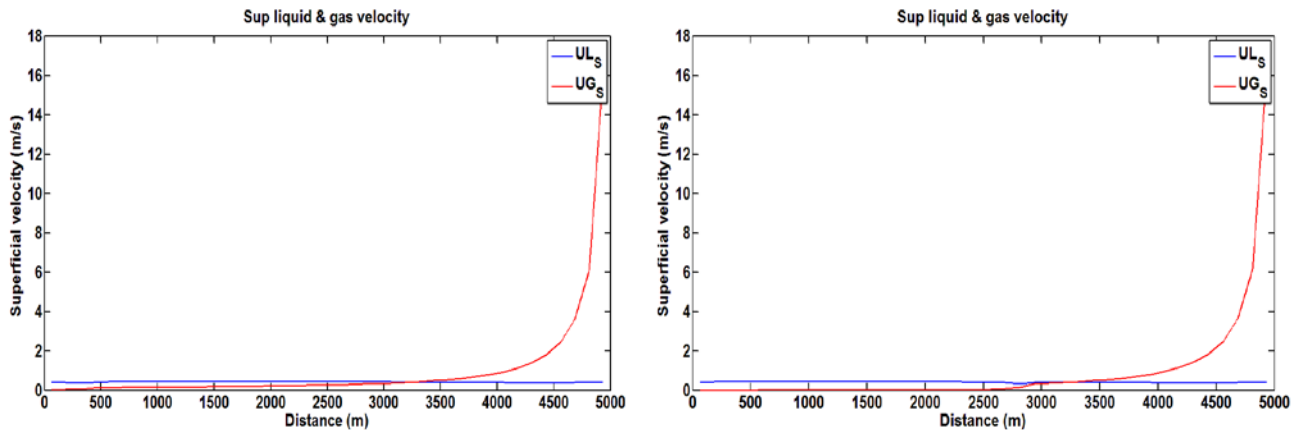


Figure 3.2 Final superficial liquid and gas velocity at the end of the simulation,  $T = 10000$  (s) for  $x_1 = 500$  (m) "left" and  $x_2 = 3000$  (m) "right".

How will pressure be affected if the injection point is changed from  $x_1=500$  to  $x_2= 3000$  (m)?

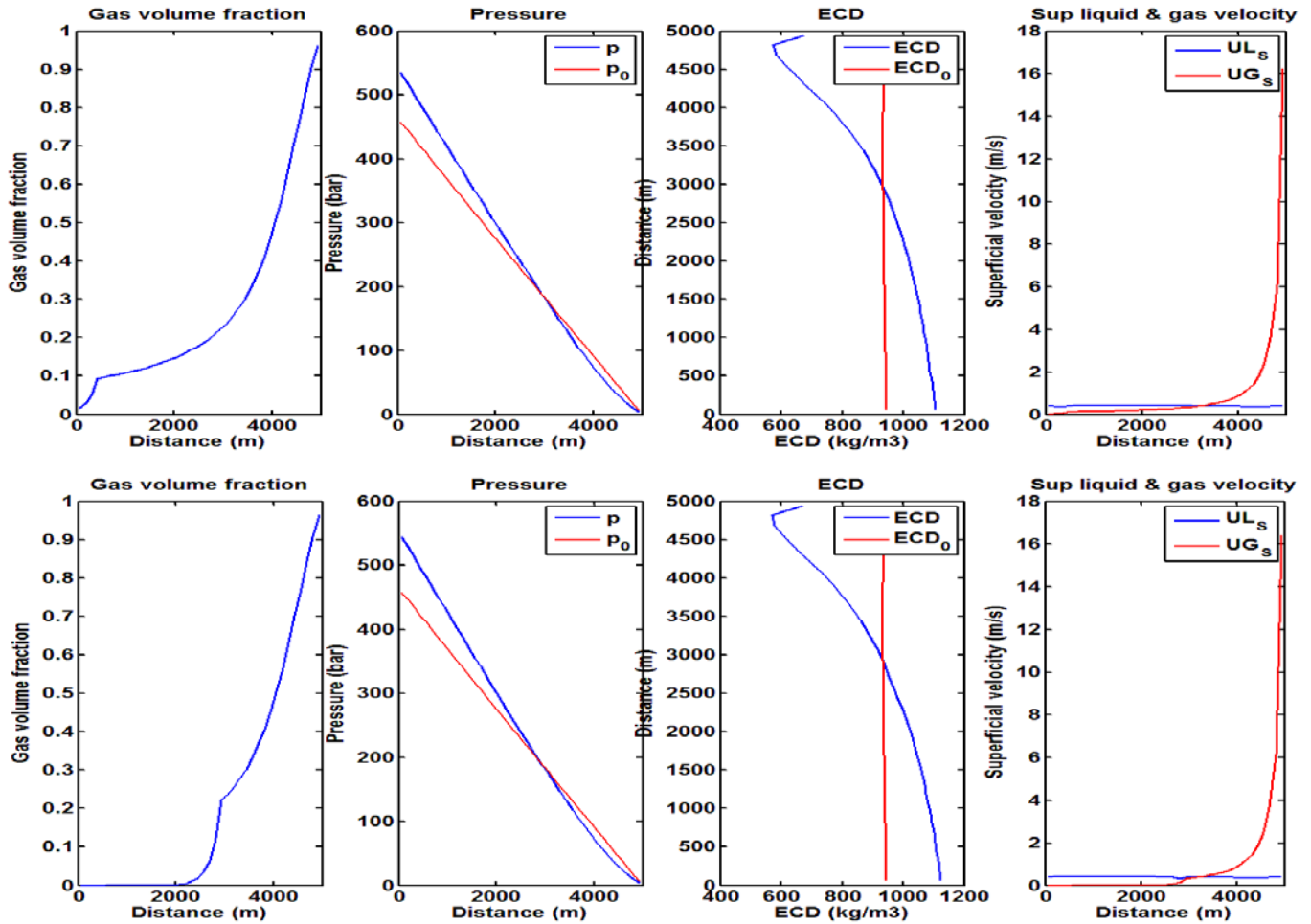


Figure 3.3 Gas fraction, pressure and ECD at  $T= 10000$  (s) for  $x_1= 500$ (m) "top" and  $x_2= 3000$ (m) "bottom".

Main observations

$x_1 = 500$  (m)

- ECD top = 675 (kg/m<sup>3</sup>)
- ECD bottom = 1103 (kg/m<sup>3</sup>)
- Pressure top = 4.14 (bar)
- Pressure bottom = 534.59 (bar)

$x_2 = 3000$  (m)

- ECD top = 669(kg/m<sup>3</sup>)
- ECD bottom = 1123 (kg/m<sup>3</sup>)
- Pressure top = 4.10 (bar)
- Pressure bottom = 543.96 (bar)

Comments

- Figure 3.3 shows a small difference in terms of ECD and pressure distribution for both injection points  $x_1= 500$  (m) and  $x_2= 3000$  (m), the reason is that the model uses a parameter  $f$  (to account for friction between the pipe wall and fluids), and it turned out that  $f$  was relatively high, therefore the friction generated by liquid rate hid the reduction in hydrostatic pressure due to gas injection, we can observe in figure 3.2 "right" that the velocity profile of liquid and gas is different for both injection points, therefore one may expect a difference in pressure distribution but as mention before the friction factor used in this simulation was relatively high.

An additional analysis is shown in figure 3.4 for the injection point where the value of  $f$  was reduced keeping constant the same gas injection rate  $q_G = 0.5$  (kg/m<sup>2</sup> s), the results are show below.

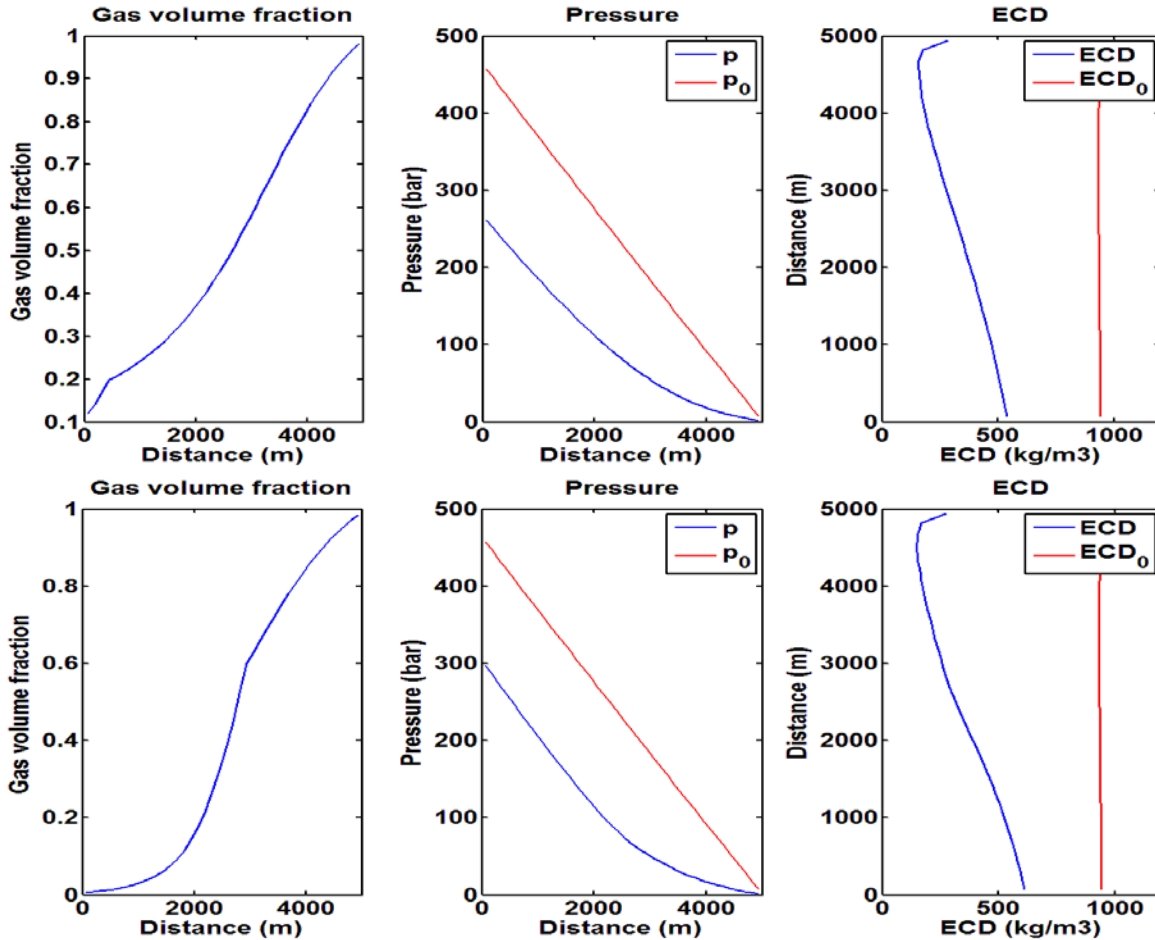


Figure 3.4 Gas fraction, pressure and ECD at  $T = 10000$  (s) for  $x_1 = 500$ (m) "top" and  $x_2 = 3000$ (m) "bottom", after modification of the friction factor  $f$ .

Main observations

|                   |                               |                   |                               |
|-------------------|-------------------------------|-------------------|-------------------------------|
| $x_1 = 500$ (m)   |                               | $x_2 = 3000$ (m)  |                               |
| – ECD top         | = 284.43 (kg/m <sup>3</sup> ) | – ECD top         | = 227.00(kg/m <sup>3</sup> )  |
| – ECD bottom      | = 540.32 (kg/m <sup>3</sup> ) | – ECD bottom      | = 612.93 (kg/m <sup>3</sup> ) |
| – Pressure top    | = 1.74 (bar)                  | – Pressure top    | = 1.69 (bar)                  |
| – Pressure bottom | = 261.71 (bar)                | – Pressure bottom | = 296.88 (bar)                |

Comments

- The injection point plays an important role on the pressure distribution, we can generally say that if we select a lower injection point we will expect a lower the pressure at bottom of the well, however later on we will demonstrate by means of different simulations that the injection rate together with the injection depth have a big impact on the pressure distribution.

If the gas velocity is high close to surface then one might think that an increment in pressure is expected, why this is not the case?

- Despite of the high gas velocity close to the surface, we know that the viscosity of the gas  $\mu_g$  is much lower than the liquid viscosity  $\mu_l$ , (see table 3.1) and the pressure generated by friction seems to be not impacted. We observe that the upper part of the well is dominated by high gas fraction and a reduction in pressure is created close to the surface, whereas the bottom of the well is dominated by the contribution of liquid to hydrostatic pressure and friction.

### 3.3. - Flow regimes for different injection points

We will make use of the current literature regarding flow patterns maps for two-phase annular flow, based on the paper published by J. Enrique Julia and Takashi Hibiki (2011) [19]. In their work they propose a new criterion to predict flow regime transitions considering 4 types of flow regimes: bubbly, cap-slug (slug), churn and annular and three transitions: bubbly to cap-slug (slug), cap-slug to churn, churn to annular, however our intention is not to develop a new model or flow pattern map, on the other hand we will use the literature review they have done and the numerical results as a basis to predict the flow regime along the wellbore. We know the flow regime is dictated by the superficial flow velocity of the gas  $\alpha_g u_g$  and superficial flow velocity of liquid  $\alpha_l u_l$ , as well as the properties of liquid-gas and the geometrical flow path (i.e. inner pipe diameter and inclination angle) as expressed by Julia and Hibiki in [19] and Shoham in [6], having demonstrated that a higher velocity of gas is observed close to the surface whereas zero velocity of gas takes place below the injection point (see Fig 3.2), then:

Plots for superficial liquid and gas velocity have been produced in three different positions along the wellbore and by means of flow regime maps and results given by simulations we will try to determine the flow pattern. In the following we will only consider the correlation proposed by Kelessidis and Duckler (1989) reported in [19].

We have selected three different arbitrary positions to evaluate the flow patterns, as shown in Fig 3.5.

- Above the injection point (Inj P.)
- Half way from the injection point to surface (Mid)
- 250 m below surface (Top)

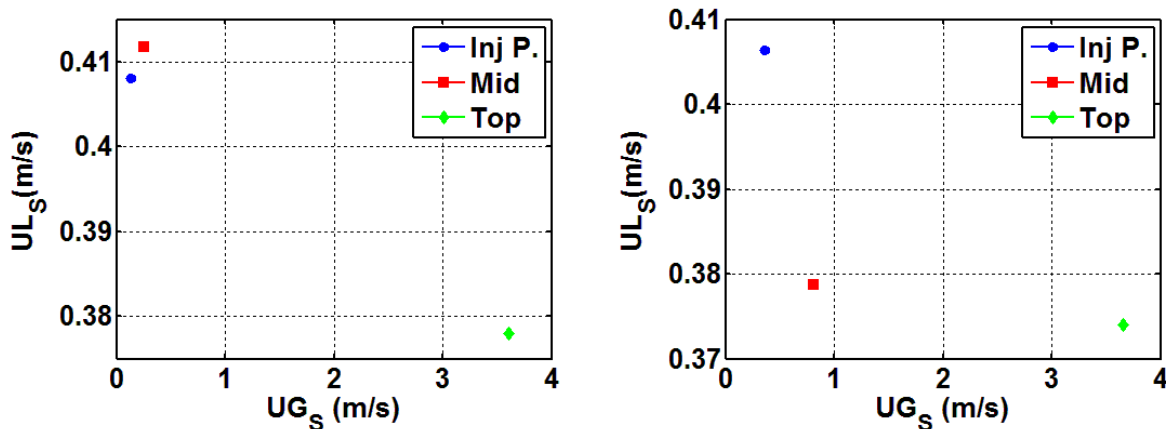


Figure 3.5 Superficial liquid and gas velocities at three different positions; *left figure* corresponds to an injection point  $x_1=500$  (m) whereas *right figure* corresponds to an injection point  $x_2=3000$  (m).  $T = 10000$  (s).

It is important to recall that the distribution parameter ( $c_0$ ) and the drift velocity ( $c_1$ ) described in (4) tends to change depending on the flow regime as stated by by Julia and Hibiki in [19] and Time et al in [11] . *For simplicity we have adopted constant values but it is important to be aware of this, moreover it gives room for improvement in further simulations of the model described on this work.*

Based on the final reading of superficial flow velocities and the literature review published by Julia and Hibiki (2011) [19], Fig 3.6. We can then suggest the following flow patterns.

Injection point x1= 500m

Injection point x2= 3000m

|        | ULs (m/s) | UGs (m/s) | Flow regime |        | ULs (m/s) | UGs (m/s) | Flow regime |
|--------|-----------|-----------|-------------|--------|-----------|-----------|-------------|
| Inj. P | 0.408     | 0.1364    | Bubbly-Slug | Inj. P | 0.4064    | 0.3620    | Slug        |
| Mid    | 0.4118    | 0.2529    | Slug        | Mid    | 0.3788    | 0.8108    | Slug        |
| Top    | 0.378     | 3.6080    | Churn       | Top    | 0.374     | 3.6500    | Churn       |

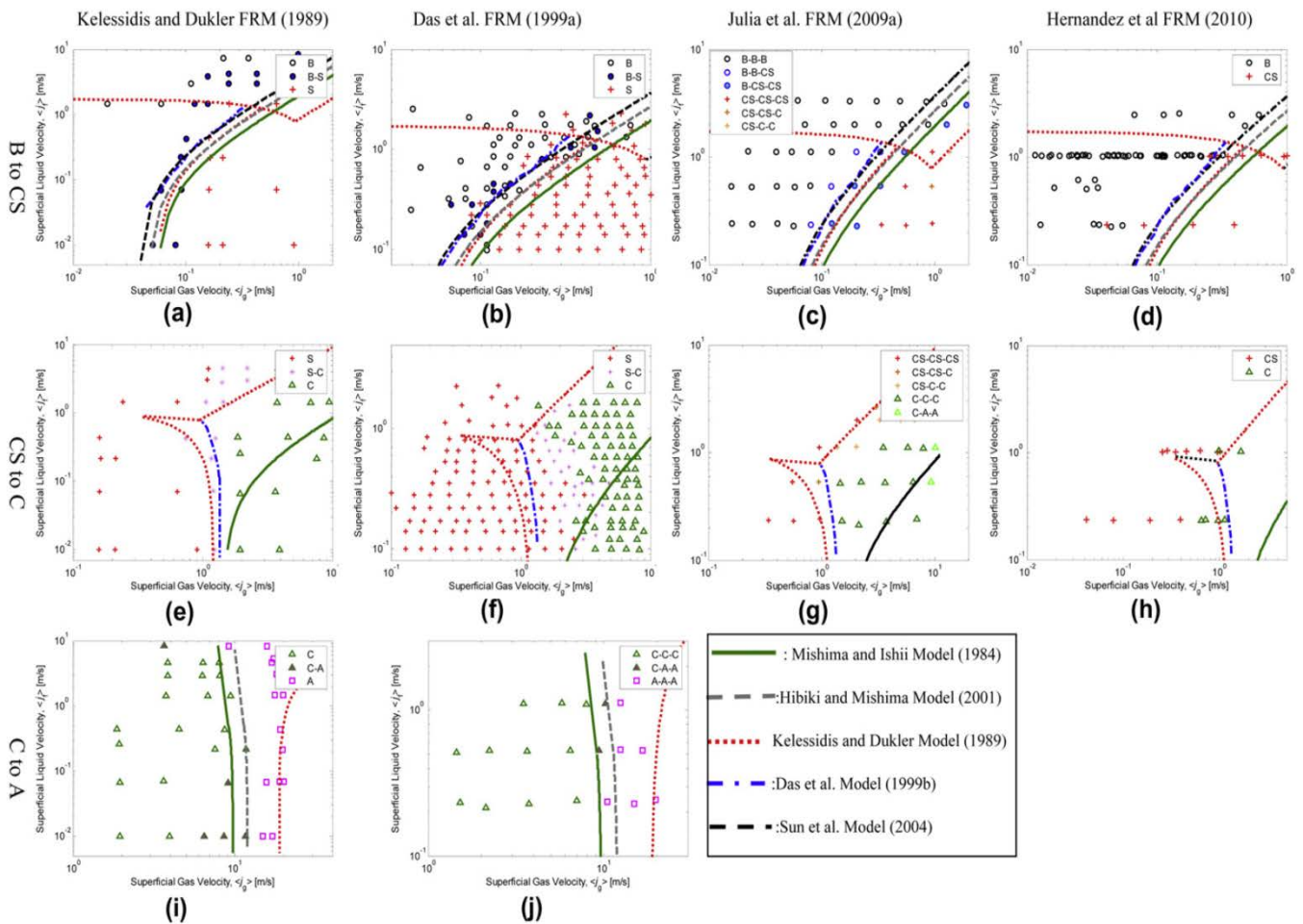


Figure 3.6 Flow regimes maps for two-phase vertical annular flow, taken from J. Enrique Julia and Takashi Hibiki (2011) [19].



General conclusions for injection point analysis:

- Since the system is initially stagnant the initial pressure profile is dictated by the density of the fluid and gravity.
- For the cases where  $x_1 = 500$  (m), the system does not come close to a stationary solution, this is because more liquid has to be displaced out of the system.
- For the case where  $x_2 = 3000$  (m) the system approaches to a stationary solution within a time  $\sim 6700$  (s) and an ECD  $\sim 980$  (kg/m<sup>3</sup>) at the bottom of the well.
- Flow regimes agree for both cases of injection points  $x_1 = 500$  (m) and  $x_2 = 3000$  (m).

### 3.4. - Variation of Injection rate

Now we want to investigate the role played by the gas injection rate by running different simulations within the period  $[0, T]$ , keeping constant liquid injection rate at the bottom of the well and the injection point  $x = 500$  (m).

Constant parameters:

- $T = 10\,000$  (s), (Simulation time)
- $q_L = 400$  (kg/m<sup>3</sup> s), (Flow rate of liquid/mud)
- $x = 500$  (m), (Position of injection)

We vary the gas injection rate, considering the following options:

- $q_G = 0.5$  (kg/m<sup>2</sup> s)
- $q_G = 1.0$  (kg/m<sup>2</sup> s)
- $q_G = 2.0$  (kg/m<sup>2</sup> s)

General observations:

The initial state corresponds to a stagnant system with the well completely filled with mud. Liquid is injected at the bottom of the well simulating only circulation of mud, there after gas injection begins at a position dictated by  $x = 500$  (m) from the bottom of the well, figures 3.7, 3.8, 3.9, 3.10 and 3.11.

**How is the pressure affected by injection rate?**

- An increment in pressure is observed when we increase the gas injection rate, see figure 3.8 on pressure curve "left", the same effect is observed on the equivalent circulating density (ECD), see figure 3.8 on ECD curve "right".

**What would be the explanation?**

- We have shown previously that when the gas comes into the well at the injection point, it pushes the liquid out of the system increasing its velocity firstly close to the injection point (see Fig 3.1 middle) and thereafter in the rest of wellbore, we have also observed that an increment in velocity creates an increment of pressure in the well due to friction, then the answer is that more pressure is generated by friction.

### What happens to the pressure distribution when more gas comes into the system?

- It's been observed in the simulations that when the gas fraction reaches an approximate value of 0.5 at the surface a significant pressure reduction is observed, and for this particular simulation that happens to be at time  $T = 2700$  (s) as shown in Fig 3.7 "left", there after the pressure gradually decreases and the pressure profile becomes highly nonlinear.

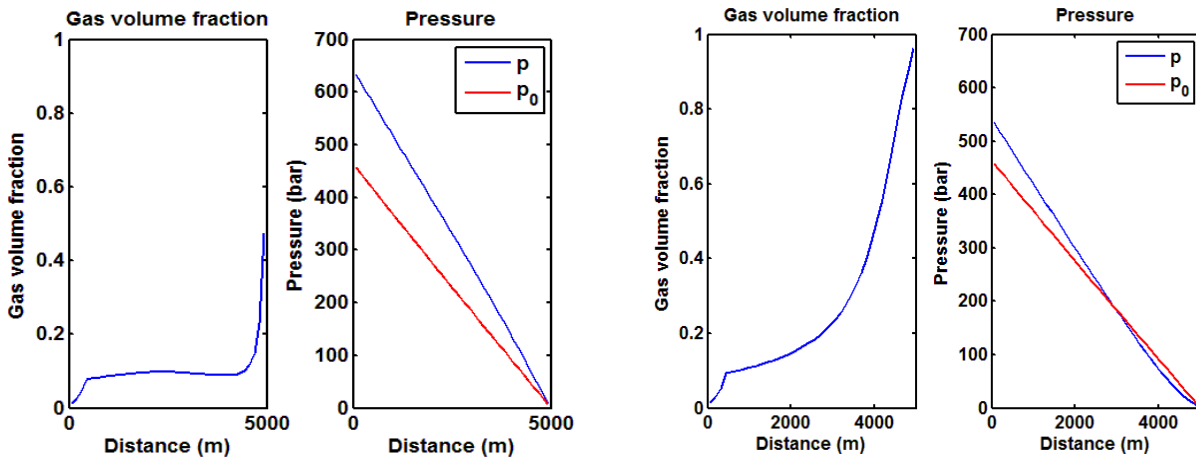


Figure 3.7 Gas fraction and pressure at  $q_G = 0.5$  (kg/m<sup>2</sup> s),  $T = 2700$  (s) left,  $x = 500$  (m),  $T = 10000$  (s) right.

### What is the role played by gas injection rate in terms of pressure distribution?

- We can say that the system is dominated by hydrostatic forces when its pressure response is considerably affected by gravity, which is the case when there is no circulation in the wellbore (i.e. the system is stagnant) and at relatively "small" gas rates; but at some point, as more and more gas enters the system the hydrostatic pressure will decrease and the contribution to pressure due to friction will increase. The behavior of the pressure will become more affected by friction rather than gravity, we can then consider that the system is dominated by friction; these two forces act on opposite ways and the combination of both can be observed on the pressure behavior of the system.
- When the gas comes into the system the increment in pressure is due to an increment in mixture velocity, which increases the friction effect on pressure. It has been shown by simulations that as more gas is being injected the hydrostatic pressure is reduced with gas being compressed at the bottom of the well and gas expansion as it comes to surface, which agrees with Steve Nas [5].
- Fig 3.8 shows the combination of both effects on the pressure at the bottom of the well "left" and ECD "right" at two different positions (bottom and shoe). We can clearly notice that when the pressure curve is starting to flatten out the system is changing from being dominated by hydrostatic forces to being dominated by friction forces and similarly happens to the ECDs curves. We can distinguish the transition because no further reduction in pressure/ECD is observed despite of the increment on gas rate.

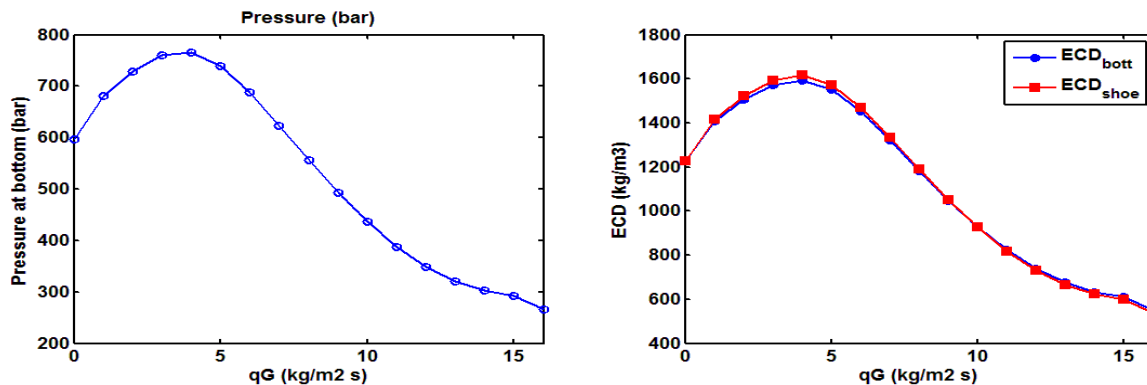


Figure 3.8 Pressure at the bottom of the well for different gas rates, "left", ECD for two different position (bottom of the well and previous casing shoe) "right".

Figure 3.9 shows the final pressure distribution along the wellbore at the end of the simulation,  $T = 10000$  (s).

- We observe a reduction in pressure as the gas injection rate increases, which is an indication that the systems is highly influenced by hydrostatic forces, the same effect on ECD is observed in Fig 3.10.

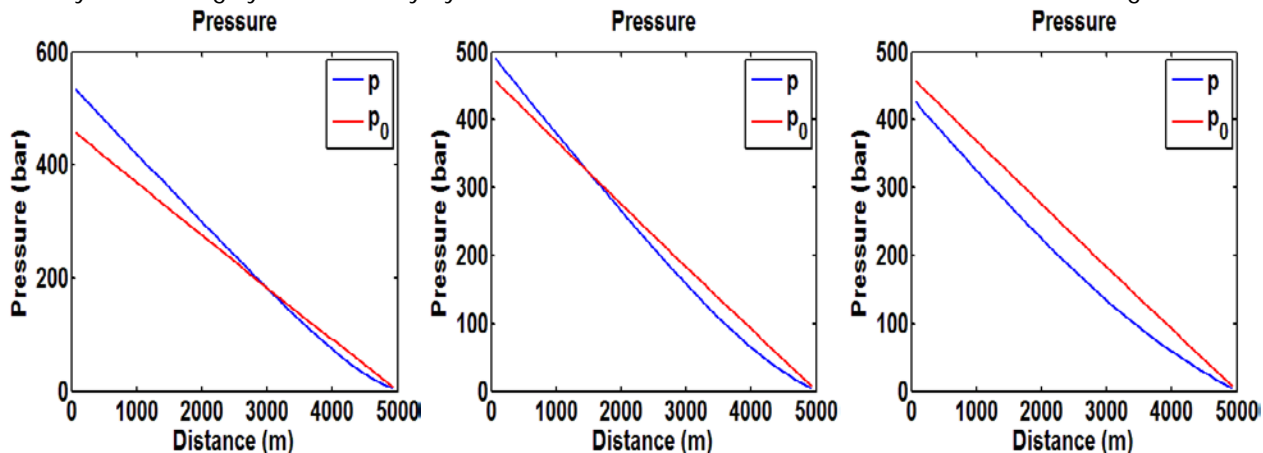


Figure 3.9 Final pressure distribution for three different gas injection rates,  $q_G = 0.5$  ( $\text{kg/m}^2 \text{ s}$ ) "left",  $q_G = 1.0$  ( $\text{kg/m}^2 \text{ s}$ ) "middle",  $q_G = 2.0$  ( $\text{kg/m}^2 \text{ s}$ ) "right",  $x = 500$  (m),  $T = 10000$ (s).

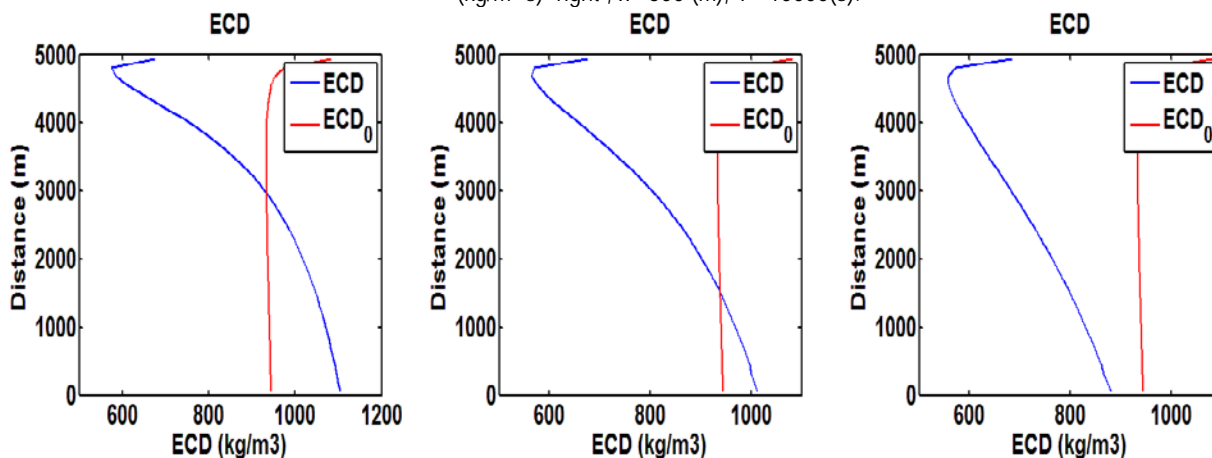


Figure 3.10 Final ECD distribution for three different gas injection rates,  $q_G = 0.5$  ( $\text{kg/m}^2 \text{ s}$ ) "left",  $q_G = 1.0$  ( $\text{kg/m}^2 \text{ s}$ ) "middle",  $q_G = 2.0$  ( $\text{kg/m}^2 \text{ s}$ ) "right",  $x = 500$  (m),  $T = 10000$ (s).

### 3.5. - Flow regimes for different injection rates

Plots for superficial liquid and gas velocity have been produced at three different positions along the wellbore and by means of numerical results from the model and flow regime maps we will try to estimate the flow pattern in three different positions along the wellbore, In the following we will only consider the classic approach proposed by **Kelessidis and Duckler** (1989) reported in [19].

Three different arbitrary positions have been selected to evaluate the flow patterns.

- Above the injection point (Inj P.)
- Half way from the injection point to surface (Mid)
- 250 m below surface (Top)

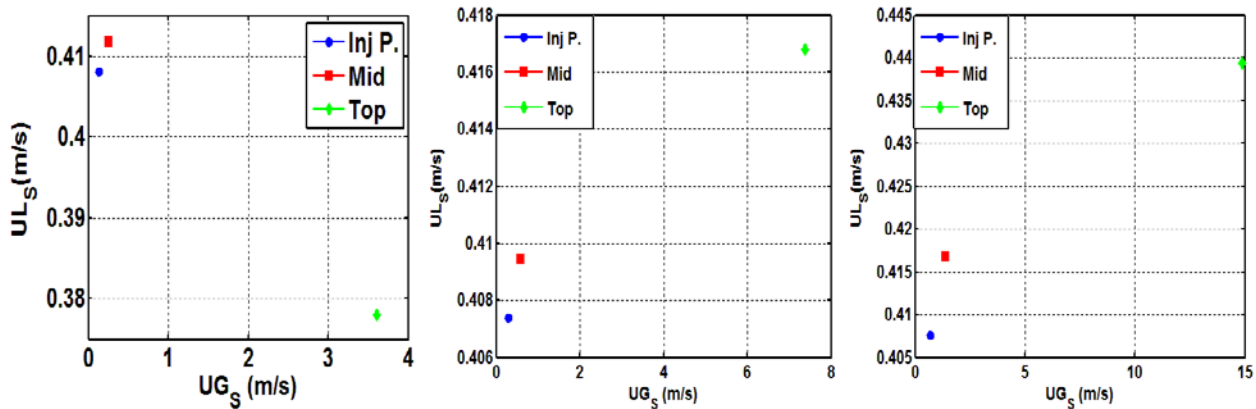


Figure 3.11 Final superficial velocities  $UL_s, UG_s$  for three different positions along the wellbore,  $x = 500$  (m),  $q_G = 0.5$  (kg/m<sup>2</sup>s) "left",  $q_G = 1.0$  (kg/m<sup>2</sup> s) "middle",  $q_G = 2.0$  (kg/m<sup>2</sup> s) "right".

The following flow patterns have been suggested, based on simulation results and correlation proposed by **Kelessidis and Duckler** (1989) reported in [19].

- $q_G = 0.5$  (kg/m<sup>2</sup> s), see Fig 3.9 "left"
- $q_G = 1.0$  (kg/m<sup>2</sup> s), see Fig 3.9 "middle"

|         | $UL_s$ (m/s) | $UG_s$ (m/s) | Flow  |         | $UL_s$ (m/s) | $UG_s$ (m/s) | Flow  |
|---------|--------------|--------------|-------|---------|--------------|--------------|-------|
| pattern |              |              |       | pattern |              |              |       |
| Inj P   | 0.1364       | 0.408        | Slug  | Inj P   | 0.4074       | 0.3003       | Slug  |
| Mid     | 0.4118       | 0.2529       | Slug  | Mid     | 0.4094       | 0.5787       | Slug  |
| Top     | 0.3780       | 3.608        | Churn | Top     | 0.4168       | 7.3770       | Churn |

- $q_G = 2.0$  (kg/m<sup>2</sup> s), see Fig 3.9 "right"

|       | $UL_s$ (m/s) | $UG_s$ (m/s) | Flow       |
|-------|--------------|--------------|------------|
| Inj P | 0.4076       | 0.6988       | Slug       |
| Mid   | 0.4168       | 1.3770       | Slug-Churn |
| Top   | 0.4933       | 14.880       | Annular    |

Main observations:

- Based on the simulations results we can generally say that higher gas injection rate produces a lower ECD when the system is influenced by hydrostatic forces, once the system becomes friction dominated an opposite effect is observed.
- Lower gas injection rate produces a faster stationary solution
- For the case of  $q_G = 0.5$  (kg/m<sup>3</sup> s) the system approaches a stationary solution within a time  $T \sim 6800$  (s) and an ECD  $\sim 1117$  kg/m<sup>3</sup>.
- For the case of  $q_G = 1.0$  (kg/m<sup>3</sup> s) the system comes close to a stationary solution within a time  $T \sim 9500$  (s) and an ECD  $\sim 1007$  kg/m<sup>3</sup>.
- For the case of  $q_G = 2.0$  (kg/m<sup>3</sup> s) the system does not reach an stationary solution, Final ECD at the bottom of the well is 873.05 kg/m<sup>3</sup>
- Flow pattern predictions agree for the three different gas injection rates at the injection point (Inj P.) and at the position half way from the injection point to surface (Mid), however for last point 250 m below surface (Top), the simulation predicts churn flow for both injection rates  $q_G = 0.5$  (kg/m<sup>2</sup> s) and  $q_G = 1.0$  (kg/m<sup>2</sup> s), and annular flow for  $q_G = 2.0$  (kg/m<sup>2</sup> s)

#### 4. – Calibration of the model

A real pressure while drilling (PWD) data file has been used as a first attempt to calibrate the model, the friction factor  $f$  used in equation (7) was modified to match the observed ECD for a given rate and depth, the casings setting depths of the well are shown in figure 4.1

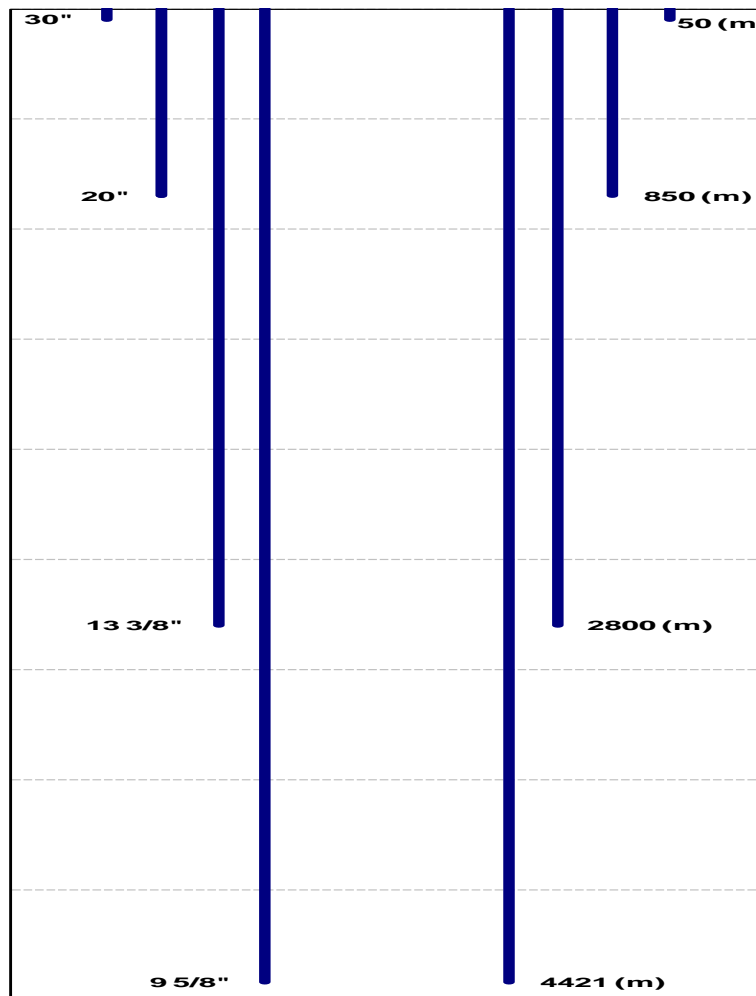


Figure 4.1 Schematic configuration of the well used to calibrate the model

#### 4.1. – Parameters used to calibrate the model

The well configuration that was used to calibrate the model is shown in figure 4.1 and the operational parameters are shown in figure 4.2; Drilling engineers sometimes lower a down hole tool into the wellbore called pressure while drilling (PWD) which is nothing but a high accuracy pressure gauge that gives annular and internal pressures in the drill string and calculates ECDs in real time, this tool is normally used to monitor the concentration of cutting added to the mud and its impact on ECD, it is also used to detect problems related to cleaning efficiency and possible issues derived, as well as kicks, swab/surge pressures and allows taking reliable pressure measurements relevant for leak off test (LOT) and formation integrity tests (FIT).

The first column of figure 4.2 shows the lithology where the transition from the high pressure zone (brown) to the reservoir (green) is depicted, the second column corresponds to the inclination of the well in ( $^{\circ}$ ), the third shows the pumping rate in (gpm), the fourth displays the current mud weight in ( $\text{gr}/\text{cm}^3$ ), the fifth column represents the ECD in ( $\text{gr}/\text{cm}^3$ ) for a given depth and rate, finally the last two columns represent the inner and annular pressure in (psi).

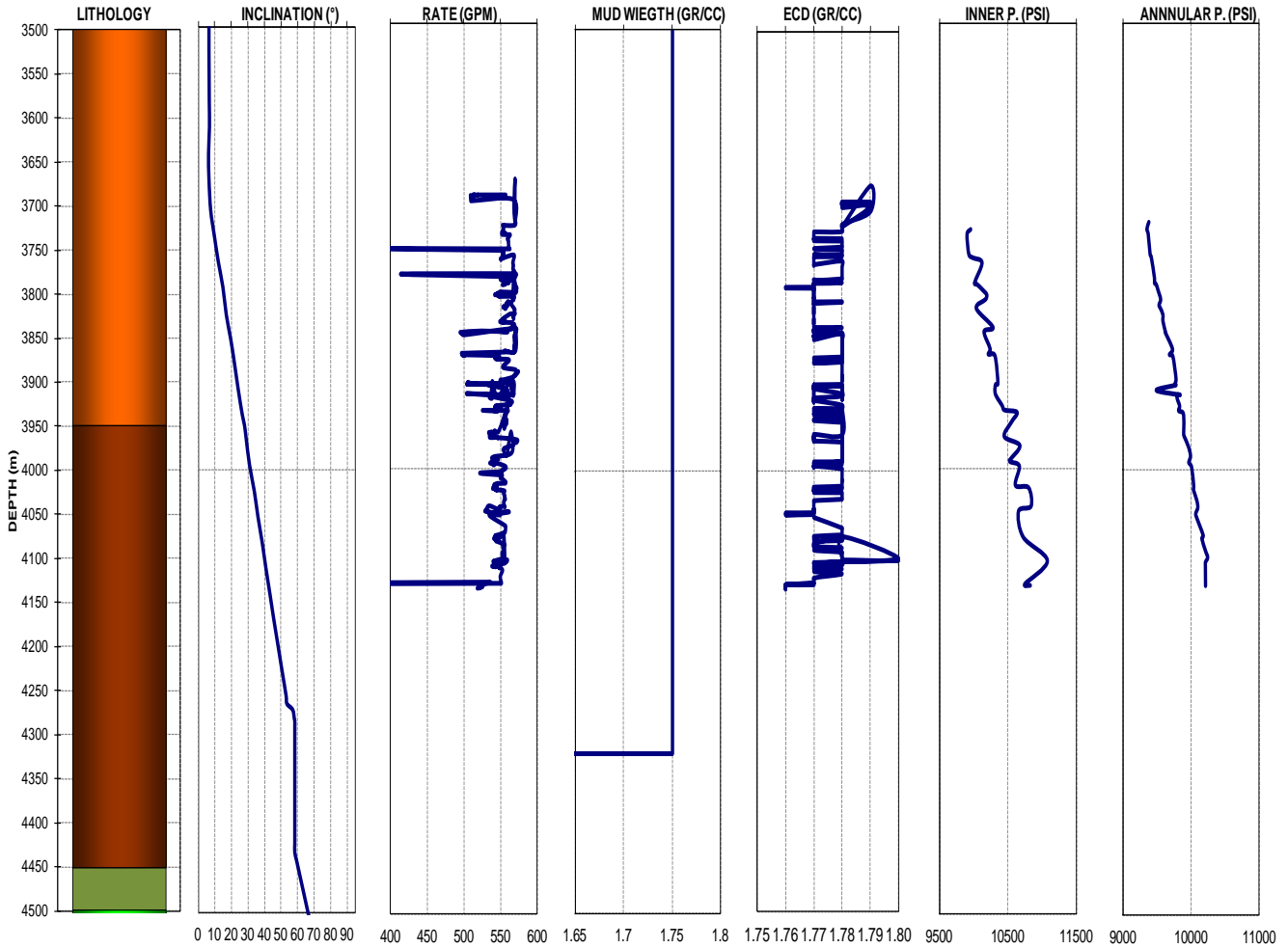


Figure 4.2 Schematic configuration of the well used to calibrate the model.

Three different depths [3693 (m), 3675(m), 3727(m)] and ECDs [1.79 ( $\text{gr}/\text{cm}^3$ ), 1.79( $\text{gr}/\text{cm}^3$ ), 1.77( $\text{gr}/\text{cm}^3$ )] respectively were used to match the observations on pressure and ECD see Table 4.1, the friction factor  $f$  was modified to match the real ECDs at three different depths, the results are shown on figure 4.3.

| Depth (m) | RATE (gpm) | ECD_Data ( $\text{gr}/\text{cm}^3$ ) |
|-----------|------------|--------------------------------------|
| 3693      | 557        | 1.79                                 |
| 3675      | 570        | 1.79                                 |
| 3727      | 553        | 1.77                                 |

Table 4.1 Parameters used for model calibration

### 4.2. – Results

The results have shown that a value of friction factor  $f = 600$  gives a good match on ECD values observed at depths 3693 (m) and 3675 (m), figure 4.3 “top-left”. However in further simulations carried out considering a friction factor  $f = 600$  the model shows a development of gas velocity profile below the injection point which is inconsistency with the physics of fluid flow, since liquid is being pumped from the bottom of the well towards the surface and the gas introduced at the injection point should follow the liquid on its way up.

This behavior of the gas can be explained if we look at equation (7) from chapter 2 “Development of the model” which allows introducing friction and gravity forces in the system ( $q = -Fu_M - gm$  with  $F = f\mu_M$ ), we can observe that the friction factor  $f$  is immerse in equation (7), which suggest that  $f$  is affecting the amount of friction in the system; now if we look at equation (8) which describes the friction gradient in the system ( $q_f = \frac{2f_f}{D-d}\rho_M u_M |u_M|$ ) we can observe that by reducing the friction factor  $f$  the friction effect will be reduced,

furthermore solving for mixture velocity from the third equation of system (10)  $u_M = -\frac{1}{F}P_x - \frac{g}{F}m$ , we can

observe that a reduction in friction factor  $f$  creates an increment on the gravitational effects which affect the mixture velocity and also each individual phase velocities. For these reasons a new friction factor has been proposed ( $f = 6000$ ) which allows performing further simulations with the confidence that the physics of fluid flow is modeled correctly, moreover it suggests that further improvements are needed in terms of model calibration which can be a good opportunity to subsequent analysis

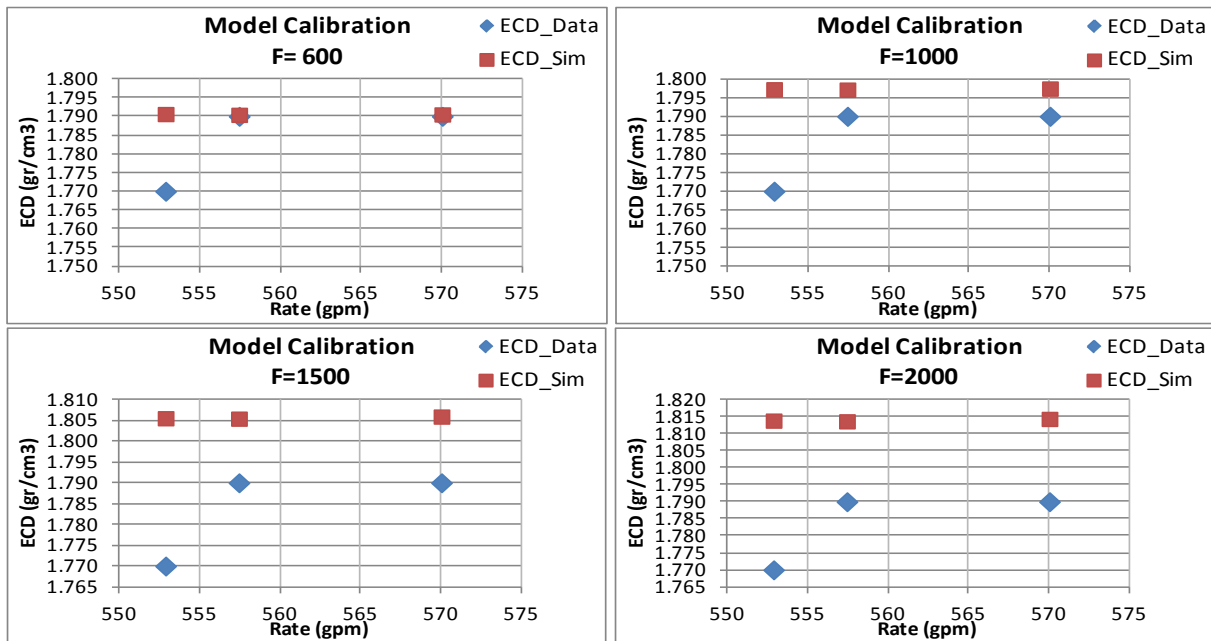


Figure 4.3 Sensitivity analysis to determine the calibrated value of friction factor to be used in further simulation, “blue” points represent actual ECD readings, “red” points represent results given by simulations.



### 5. – Numerical Simulations (directional geometry)

#### 5.1. – Directional well path

The simulations have been performed with a directional well path of 82° of final inclination, a kick off point (KOP) at 3780 (m) has been selected, a build up rate (BUR) of 3°/30m has been used for the first build up section, until the well reaches an inclination of 60° at 4380 (m), and a second build up rate (BUR) of 2.5°/30m until the well reaches a final inclination of 82° at 4660 (m); there after the inclination is kept constant until the end of the trajectory 5000 (m) measured depth , giving a total displacement of 880 (m) and a horizontal section of 350 (m). The modification of the friction factor  $f$  has been done and from this point the analysis is performed using a value of  $f = 6000$ .

The well path details are shown in Fig 5.0.

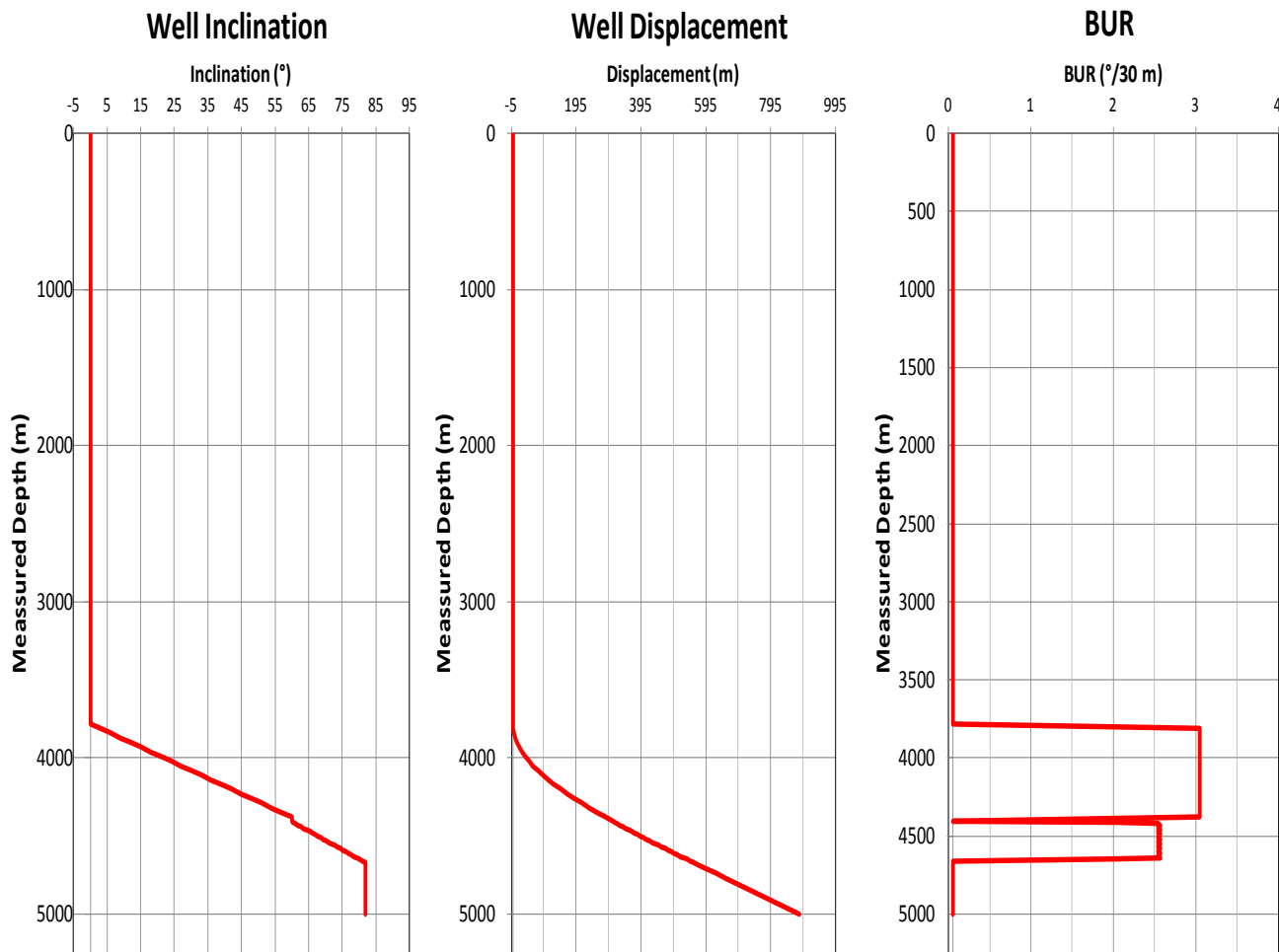


Figure 5.0 Directional well path, well inclination (°) "left", well displacement (m) "middle", BUR (°/30m) "right".

### 5.2. – Wellbore architecture

The following casings setups have been considered for the numerical simulations. The “left” well configuration has been used to model the concentric nitrogen injection whereas the “right” configuration has been used to model the direct nitrogen injection.

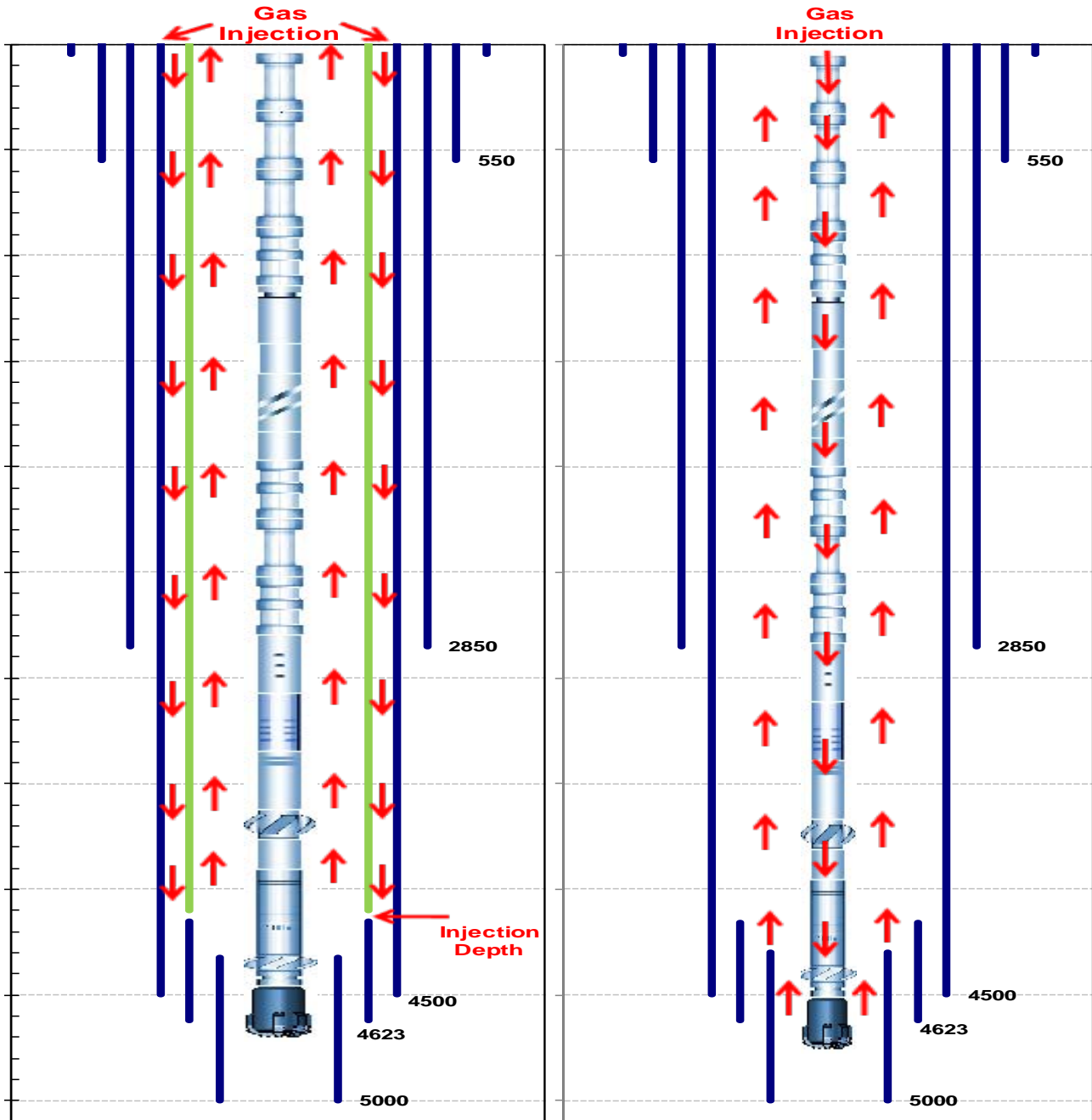


Figure 5.1 Well architecture; concentric nitrogen injection “left”, direct nitrogen Injection “right”

### 5.3. – Specification of parameters

Table 5.1 gives the details of the parameters used in the numerical simulation for the horizontal well. The new friction factor  $f = 6000$ , has been included in this section and an increment on liquid viscosity has been done to avoid issues related with stability of the model.

|                   |         |
|-------------------|---------|
| $\rho_{L,0}$ (kg) | 920     |
| $p_0$ (Pa)        | $10^5$  |
| $a_L$ (m/s)       | 1000    |
| $a_G$ (m/s)       | 316.3   |
| $f$ ( )           | 6000    |
| $\mu_L$ (Pa-s)    | 1.0     |
| $\mu_G$ (Pa-s)    | 0.00005 |
| $L$ (m)           | 5000    |
| $N$ ( )           | 40      |

Table 5.1 Parameters used for the numerical examples (Directional Well)

### 5.4. – Variation of Injection point

In this chapter we would like to investigate the role played by the position of injection point “x” by running different simulations within the period  $[0, T]$ , we will make particular emphasis on the differences observed between a vertical well previously studied and the new directional geometry, we set constant liquid and gas injection rate at the bottom of the well, and we will vary the injection point “x” considering two different positions; The time of the simulation has been reduced from  $T = 10000$ (s) to  $T = 8000$  (s), In other words:

Constant parameters:

- $T = 8000$  (s), (Simulation time)
- $q_L = 400$  (kg/m<sup>2</sup> s), (Flow rate of liquid/mud)
- $q_G = 0.5$  (kg/m<sup>2</sup> s) , (Flow rate of gas)

And we will vary the injection point considering two different positions

- $x_1 = 500$  (m)
- $x_2 = 3000$  (m)

General observations:

We now consider a directional well path with a final inclination of  $82^\circ$ , see figure 5.0; the initial state corresponds to a stagnant system with the well completely filled with mud. Liquid is injected at the bottom of the well simulating only circulation trough the drill string, there after gas injection begins at a position dictated by “x”.

Some natural questions include the following:

What would be the difference in terms of initial pressure profile between a vertical and a horizontal well?

- The initial pressure distribution is dictated by the fluid density and the true vertical depth, for instance for the same length of the well  $L=5000$  (m), the bottom hole pressure in a vertical well is larger than in a horizontal well, the geometry plays an important role on gravitational forces, in other words for a horizontal well the hydrostatic pressure will approach to a constant value close to the bottom because the true vertical depth remains constant. We can observe this effect in figure 5.2.

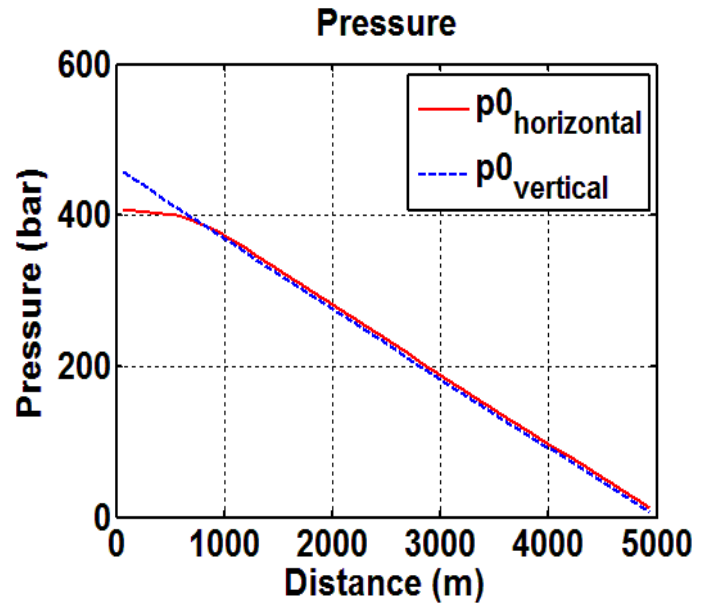


Figure 5.2 Initial pressure profile for a horizontal well

What would one expect when the circulation begins?

- As we see in figure 5.3 a considerable increment in pressure is observed close to the bottom of the well, this is due to the increment in liquid velocity in the horizontal section which will create more friction and therefore an increment in pressure is observed. It's interesting to notice that a gradual increment in pressure is observed as depth is increased. **What would be a possible explanation?**

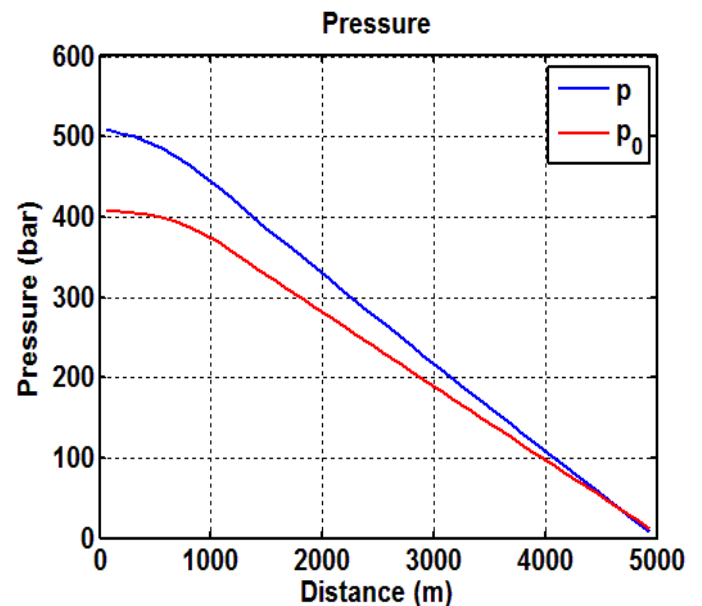


Figure 5.3 Pressure profile for  $T=0$  (s) and  $T=80$  (s).

What can we say about the continuous increment on pressure difference towards the bottom of the well?

- This effect can be explained if we look at the liquid velocity profile along the entire wellbore, we have to remember that up to this point no gas has been injected and the increment in pressure in the system is due to pure friction between the wall pipe and the liquid, then the increment in pressure close to the bottom that we observe in figure 5.3 is due to a increment in fluid velocity caused by the **well geometry**, see well inclination figure 5.0 "left", and for the rest of the wellbore the liquid velocity lowers down towards the surface, see figure 5.4; which creates a reduction in pressure in the rest of the wellbore.

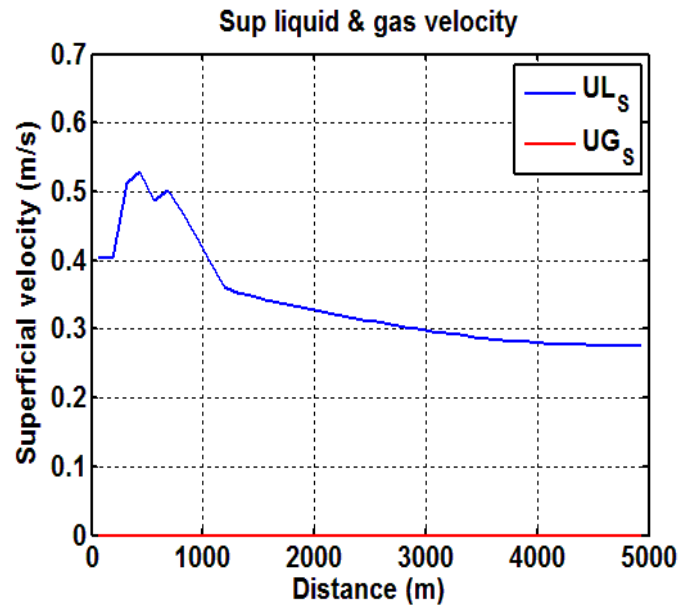


Figure 5.4 Superficial liquid velocity profile for T= 80 (s)

What happens when gas comes into the system? Since the gas is being injected at a position dictated by "x"

- For the case where the injection point is  $x_1 = 500$  (m); right after gas injection we observe:
  - A negligible increment on pressure in the system, Fig 5.5 "left" (dashed line).
  - A minimum increment in liquid velocity along the wellbore Fig 5.5 "middle" (dashed line).
  - An increment of liquid mass rate in both positions bottom and top (Liquid is being pushed out of the system at a higher rate due to the gas influx), Fig 5.5 "right".

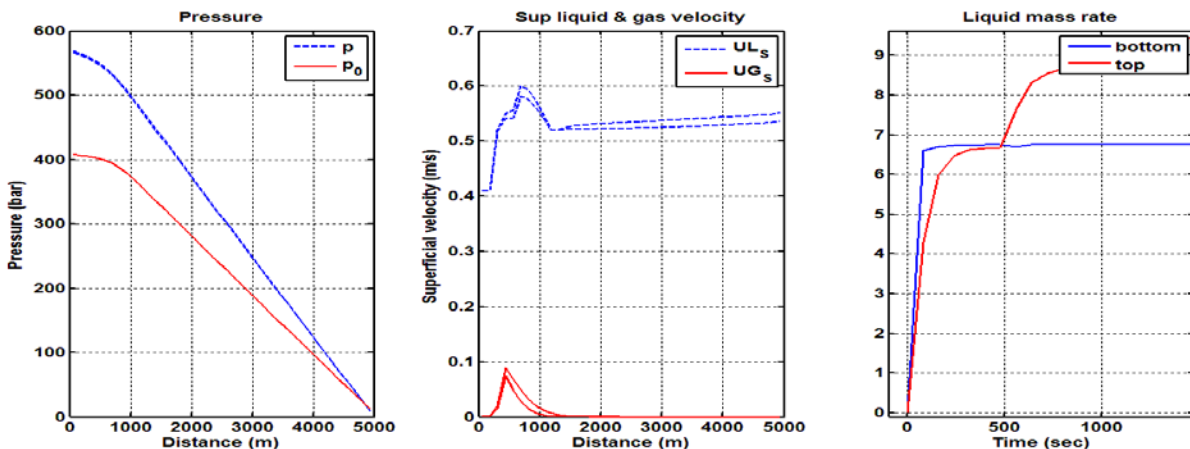


Figure 5.5 Pressure "left", superficial liquid and gas velocities "middle" and liquid mass rate "right" at 140 (s) and 220(s) after gas injection,  $x_1 = 500$  (m) and  $q_G = 0.5$  (kg/m<sup>2</sup> s).

- For the case where the injection point is  $x_2= 3000$  (m); right after gas injection we see:
  - A considerable increment on pressure along the wellbore, Fig 5.6 “left” (dashed line).
  - No increment in liquid velocity in the directional section(1000 m) , but considerable increment of liquid velocity close to the injection point Fig 5.6 “middle” (dashed line).
  - A considerable increment of liquid mass rate at top of the wellbore (Liquid is being expelled out of the system) Fig 5.6 “right”.

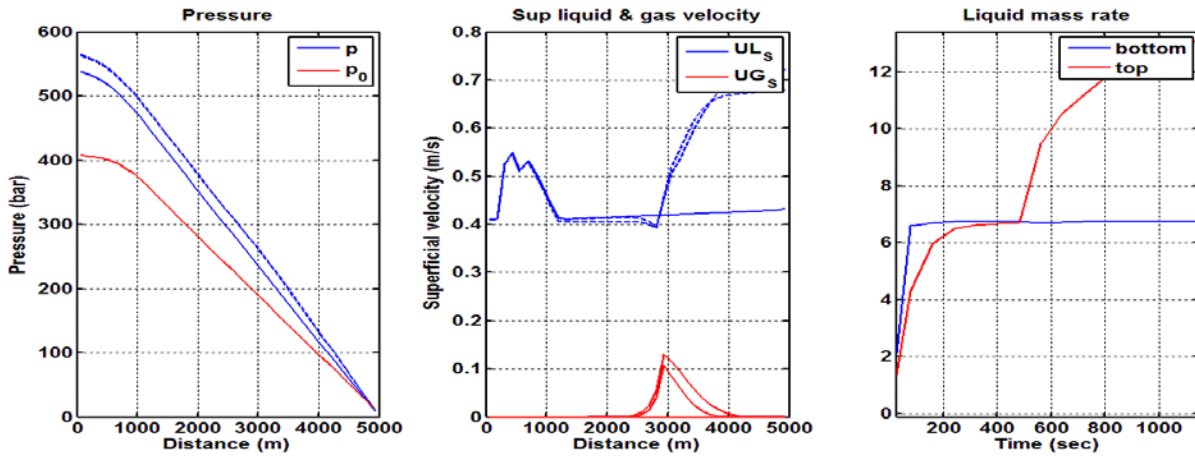


Figure 5.6 Pressure “left”, superficial liquid and gas velocities “middle” and liquid mass rate “right” at 140 (s) and 220(s) after gas injection,  $x_2= 3000$  (m) and  $q_G= 0.5$  (kg/m<sup>2</sup> s).

- We can observe that the liquid velocity profile is the governing parameter for friction at earlier stages (see figure 5.5 and 5.6), we can therefore associate the change in liquid velocity with a change in pressure. For the case where the injection point is  $x_1=500$  (m) it is observed that the influx of gas is not affecting the liquid velocity significantly, this effect can be explained by looking at the wellbore geometry; for this particular case the injection point  $x_1= 500$  coincide with a wellbore inclination of  $\sim 70^\circ$ , see figure 5.0 “left” and the wellbore geometry has a stronger effect in liquid velocity resulting in a minimum boost in liquid velocity created by the gas influx, in other words the increment experienced in liquid velocity is minimum and the effect on pressure increment resulted negligible, see figure 5.5 “left”. On the other hand if we analyze the case where the injection point is  $x_2= 3000$  (m) we can clearly observe a significant increment in liquid velocity close to the gas influx point, performing the same analysis, if we look at the wellbore geometry at  $x_2= 3000$  (m) we may realize that the wellbore has an inclination is  $0^\circ$  (vertical geometry), see figure 5.0 “left”, and the gas influx resulted in a bigger impact in liquid velocity profile, the effect on friction generated by the increment in liquid velocity is more notorious and can be clearly observed in figure 5.6 “left”
- Continuing with the same analysis but now using a different approach; we can observe(see figure 5.5 “left” and “middle”) that in the horizontal and directional section (e.g.  $x_1= 500$  m) the pressure behavior is dominated by friction and the gravity force has minimum effect in pressure response (since the wellbore inclination tends to  $90^\circ$ ), on the other hand for other wellbore configurations where the inclination is significantly different from  $90^\circ$  (e.g.  $x_2=3000$  m ) the gravity effect has a bigger impact on the pressure.

What can we expect if more and more gas comes into the system?

- Eventually the pressure will be lowered because a lighter fluid is displacing a heavier one, up to this point the system is still dominated by hydrostatic forces, it will be demonstrated later on that if we keep injecting gas continuously there will be a point where the pressure will not decrease anymore, we can generally say that the system will change from hydrostatic dominated to friction dominated as stated by Steve Nas in [5]. (See appendix 1, 2 and 3), similar effect is observed in a vertical well, see figure 3.8.

How will the velocity profile be along the wellbore for a horizontal geometry?

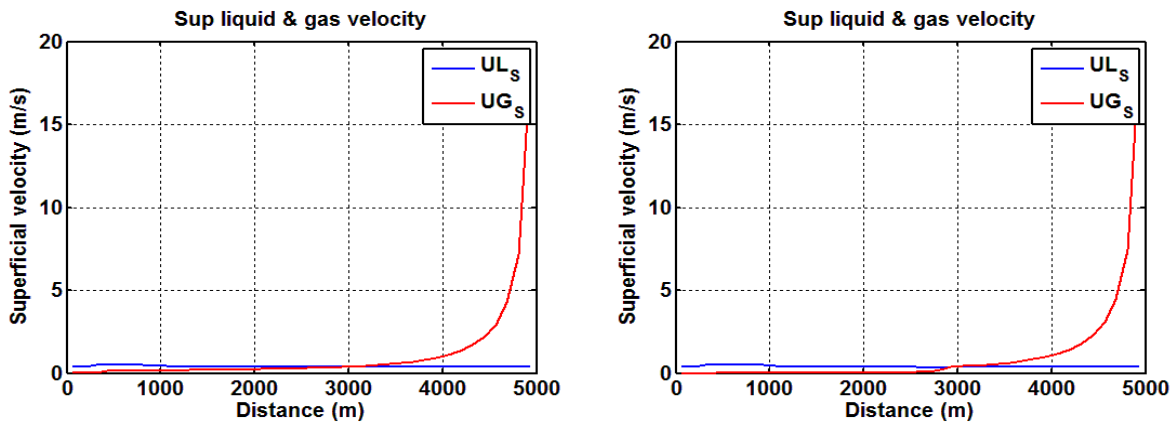


Figure 5.7 Final superficial liquid and gas velocity at the end of the simulation, for  $x_1= 500$  (m) “left”, for  $x_2= 3000$  (m) “right”.  $T= 8000$  (s)

- For both injection points  $x_1= 500$ (m) and  $x_2=3000$ (m) we observe:
  - At early times a system dominated by the geometry of the well, where the highest liquid velocity is observed at the bottom of the well (directional section) and a steady liquid velocity profile after the directional section has been overcome, see figures 5.5 and 5.6 “middle”
  - At late times a typical behavior of the system is reached, gas is being expanded as it comes close to surface creating a continuous increment in velocity and a liquid velocity profile approaching to a steady state profile, see figure 5.7
  - Both injection points ( $x_1=500$  m and  $x_2=3000$  m ) have been produced a similar steady state velocity profile, with a gas velocity value of 18.65 m/s for  $x_1= 500$  m and 19.22 m/s for  $x_2= 3000$  m, in the last cell of the model.

How will pressure be affected if the injection point is changed from  $x_1=500$  to  $x_2= 3000$  (m)?

Main observations: (see figure 5.8.)

- |                   |                              |                    |                              |
|-------------------|------------------------------|--------------------|------------------------------|
| • $x_1 = 500$ (m) |                              | • $x_2 = 3000$ (m) |                              |
| - ECD top         | = 590.0 (kg/m <sup>3</sup> ) | - ECD top          | = 571.3 (kg/m <sup>3</sup> ) |
| - ECD bottom      | = 915.5 (kg/m <sup>3</sup> ) | - ECD bottom       | = 931.3 (kg/m <sup>3</sup> ) |
| - Pressure top    | = 3.617 (bar)                | - Pressure top     | = 3.50 (bar)                 |
| - Pressure bottom | = 443.4 (bar)                | - Pressure bottom  | = 451.1 (bar)                |

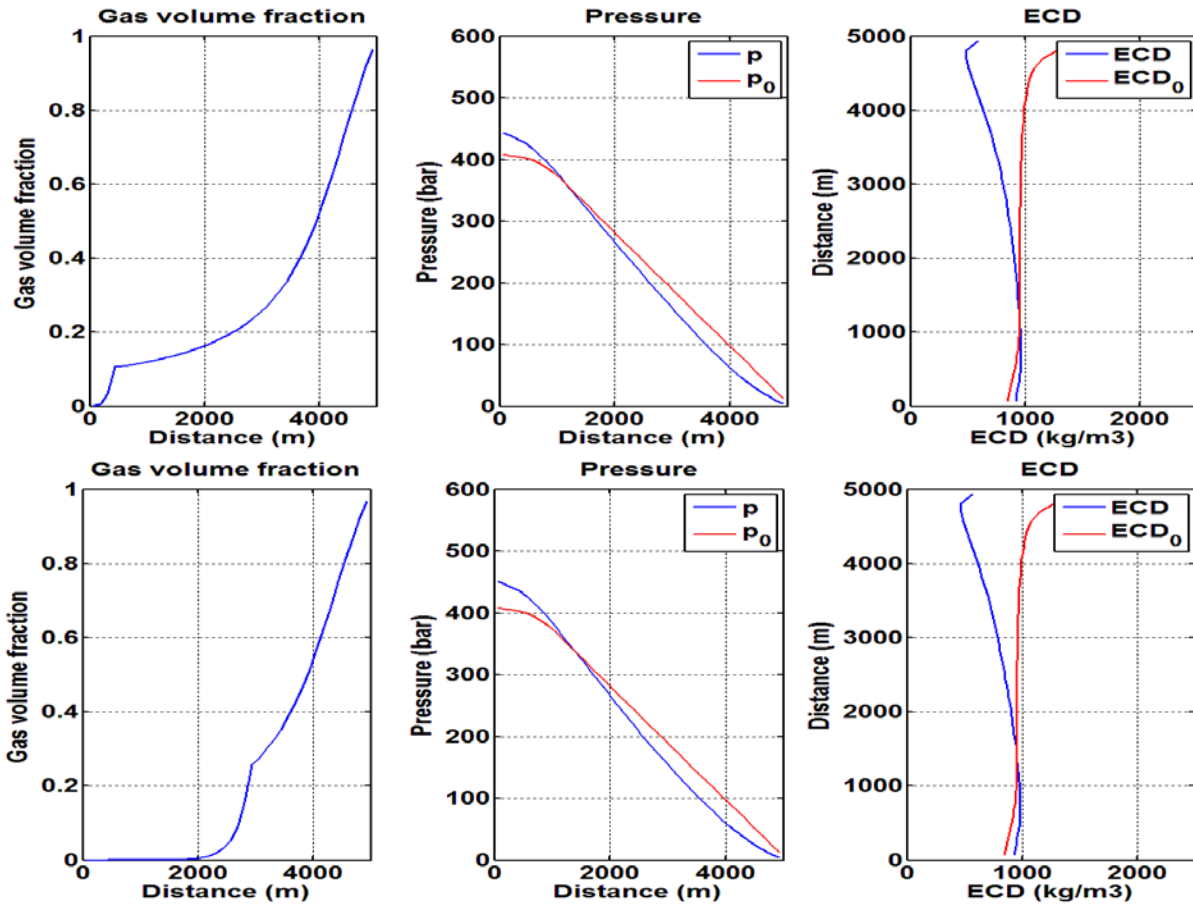


Figure 5.8 Gas fraction “left”, pressure “middle” and ECD “right” at  $T = 8000$  (s) for  $x_1 = 500$ (m) “top” and  $x_2 = 3000$ (m) “bottom”.

Comments

- For the case of a directional well we can observe that the injection point apparently have a minimum impact on pressure distribution; For this particular case the injection rate was  $q_G = 0.5$  (kg/m<sup>2</sup> s), we will demonstrate later on that if we select a lower injection point, a lower the pressure at bottom of the well will be obtained, as long as the system is dominated by gravitational forces, see appendix 1 and 2.

5.5. – Flow regimes for different injection points

I would like to recall once again that the distribution parameter ( $c_0$ ) and the drift velocity ( $c_1$ ) described in (4) tends to change depending on the flow regime as stated by by J.Enrique Julia and Takashi Hibiki in [19]. It has been adopted constant values but it is important to be aware of this, moreover it gives room for improvement.

In the following we will make only consider the two upper points to evaluate the possible flow regime using the flow map provided in the paper published by J. Enrique Julia and Takashi Hibiki (2011) [19], since the correlation given is valid only for vertical annuli, and we will stick to the classical approach proposed by Kelessidis and Duckler (1989) reported in [19].



We have selected two different arbitrary positions to evaluate the flow patterns, as shown in Fig 5.9

- Half way from the injection point to surface (Mid)
- 250 m below surface (Top)

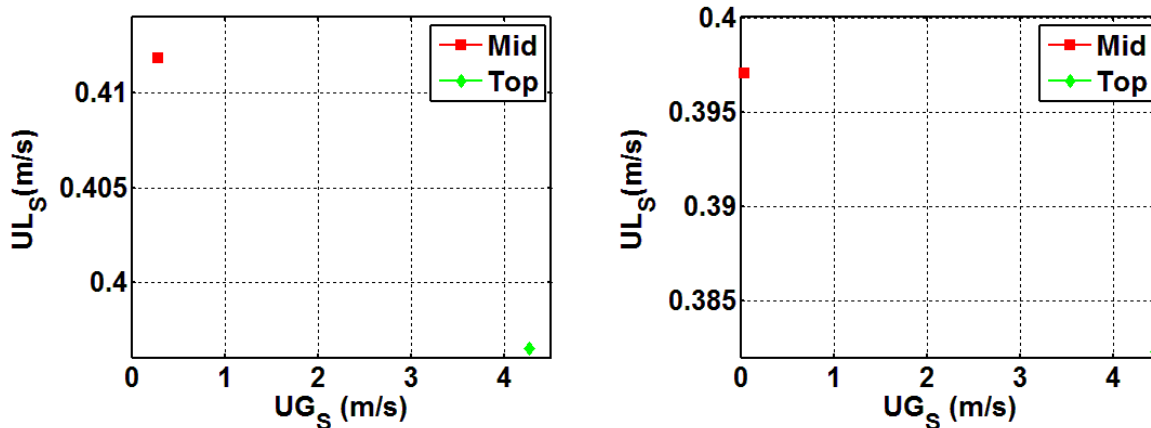


Figure 5.9 Superficial liquid and gas velocities at three different positions; *left figure* corresponds to an injection point  $x_1= 500$  (m) whereas *right figure* corresponds to an injection point  $x_2= 3000$  (m). Final time,  $T = 8000$  (s).

Based on the final reading of superficial flow velocities given by the simulation and the flow map published by J. Enrique Julia and Takashi Hibiki (2011) [19], Fig 3.6. We can then suggest the following flow patterns.

Injection point  $x_1= 500\text{m}$

|     | $U_{L_s}$ (m/s) | $U_{G_s}$ (m/s) | Flow |
|-----|-----------------|-----------------|------|
| Mid | 0.4118          | 0.2871          | Slug |
| Top | 0.3965          | 4.266           | Slug |

Injection point  $x_2= 3000\text{m}$

|     | $U_{L_s}$ (m/s) | $U_{G_s}$ (m/s) | Flow        |
|-----|-----------------|-----------------|-------------|
| Mid | 0.3971          | 0.03891         | Bubbly-Slug |
| Top | 0.3823          | 4.4530          | Churn       |

General conclusions for injection point analysis:

- At early times the pressure distribution is highly influenced by the well geometry, whereas at late times the injection rate as well as the well geometry has a considerable impact on the pressure profile along the system.
- An increment in pressure (i.e. friction) is generated in the directional section, due to an increment of liquid fluid velocity.
- In terms of velocity profile we observe higher velocity of gas close surface for a vertical well when the injection point is closest to the surface, whereas for a horizontal geometry the simulation show the same gas velocity close to surface for both injection points ( $x_1= 500$  m and  $x_2= 3000$  m)
- Final pressure profile is also dependent on liquid rate; we can generally state that bigger liquid rate produce a higher pressure profile

## 5.6. – Variation of Injection rate

In this section we aim to answer some questions regarding the main differences observed when we change the rate and the injection point compared to the previous analysis for a vertical well, by running different simulations within the period  $[0, T]$ , keeping constant liquid injection rate at the bottom of the well and the injection point  $x=500$  (m). We have reduced the time of the total simulation from  $T=10000$  (s) to  $T=8000$  (s).

Constant parameters:

- $T = 8000$  (s), (Simulation time)
- $q_L = 400$  (kg/m<sup>3</sup> s), (Flow rate of liquid/mud)
- $x = 500$  (m), (Position of injection)

We vary the gas injection rate, considering the following options:

- $q_G = 0.5$  (kg/m<sup>2</sup> s)
- $q_G = 1.0$  (kg/m<sup>2</sup> s)
- $q_G = 2.0$  (kg/m<sup>2</sup> s)

General observations:

We consider a directional well path with a final inclination of  $82^\circ$ , see figure 5.1; the initial state corresponds to a stagnant system with the well completely filled with mud. Liquid is pumped at the bottom of the well simulating single phase circulation, there after gas injection begins at a fixed distance  $x = 500$  (m) from the bottom of the well.

### How is the pressure affected by injection rate?

- According to the simulations for liquid rate bigger than 125 gal/min (see appendix 1, 2 and 3), the pressure in the system is increased when we increase the gas injection rate up to 1.0 (kg/m<sup>2</sup> s) roughly speaking, there after the pressure in the bottom of the wellbore tends to decrease because the system at this stage is highly influenced by gravity forces, eventually the pressure will stabilize at high injection rates, at that point the system will have changed to friction dominated.

### What is the role played by gas injection rate in terms of pressure distribution?

- As stated by Steve Nas in [5], as more gas is being injected the hydrostatic pressure is reduced with gas being compressed at the bottom of the well and gas expansion as it comes to surface.
- It has been also demonstrated that as gas comes into the system an increment in pressure generated by rise in mixture velocity followed by a reduction in hydrostatic pressure as long as sufficient gas has come in the system, this statement is valid as long as the system is in the hydrostatic dominated zone.

We observe a reduction in pressure as the gas injection rate increases, the same effect on ECD is observed on figure 5.11; Figure 5.10 shows the final pressure distribution along the wellbore at the end of the simulation,  $T=8000$  (s).

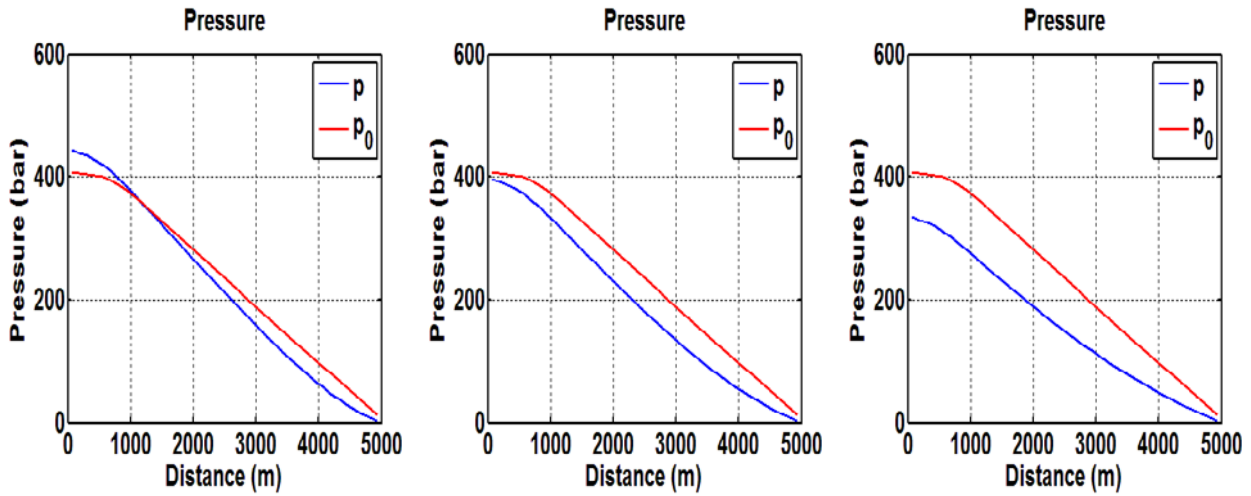


Figure 5.10 Final pressure distribution for three different gas injection rates,  $q_G = 0.5 \text{ (kg/m}^2 \text{ s)}$  "left",  $q_G = 1.0 \text{ (kg/m}^2 \text{ s)}$  "middle",  $q_G = 2.0 \text{ (kg/m}^2 \text{ s)}$  "right",  $x = 500 \text{ (m)}$ ,  $T = 8000 \text{ (s)}$ .

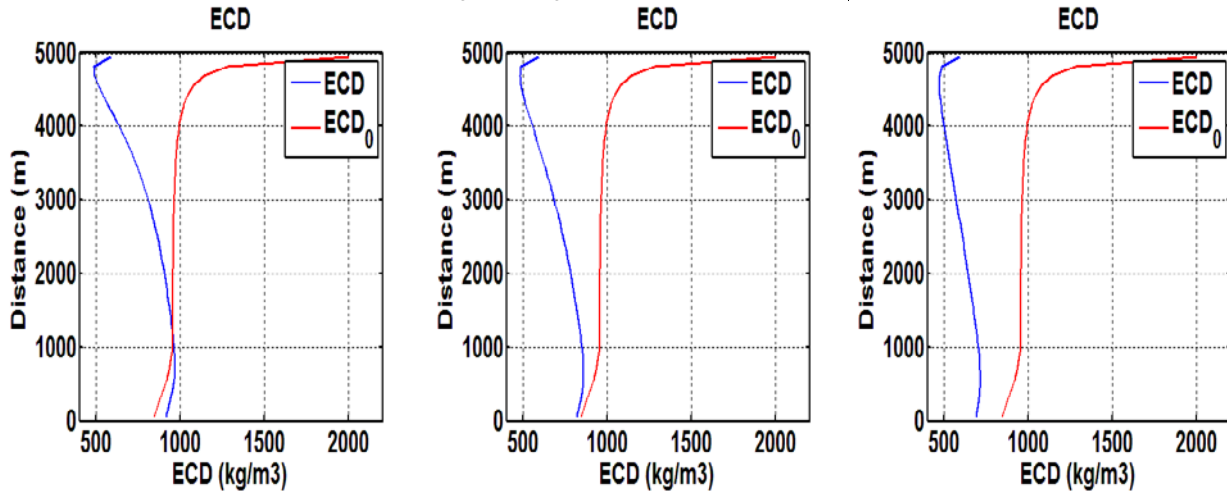


Figure 5.11 Final ECD distribution for three different gas injection rates,  $q_G = 0.5 \text{ (kg/m}^2 \text{ s)}$  "left",  $q_G = 1.0 \text{ (kg/m}^2 \text{ s)}$  "middle",  $q_G = 2.0 \text{ (kg/m}^2 \text{ s)}$  "right",  $x = 500 \text{ (m)}$ ,  $T = 8000 \text{ (s)}$ .

So far we have explained what happens in the system when we increase the injection rate, but we have to recall that we have used only three different rates in the simulations (i.e.  $q_G = 0.5 \text{ (kg/m}^2 \text{ s)}$ ,  $q_G = 1.0 \text{ (kg/m}^2 \text{ s)}$ ,  $q_G = 2.0 \text{ (kg/m}^2 \text{ s)}$ ), then a natural question would be:

**What will happen if the gas injection rate is constantly increased?**

We will consider the following assumptions for the analysis:

- A fixed injection point  $x = 1000 \text{ (m)}$ .
- For simplicity only a vertical well will be considered and the bottom hole pressure will be analyzed.
- Four different liquid rates ( 125 (gpm), 150 (gpm), 200 (gpm), 225 (gpm) )

And we will make use of figure A1.1.6 presented in Appendix 1, shown below.

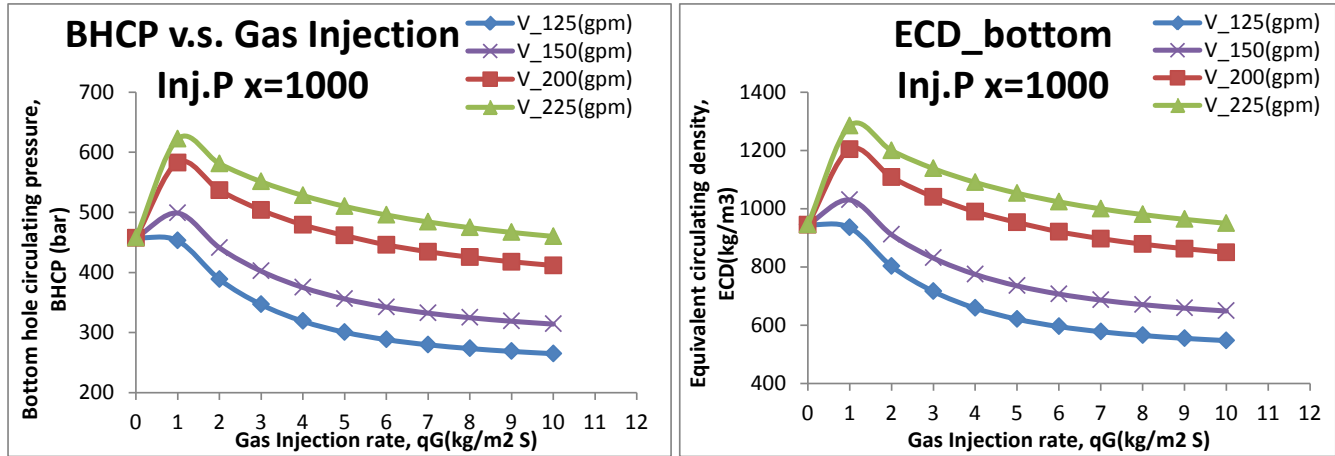


Figure A1.1.6 Sensitivity analysis of gas-liquid injection rate for a vertical well @ bottom, "Injection point  $x= 1000$  (m)",  $f = 6000$

Main observations:

- An increment in pressure is observed in the system as soon as we start gas injection up to an approximately value of gas injection rate of  $q_G = 1.0$  (kg/m<sup>2</sup> s). This pressure increment is caused by an increment of friction in the system, as explained before.
- A transition period where a decrement in pressure is observed after  $q_G = 1.0$  (kg/m<sup>2</sup> s), this is a clear indication that the system is strongly affected by hydrostatic forces.
- A stabilized pressure at late times. This indicates that the system has reached the zone where it becomes dominated by friction forces.
- The transition from hydrostatic-friction dominated system depends also on the liquid rate, (i.e. for lower liquid injection rates, the time is shorter whereas for higher liquid injection rates the transition time is larger).

### 5.7. - Flow regimes for different injection rates

For this directional geometry we have produced the same kind of plots for superficial liquid and gas velocity in three different positions along the wellbore but we will only consider the two upper most points and by means of flow regime maps we will try to determine the flow pattern, In the following we will keep our analysis using the classic approach proposed by **Kelessidis and Duckler** (1989) reported in [19].

Only two different arbitrary positions have been selected to evaluate the flow patterns

- Half way from the injection point to surface (Mid)
- 250 m below surface (Top)

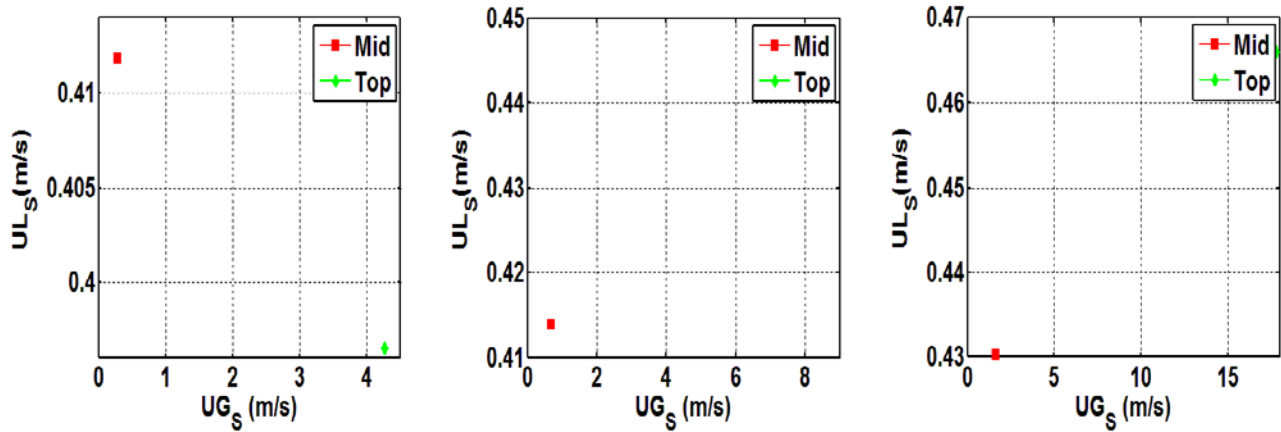


Figure 5.12 Final superficial velocities  $u_{LS}$ ,  $u_{GS}$  for three different positions along the wellbore,  $x= 500$  (m),  $q_G= 0.5$  (kg/m<sup>2</sup>s) "left",  $q_G= 1.0$  (kg/m<sup>2</sup> s) "middle",  $q_G= 2.0$  (kg/m<sup>2</sup> s) "right".

The following flow patterns have been suggested, based on simulation results and correlation proposed by Kelessidis and Duckler (1989) reported in [19].

–  $q_G= 0.5$  (kg/m<sup>2</sup> s), see Fig 3.9 "left"

|     | $U_{LS}$ (m/s) | $U_{GS}$ (m/s) | Flow P. |
|-----|----------------|----------------|---------|
| Mid | 0.4118         | 0.2871         | Slug    |
| Top | 0.3965         | 4.2660         | Churn   |

–  $q_G= 1.0$  (kg/m<sup>2</sup> s), see Fig 3.9 "middle"

|     | $U_{LS}$ (m/s) | $U_{GS}$ (m/s) | Flow P. |
|-----|----------------|----------------|---------|
| Mid | 0.4139         | 0.6748         | Slug    |
| Top | 0.4423         | 8.7160         | Churn   |

–  $q_G= 2.0$  (kg/m<sup>2</sup> s), see Fig 3.9 "right"

|     | $U_{LS}$ (m/s) | $U_{GS}$ (m/s) | Flow P. |
|-----|----------------|----------------|---------|
| Mid | 0.4303         | 1.6520         | Churn   |
| Top | 0.4660         | 17.820         | Annular |

Main observations:

- We can generally say that higher gas injection rate produces a lower equivalent circulating density ECD at the bottom of the well, as long as the system is strongly affected by gravity forces, once the system becomes friction dominated higher gas injection rates will not an reduction of pressure in the system.
- Lower gas injection rate produces a faster stationary solution.
- Numerical results have shown that a value of gas injection rate  $q_G = 1.0$  (kg/m<sup>2</sup> s) is the starting point where the stationary pressure response of the system shows a decrement at the two positions analyzed (bottom of the wellbore and casing shoe), see appendix 1, 2 and 3; whereas for values higher than  $q_G = 1.0$  (kg/m<sup>2</sup> s) the stationary solution of the system shows a decrement in pressure for both positions (bottom of the wellbore and casing shoe).
- The transition period of the system from being dominated by gravitational force to friction forces depends also on the liquid injection rate, (i.e. for lower liquid injection rates, the time is shorter whereas for higher liquid injection rates the transition time is larger).
- A stabilized pressure profile at late times is an indication that the system has reached the zone where it becomes dominated by friction.
- Flow pattern predictions for both positions (Middle way from injection point to surface and 250(m) below surface) agree for the first two injection rates [ $q_G = 0.5$  (kg/m<sup>2</sup> s) and  $q_G = 1.0$  (kg/m<sup>2</sup> s)]; for the last injection rate  $q_G = 2.0$  (kg/m<sup>2</sup> s) the results have shown different outcomes because more gas has been introduced in the system and therefore more gas is being expanded as it flows upward towards the surface.

## Appendix 1 – Sensitivity of liquid-gas rate at bottom hole

In this section different simulations have been performed considering both friction factors ( $f = 600$  and  $f = 6000$ ), several gas injection rates were simulated along with different liquid injection rates.

For the case where  $f = 600$  the simulations include the following liquid rates:

- 200 (gmp)
- 250 (gmp)
- 300 (gmp)
- 400 (gmp)
- 500 (gmp)

For the case where  $f = 6000$  the simulations consider the following liquid rates:

- 125 (gmp)
- 150 (gmp)
- 200 (gmp)
- 225 (gmp)

The purpose of appendixes 1 and 2 is to give the reader a set of different results in terms of equivalent circulating density (ECD) and pressure at two different positions (bottom hole and previous casing shoe), therefore if there is need to know what would be the expected pressure or ECD at bottom hole,  $x_1 = 500$  (m),  $x_2 = 1000$  (m),  $x_3 = 1500$  (m) and  $x_4 = 2000$  (m) for a given configuration (vertical well and horizontal well) the reader may find it on appendixes 1 and 2.

We can observe in all figures from appendix 1, 2 and 3 that a higher friction factor ( $f$ ) produces more friction in the system, reflected in the stationary pressure solution at the points of interest (bottom hole and shoe) for both well geometries (vertical well and horizontal).

### A1. – Analysis of pressures and ECDs at bottom hole

The constant monitoring and analysis of pressure at the bottom of the well in real time is particularly important during drilling operations, simply because we want to keep the mud weight and equivalent circulating density within the operational window normally dictated by the pore pressure and the fracture pressure/lost circulation.

The analysis may be divided as follows:

#### A1.1 Vertical Well

- **Direct nitrogen injection**

In the direct injection set up, nitrogen is injected directly through the drill string; as mention previously this method has limitations in terms of the gas injection rate that the tools can handle and issues with communication of parameters from the MWD tool to the surface.

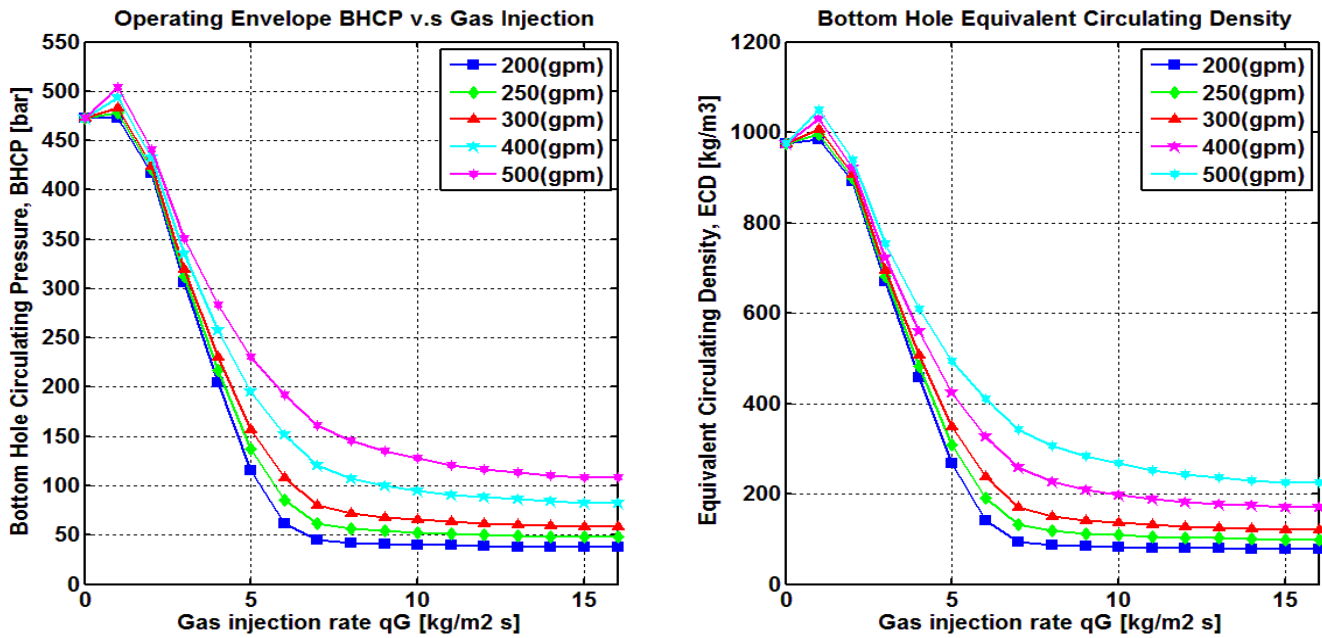


Figure A.1.1 Sensitivity analysis of gas-liquid injection rate for a vertical well @ bottom, "Direct Nitrogen Injection",  $f = 600$

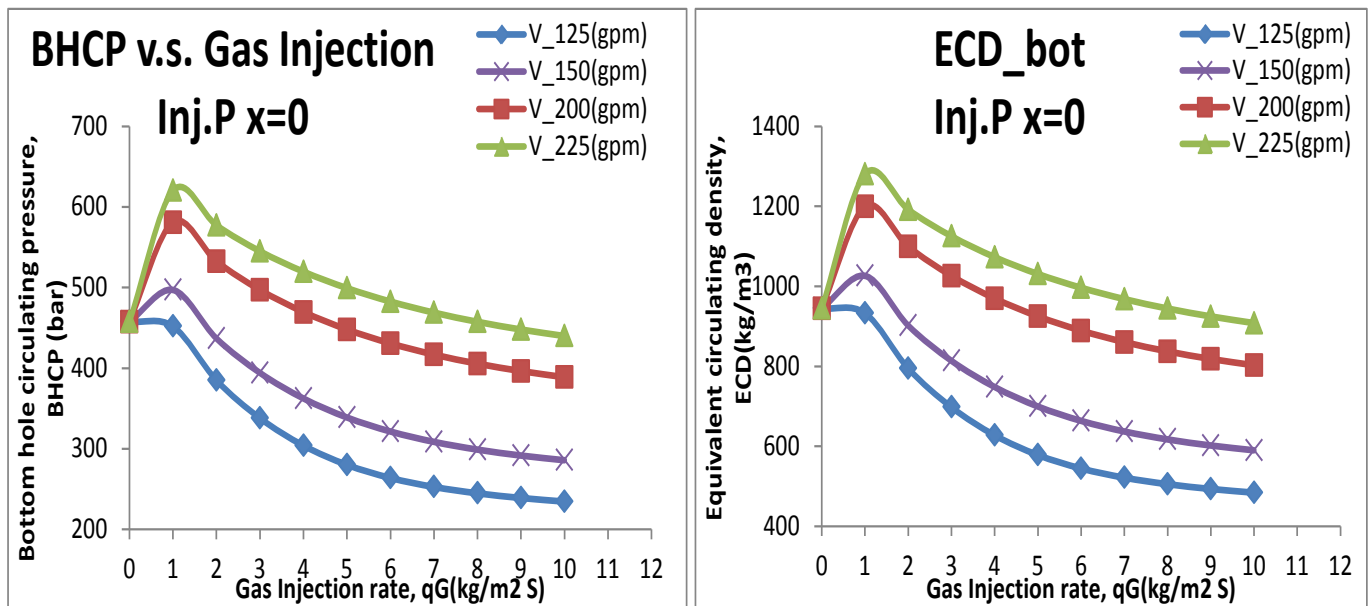


Figure A1.1.2 Sensitivity analysis of gas-liquid injection rate for a vertical well @ bottom, "Direct Nitrogen Injection",  $f = 6000$



– Injection point  $x_1 = 500$  (m)

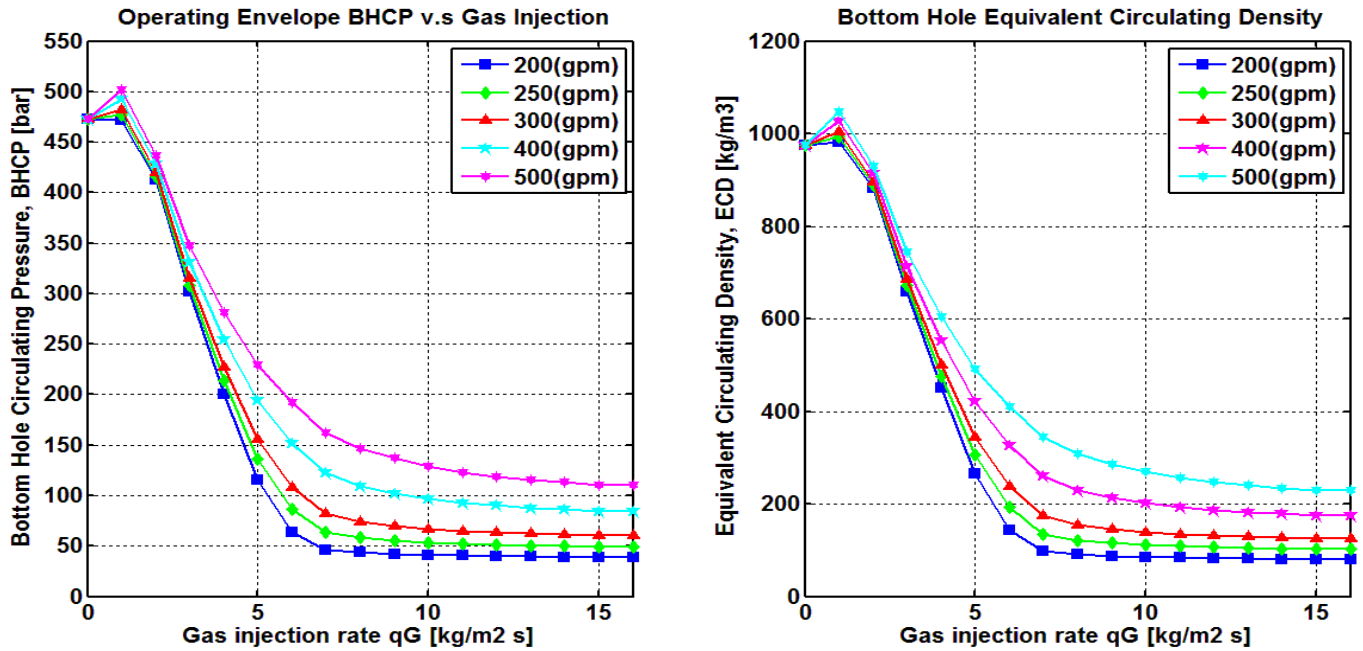


Figure A1.1.3 Sensitivity analysis of gas-liquid injection rate for a vertical well @ bottom, "Injection point  $x_1 = 500$  (m)",  $f = 600$

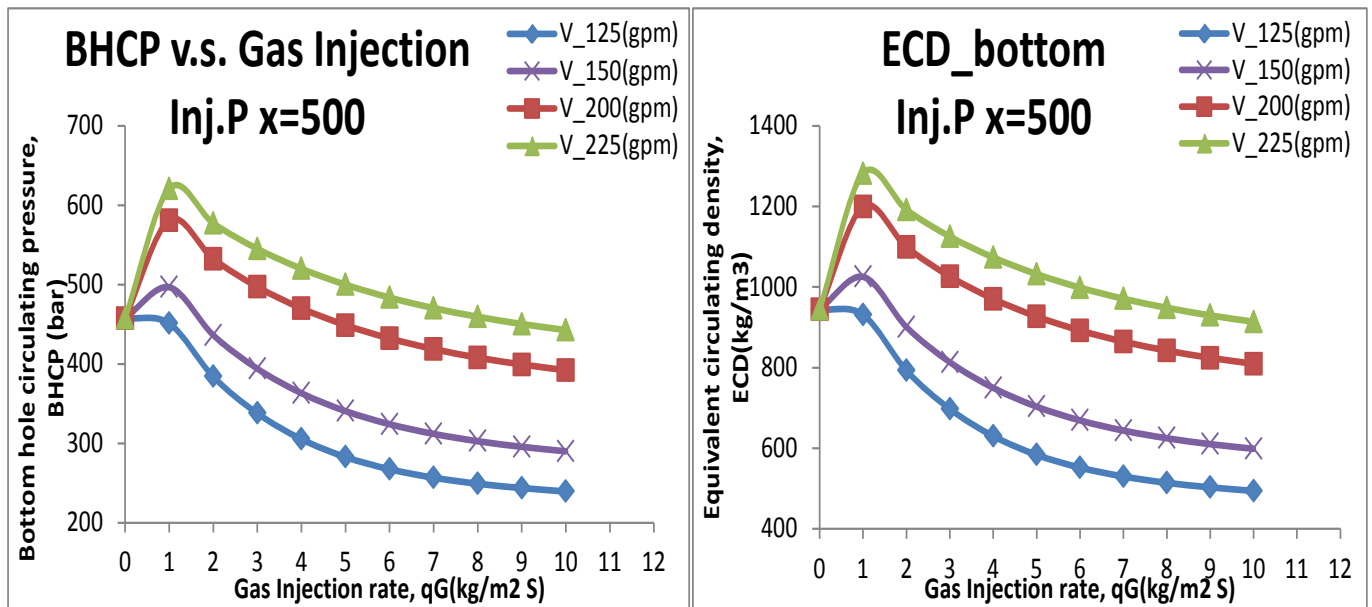


Figure A1.1.4 Sensitivity analysis of gas-liquid injection rate for a vertical well @ bottom, "Injection point  $x_1 = 500$  (m)",  $f = 6000$

– Injection point  $x_2 = 1000$  (m)

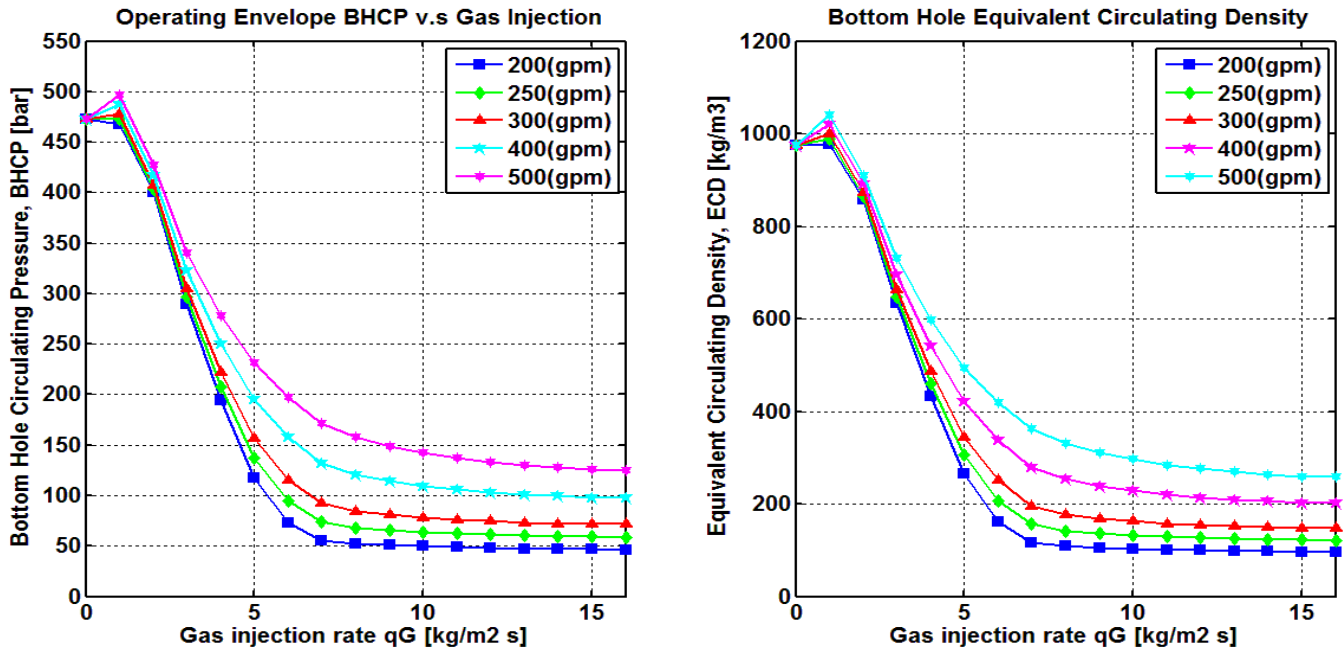


Figure A1.1.5 Sensitivity analysis of gas-liquid injection rate for a vertical well @ bottom, "Injection point  $x_2= 1000$  (m)",  $f = 600$

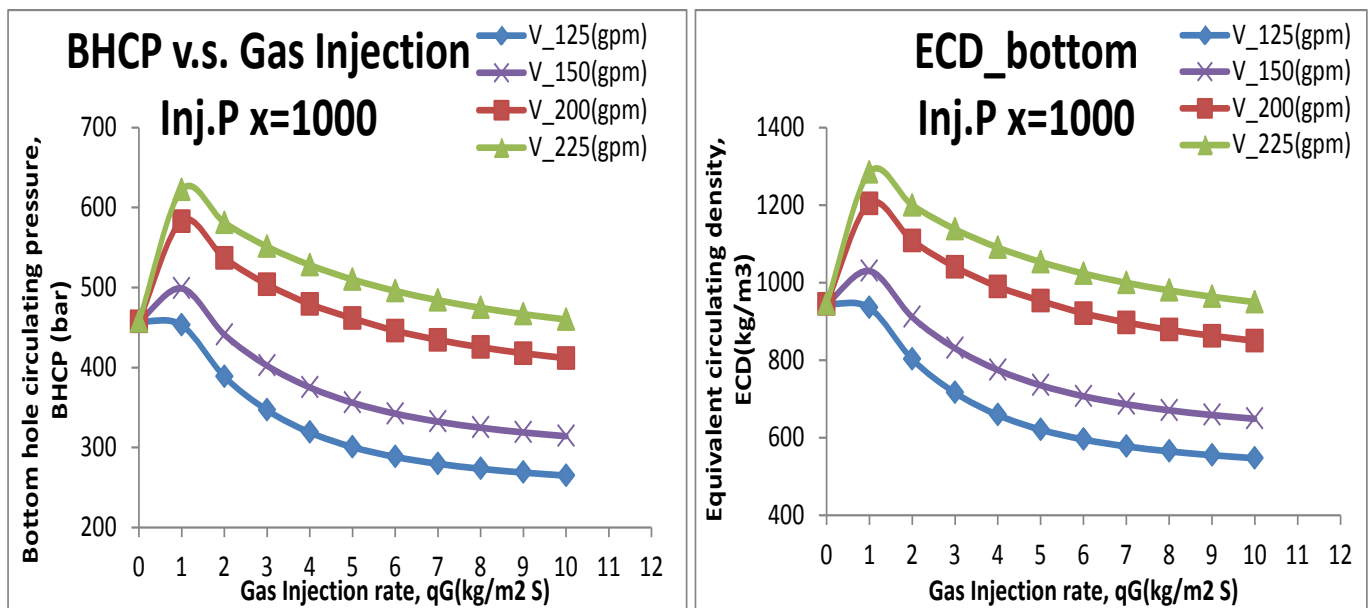


Figure A1.1.6 Sensitivity analysis of gas-liquid injection rate for a vertical well @ bottom, "Injection point  $x_2= 1000$  (m)",  $f = 6000$

– Injection point  $x_3 = 1500$  (m)

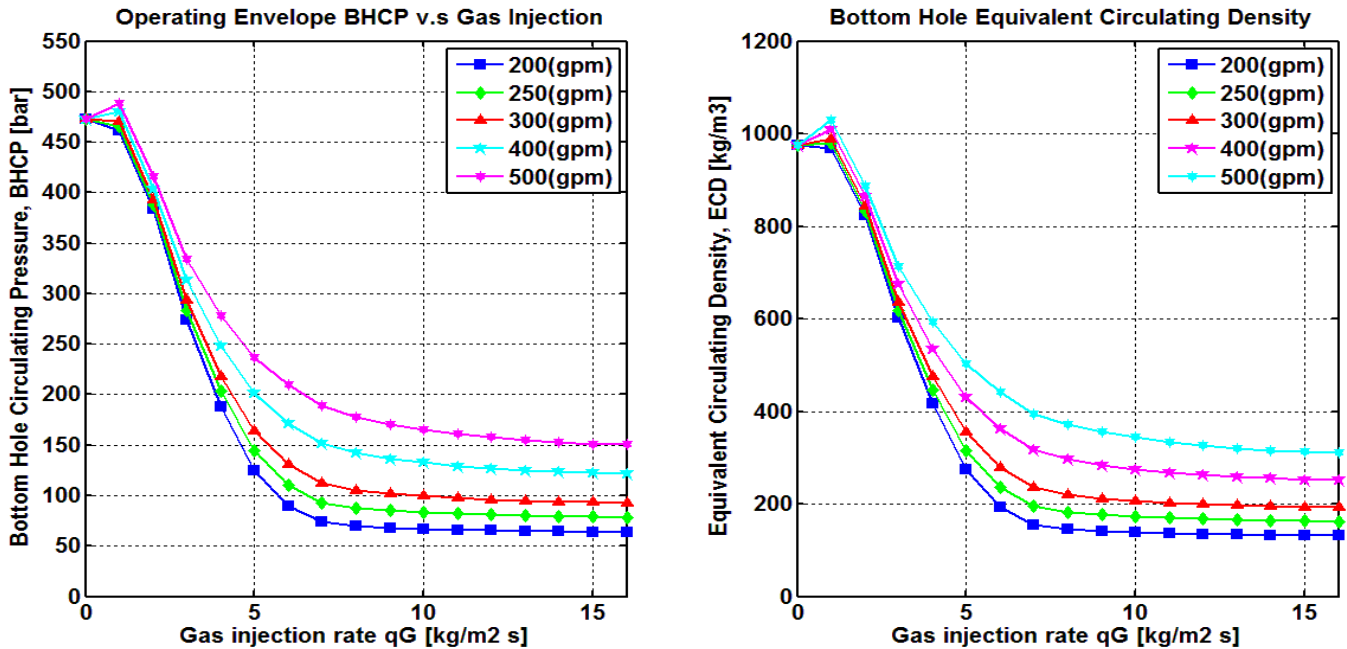


Figure A1.1.7 Sensitivity analysis of gas-liquid injection rate for a vertical well @ bottom, "Injection point  $x_3=1500$  (m)",  $f = 600$

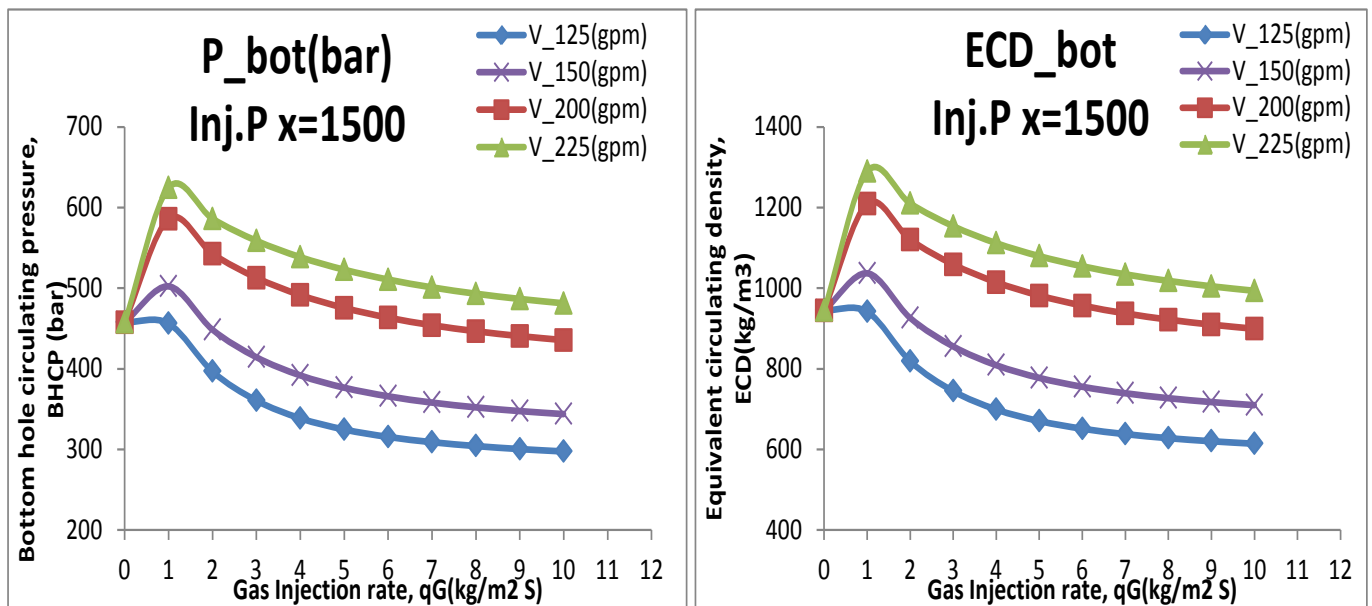


Figure A1.1.8 Sensitivity analysis of gas-liquid injection rate for a vertical well @ bottom, "Injection point  $x_3=1500$  (m)",  $f = 6000$

– Injection point  $x_4 = 2000$  (m)

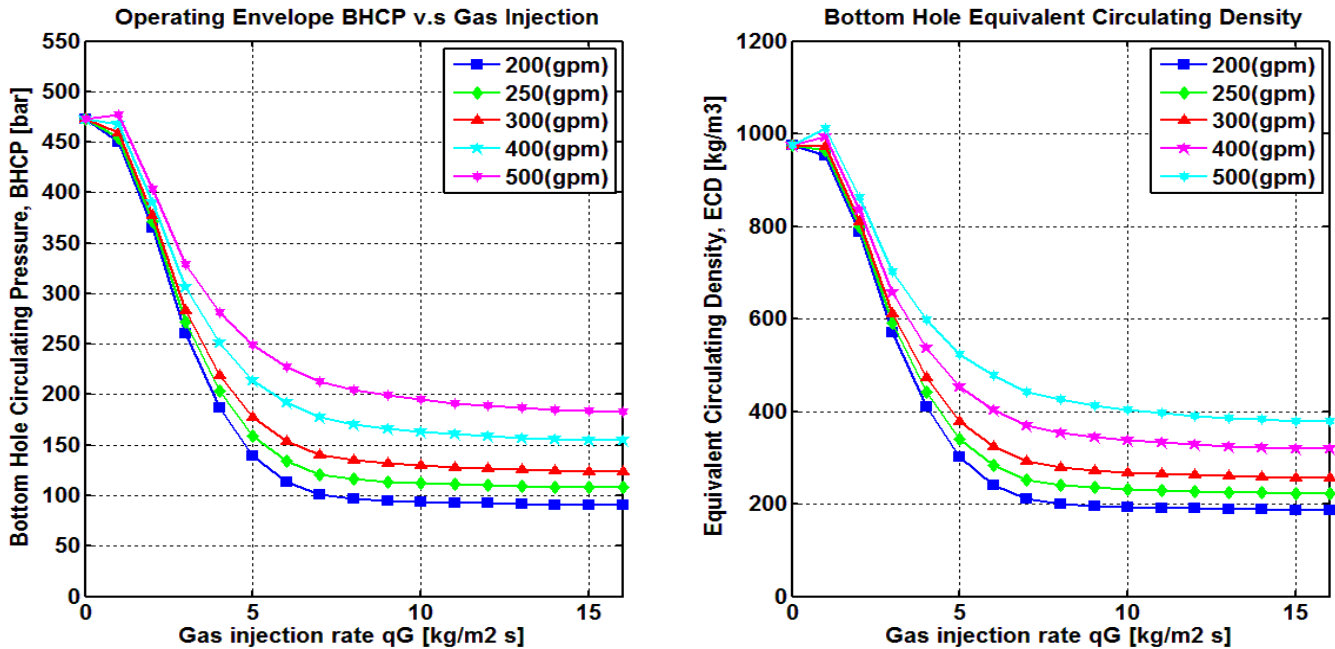


Figure A1.1.9 Sensitivity analysis of gas-liquid injection rate for a vertical well @ bottom, "Injection point  $x_4 = 2000$  (m)",  $f = 600$

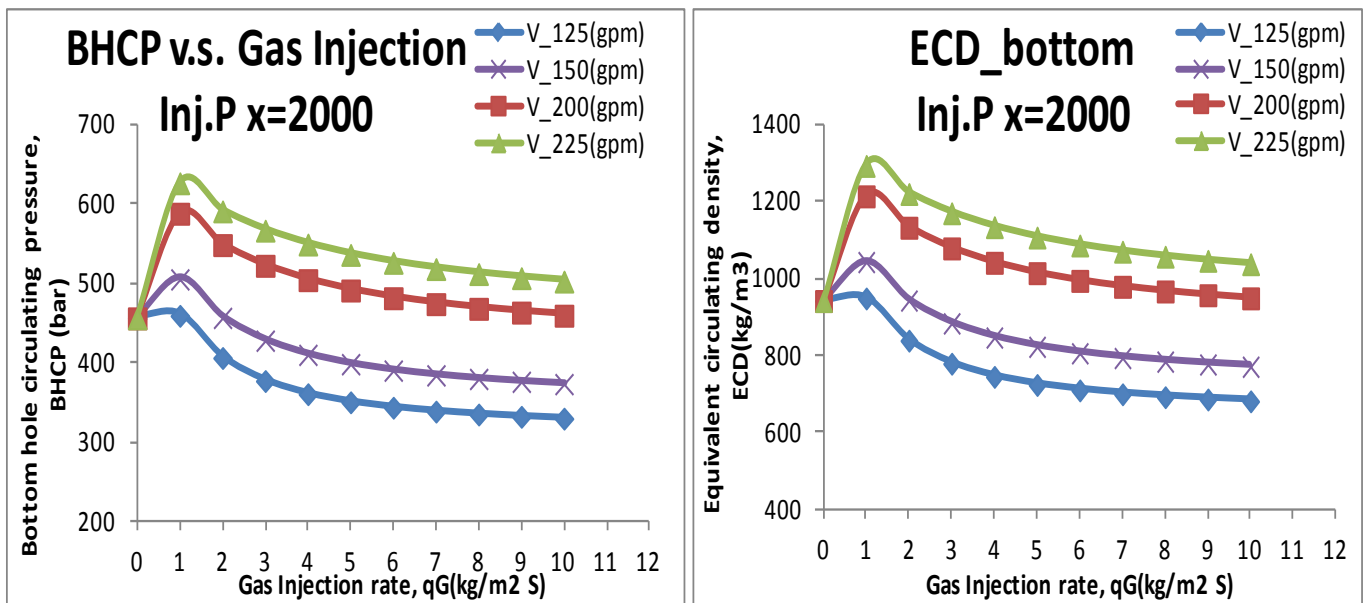


Figure A1.1.10 Sensitivity analysis of gas-liquid injection rate for a vertical well @ bottom, "Injection point  $x_4 = 2000$  (m)",  $f = 6000$

A1.2 Directional well

– Direct nitrogen injection

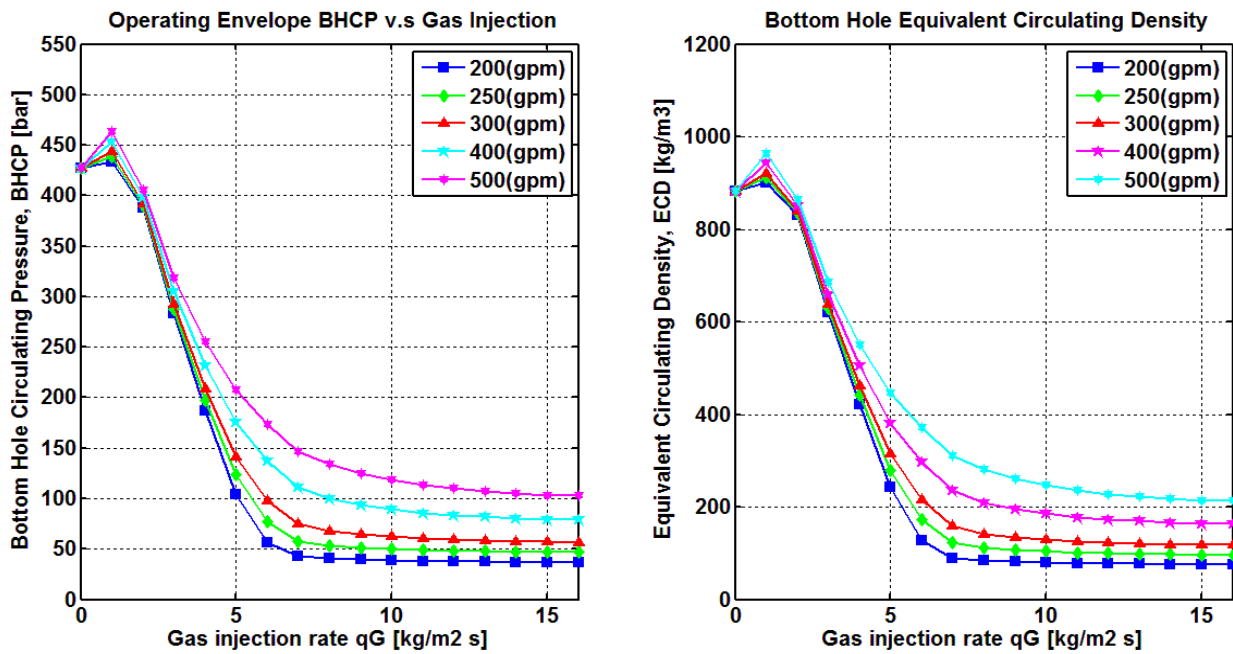


Figure A1.2.1 Sensitivity analysis of gas-liquid injection rate for a horizontal well @ bottom, "Direct Nitrogen Injection",  $f = 600$

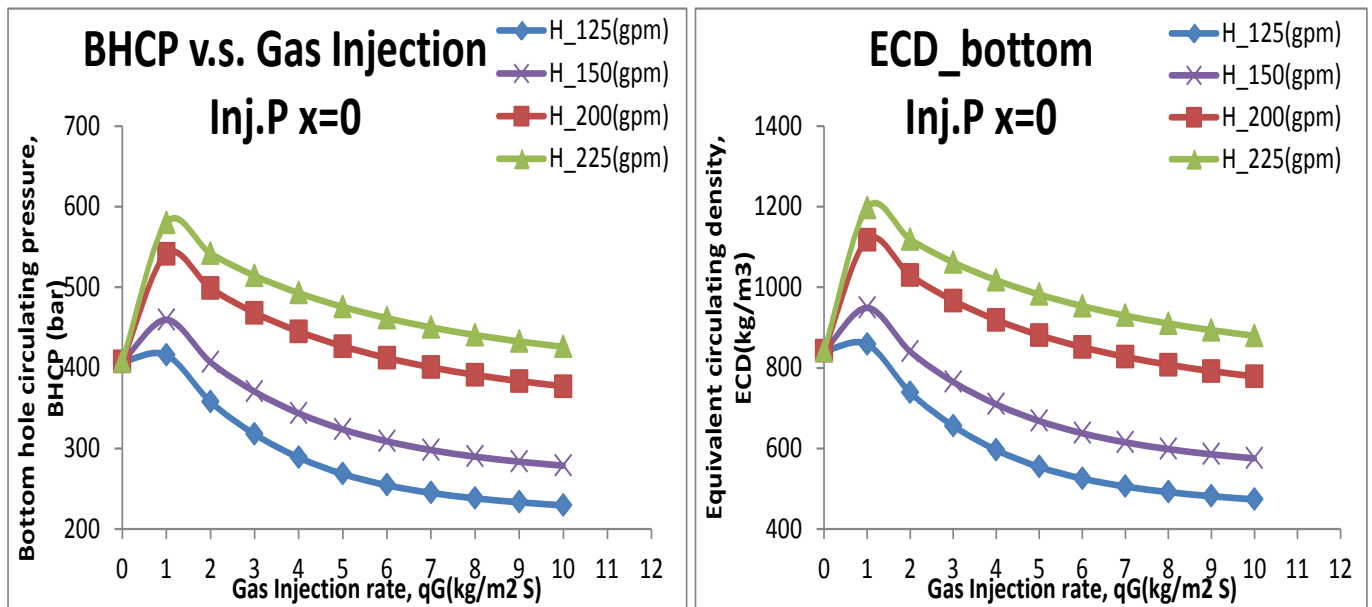


Figure A1.2.2 Sensitivity analysis of gas-liquid injection rate for a horizontal well @ bottom, "Direct Nitrogen Injection",  $f = 6000$

– Injection point  $x_1 = 500$  (m)

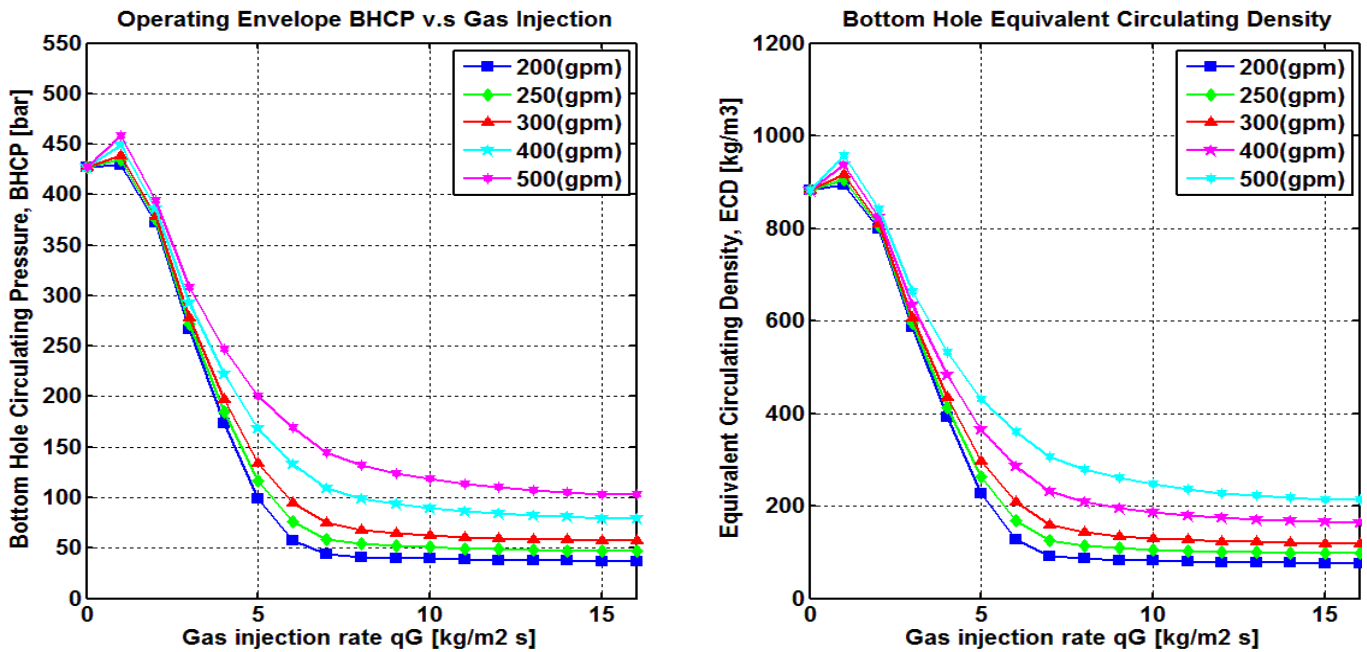


Figure A1.2.3 Sensitivity analysis of gas-liquid injection rate for a horizontal well @ bottom, "Injection point  $x_1 = 500$  (m)",  $f = 600$

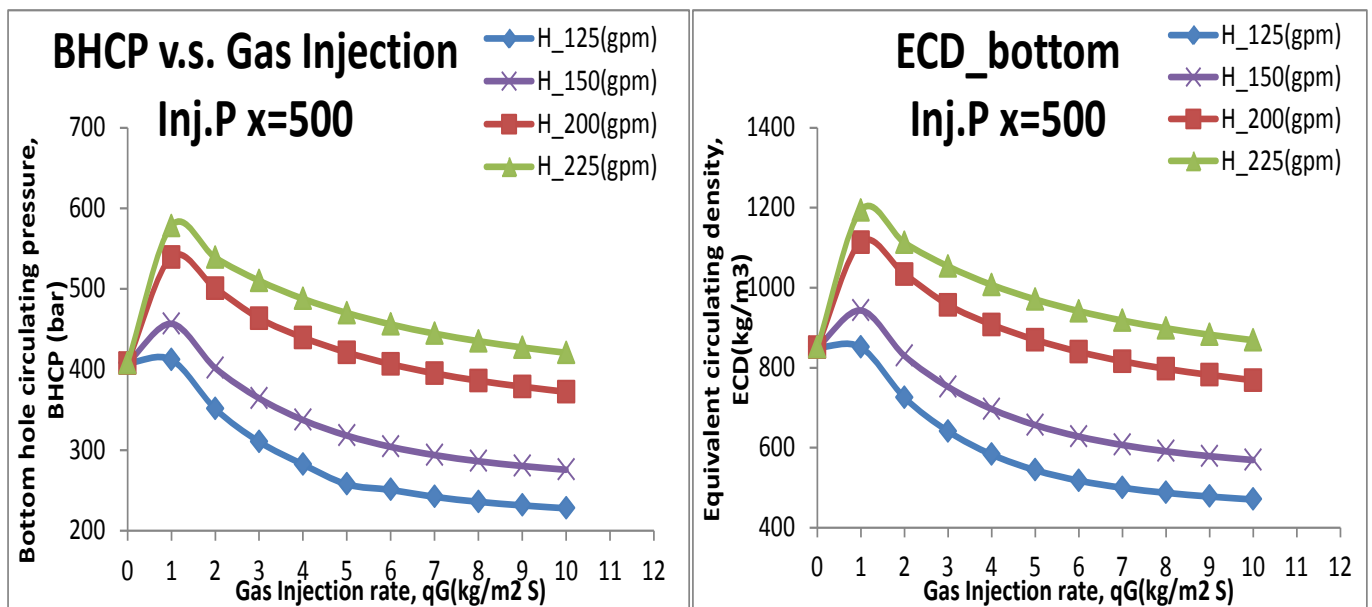


Figure A1.2.4 Sensitivity analysis of gas-liquid injection rate for a horizontal well @ bottom, "Injection point  $x_1 = 500$  (m)",  $f = 6000$

– Injection point  $x_2 = 1000$  (m)

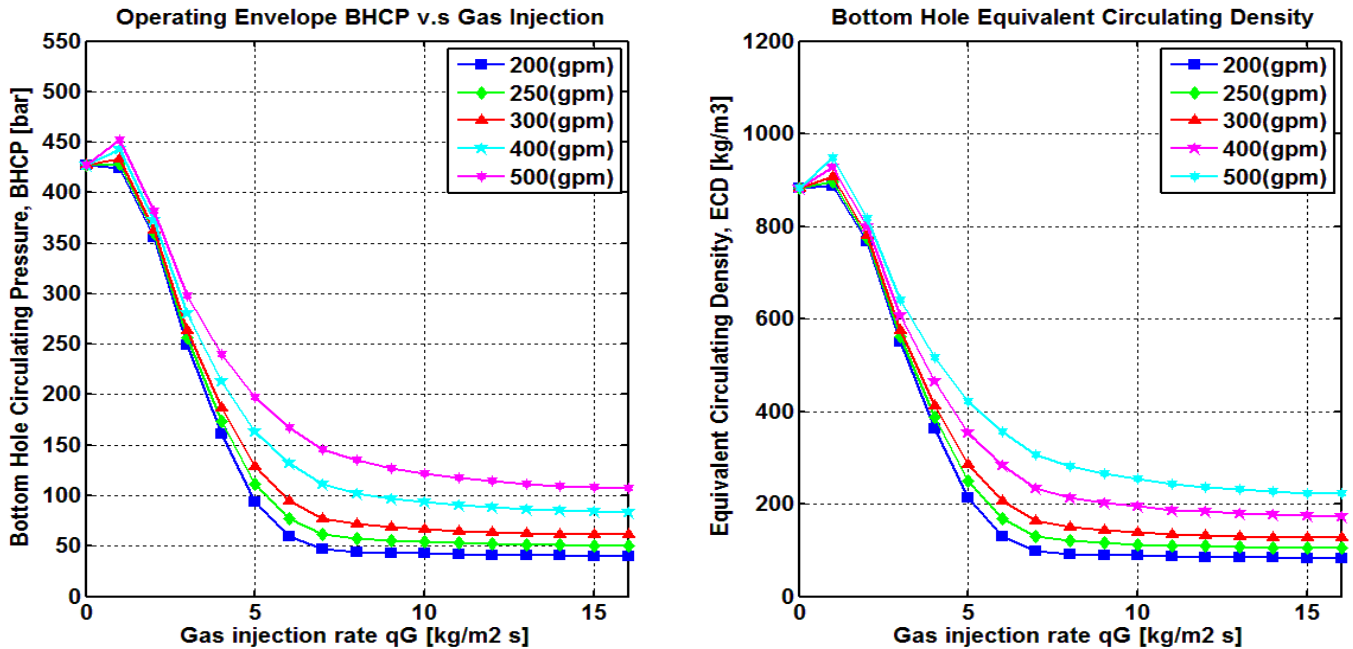


Figure A1.2.5 Sensitivity analysis of gas-liquid injection rate for a horizontal well @ bottom, "Injection point  $x_2 = 1000$  (m)",  $f = 600$

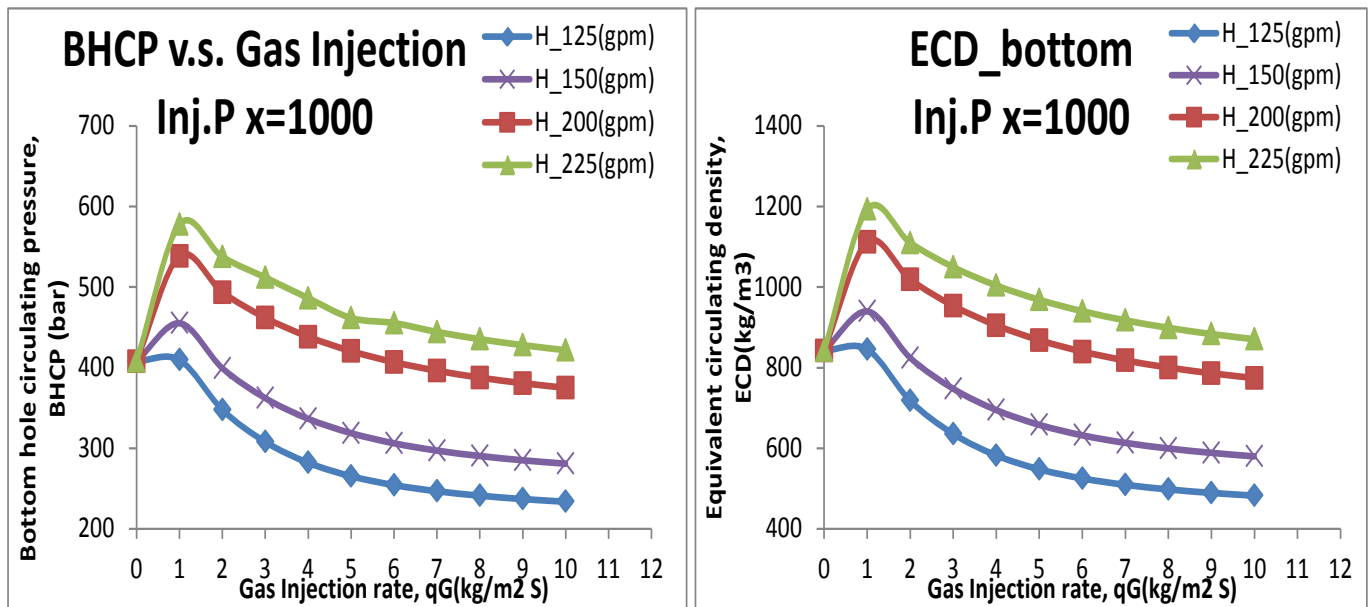


Figure A1.2.6 Sensitivity analysis of gas-liquid injection rate for a horizontal well @ bottom, "Injection point  $x_2 = 1000$  (m)",  $f = 6000$

– Injection point x3 = 1500 (m)

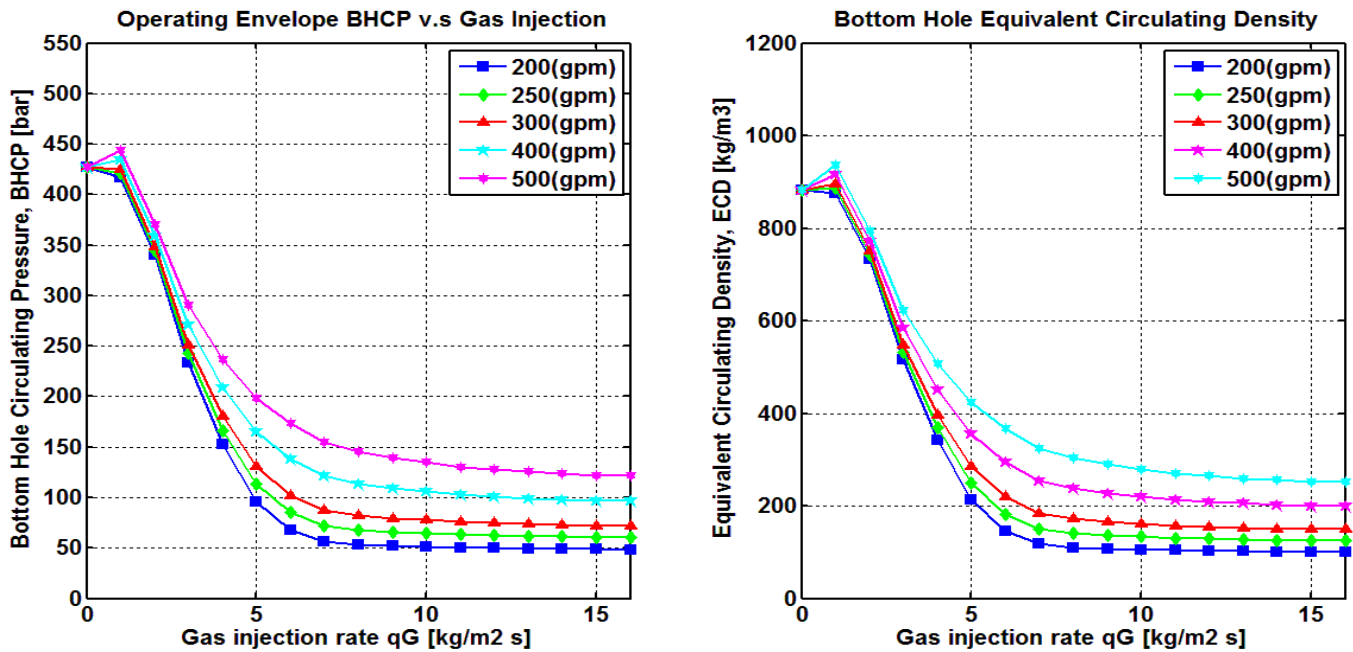


Figure A1.2.7 Sensitivity analysis of gas-liquid injection rate for a horizontal well @ bottom, "Injection point x3= 1500 (m)",  $f = 600$

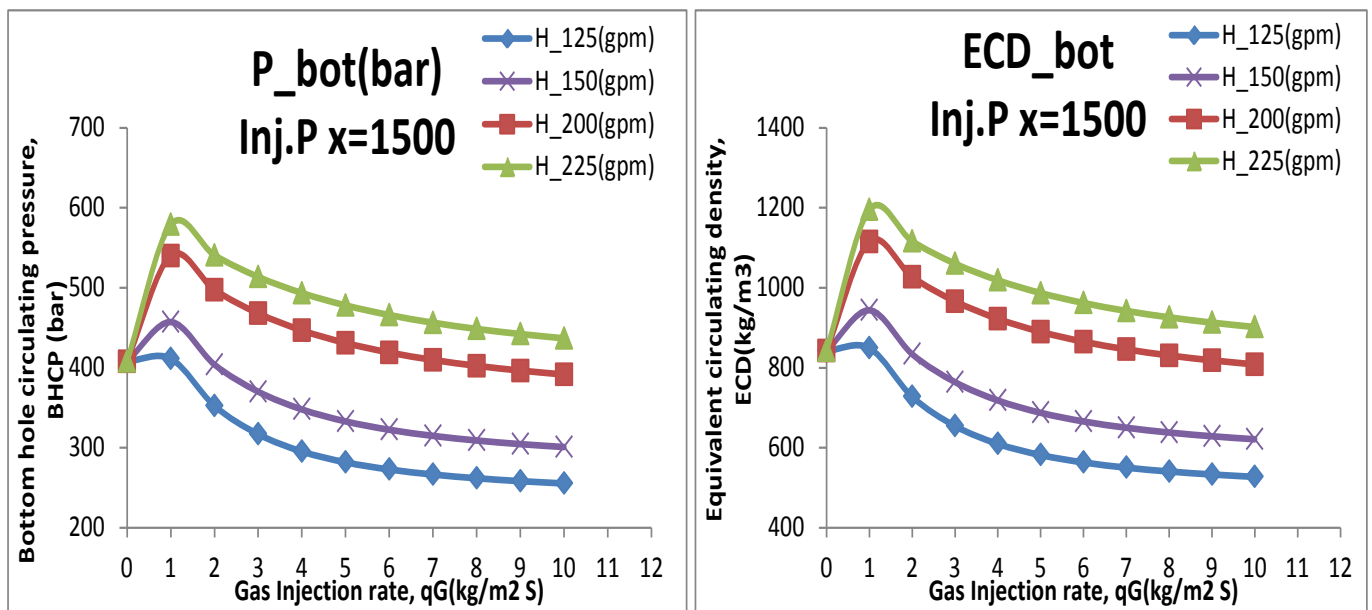


Figure A1.2.8 Sensitivity analysis of gas-liquid injection rate for a horizontal well @ bottom, "Injection point x3= 1500 (m)",  $f = 6000$



– Injection point x4 = 2000 (m)

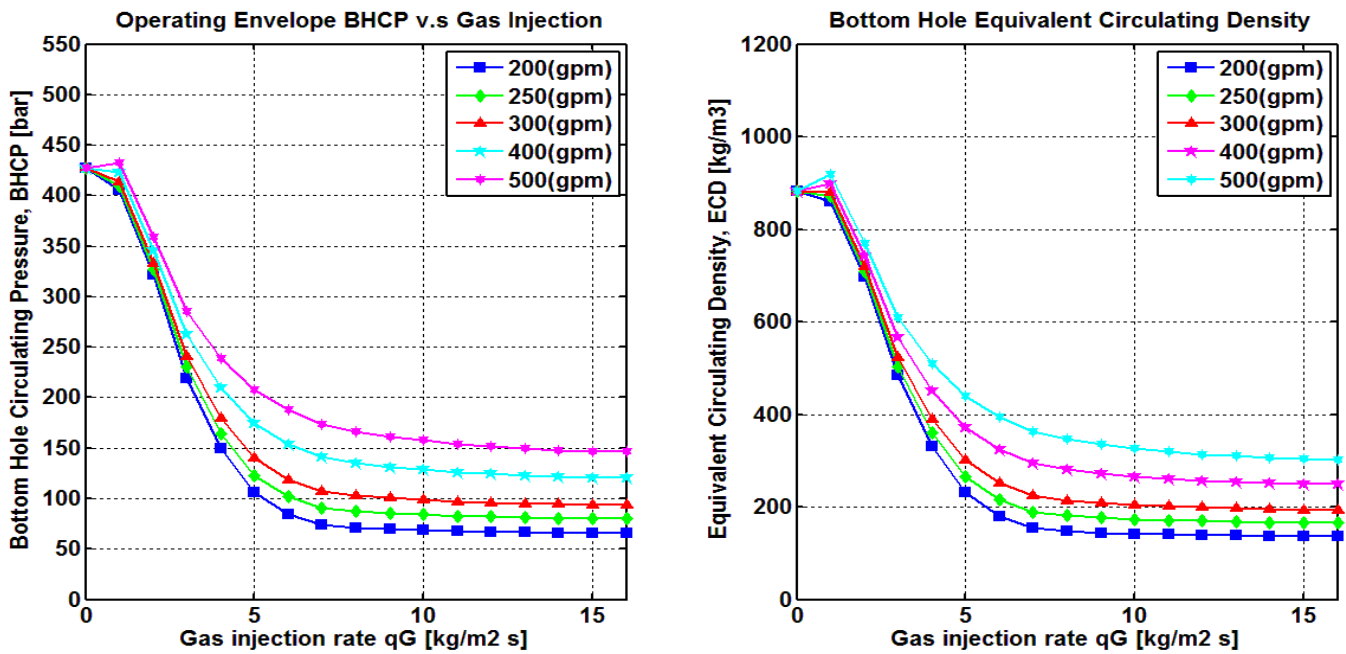


Figure A1.2.9 Sensitivity analysis of gas-liquid injection rate for a horizontal well @ bottom, "Injection point x4= 2000 (m)",  $f = 600$

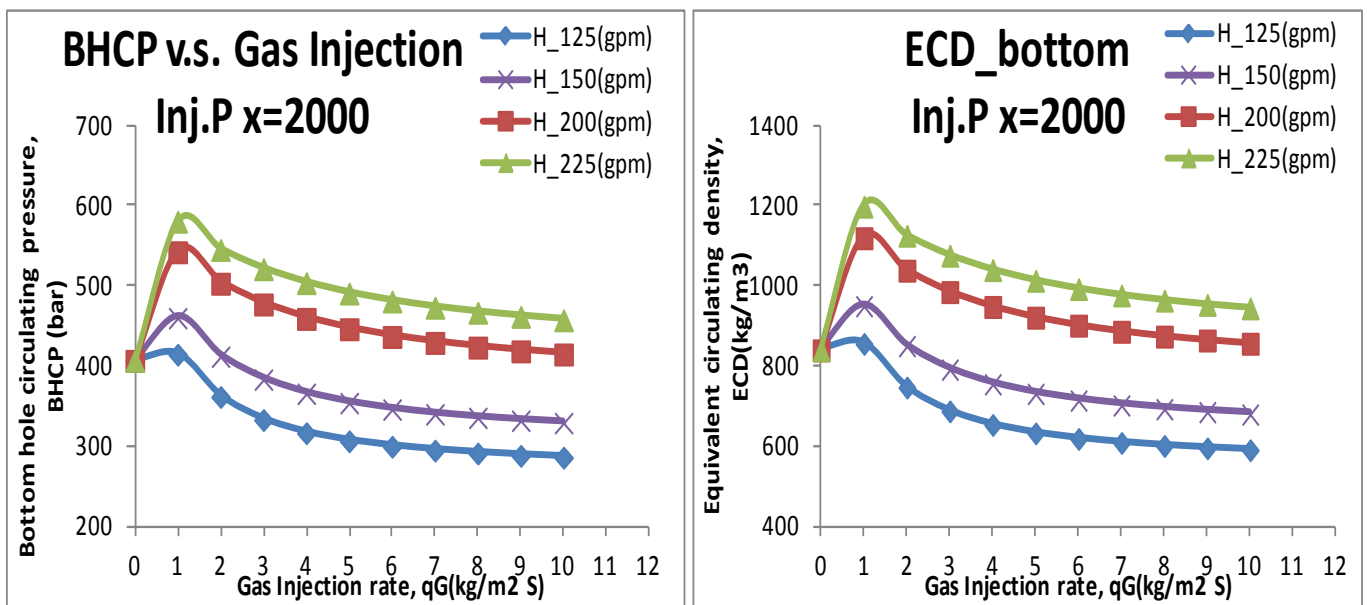


Figure A1.2.10 Sensitivity analysis of gas-liquid injection rate for a horizontal well @ bottom, "Injection point x4= 2000 (m)",  $f = 6000$

## Appendix 2 – Sensitivity of liquid-gas rate at the shoe

### A. 2. – Analysis of pressures and ECDs at shoe

The importance of pressure monitoring at the well shoe relies on the fact that an increment in pressure due to a bad operational practice may cause an undesired situation in the wellbore, (e.g. a fracture at the previous shoe), leading enormous problems during drilling operations, for example lost of circulation, open hole collapse, friction and drag issues and eventually casing collapse or borehole collapse resulting in side tracks and significant monetary losses plus safety concerns.

It is also well known that during overbalanced drilling operations the mud weight and the equivalent circulating density (ECD) have to be within the operational window dictated by pore pressure and borehole collapse/fracture pressure; therefore it is highly relevant to account with reliable models that will help us to predict the pressure distribution along the wellbore (specially at bottom hole and previous casing shoe), in addition some tools like pressure while drilling (PWD) can help us to monitor drilling parameters in real time, these tools can be particularly useful tool to calibrate modes like the one we are using in this work.

The analysis may be divided as follows:

#### A2.1 Vertical well

##### – Direct nitrogen injection

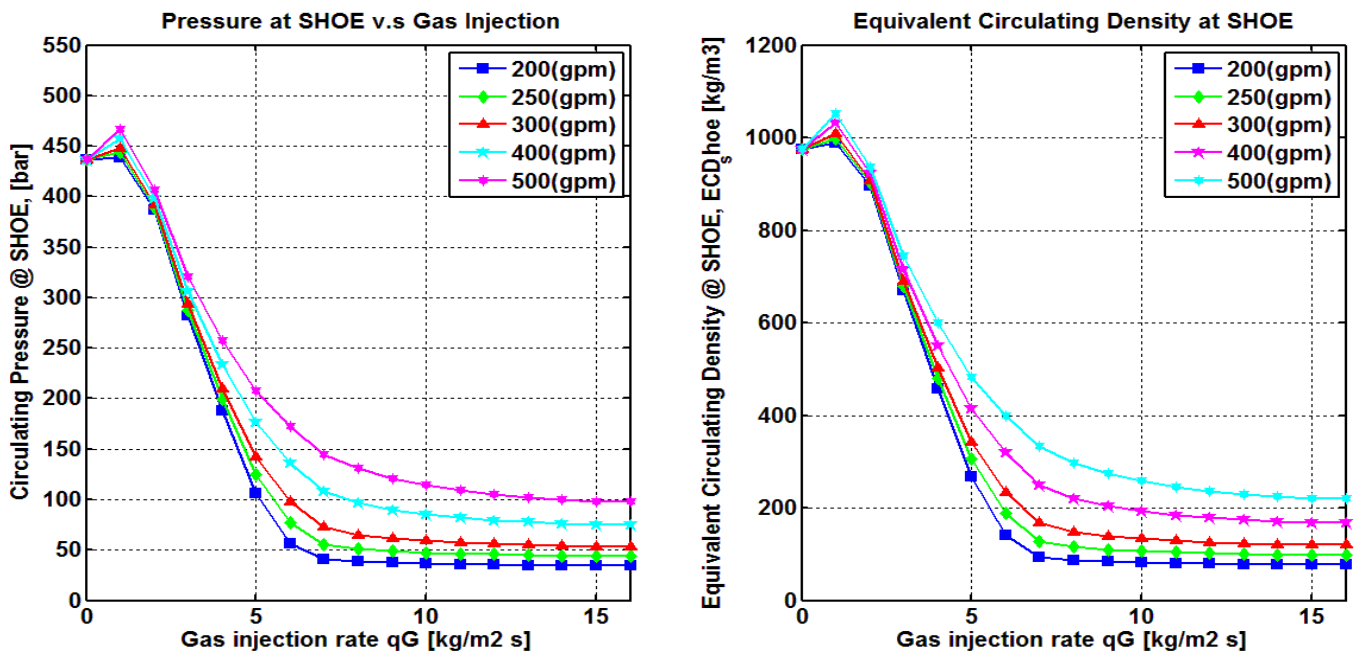


Figure A2.1.1 Sensitivity analysis of gas-liquid injection rate for a vertical well @ shoe, "Direct Nitrogen Injection",  $f = 600$

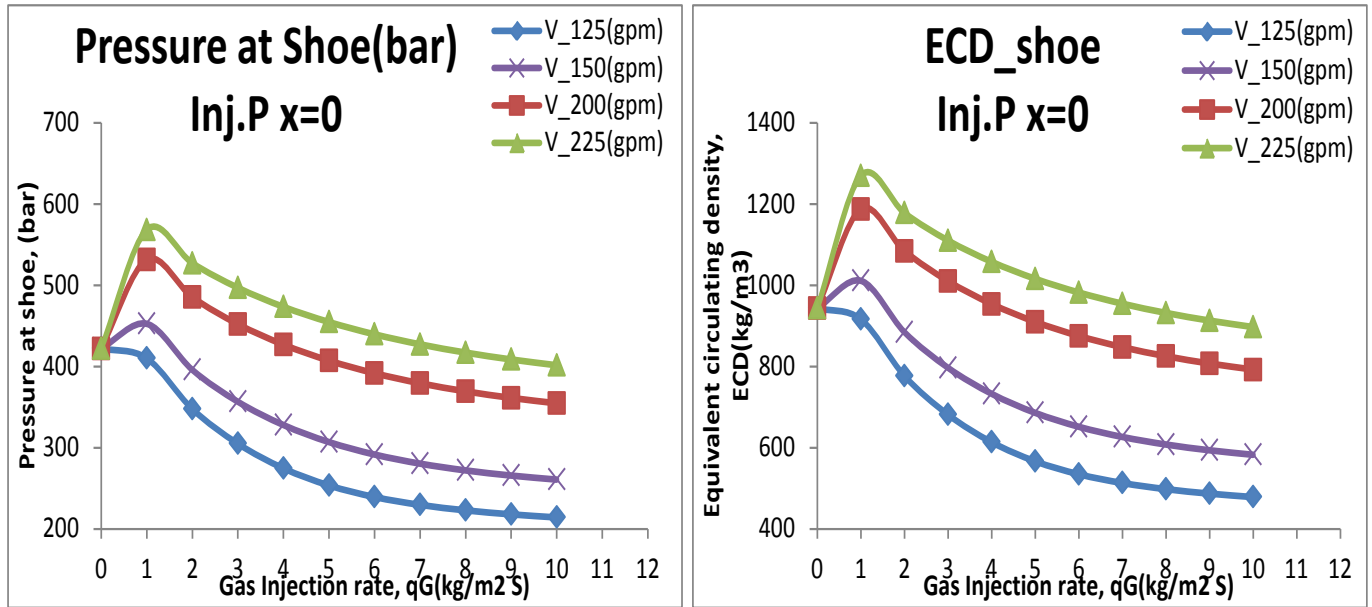


Figure A2.1.2 Sensitivity analysis of gas-liquid injection rate for a vertical well @ shoe, "Direct Nitrogen Injection",  $f = 6000$

– Injection point  $x_1 = 500$  (m)

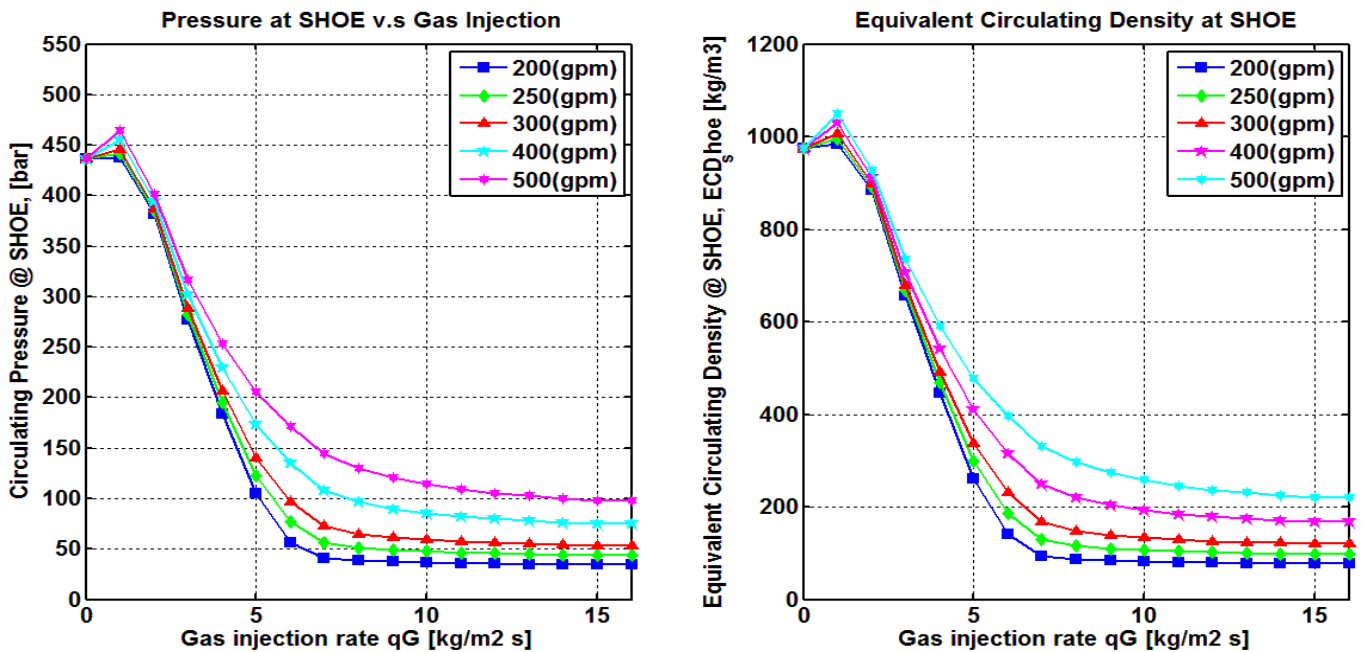


Figure A2.1.3 Sensitivity analysis of gas-liquid injection rate for a vertical well @ shoe, "Injection point  $x_1 = 500$  (m)",  $f = 600$

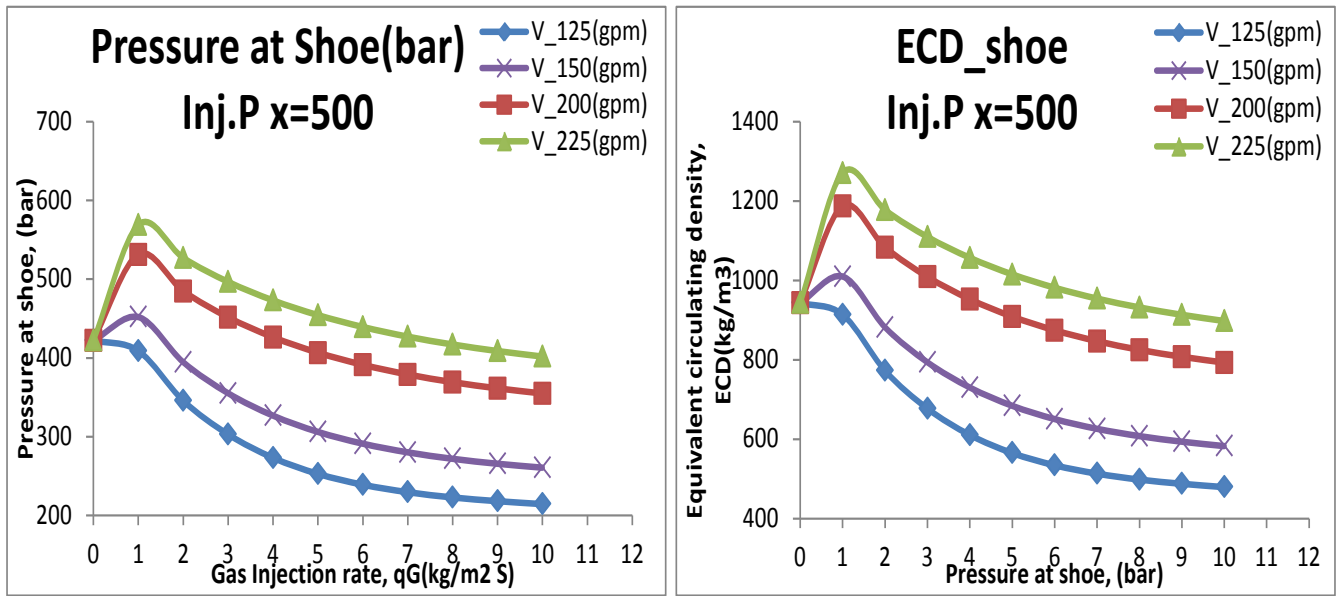


Figure A2.1.4 Sensitivity analysis of gas-liquid injection rate for a vertical well @ shoe, "Injection point x1= 500 (m)",  $f = 6000$

– Injection point x2 = 1000 (m)

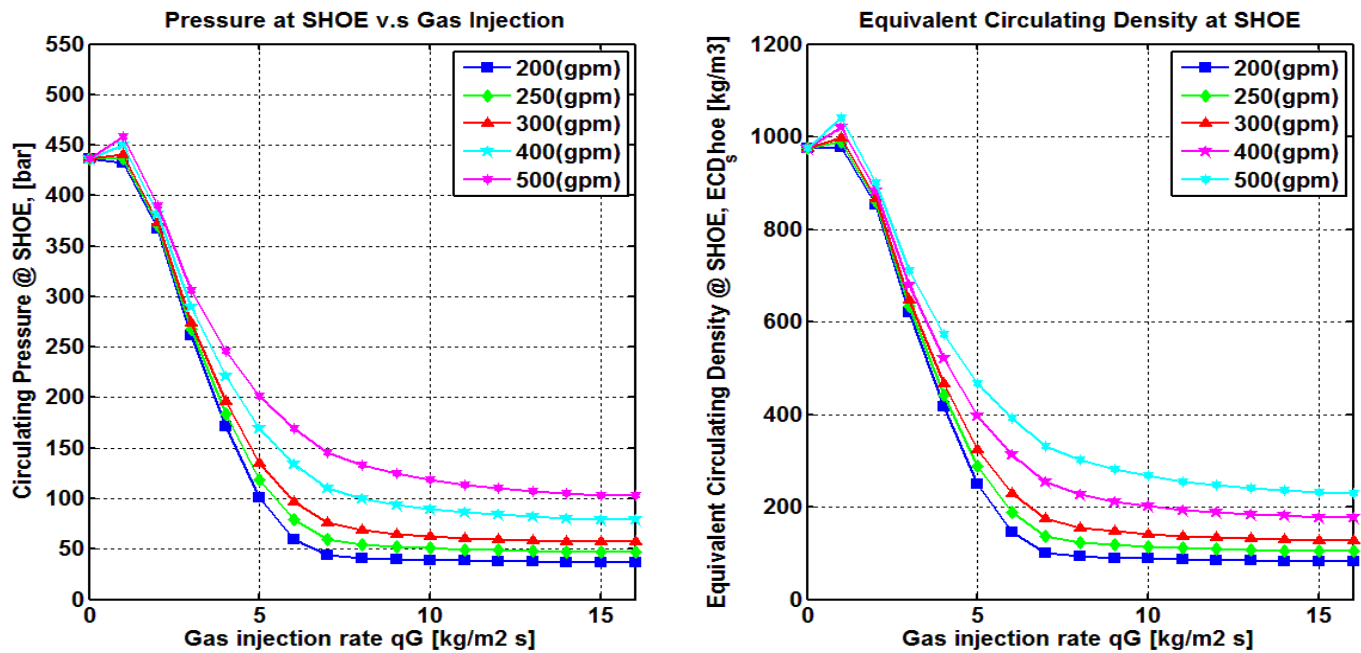


Figure A2.1.5 Sensitivity analysis of gas-liquid injection rate for a vertical well @ shoe, "Injection point x2= 1000 (m)",  $f = 600$

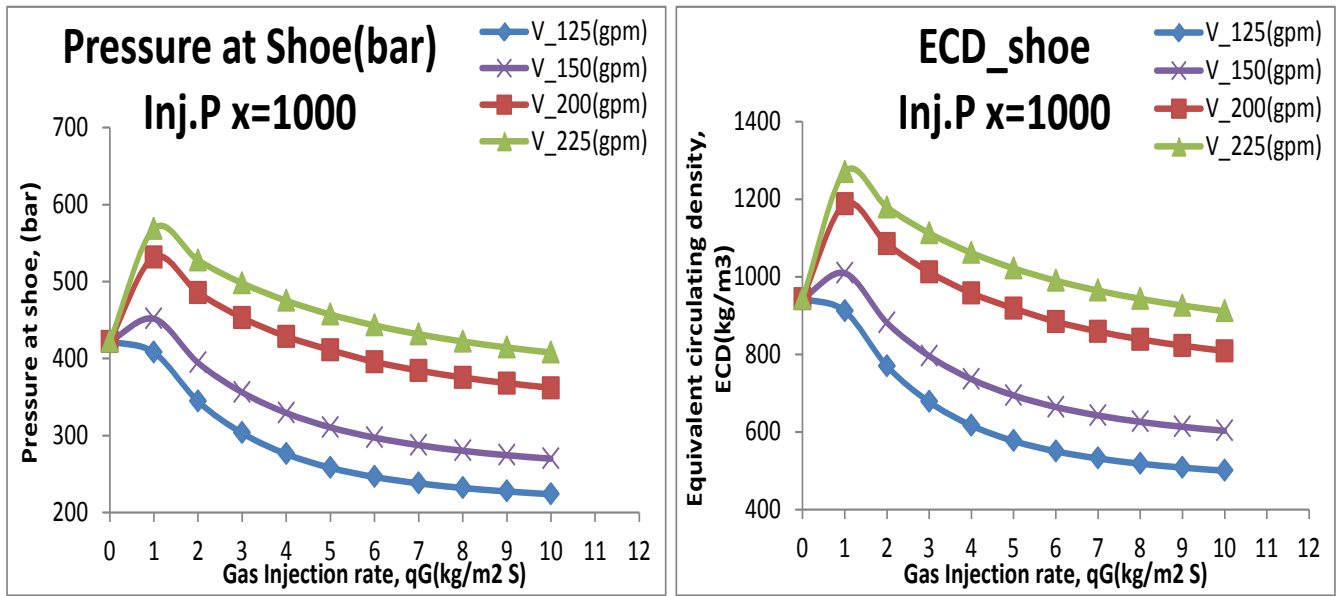


Figure A2.1.6 Sensitivity analysis of gas-liquid injection rate for a vertical well @ shoe, "Injection point x2= 1000 (m)",  $f = 6000$

– Injection point x3 = 1500 (m)

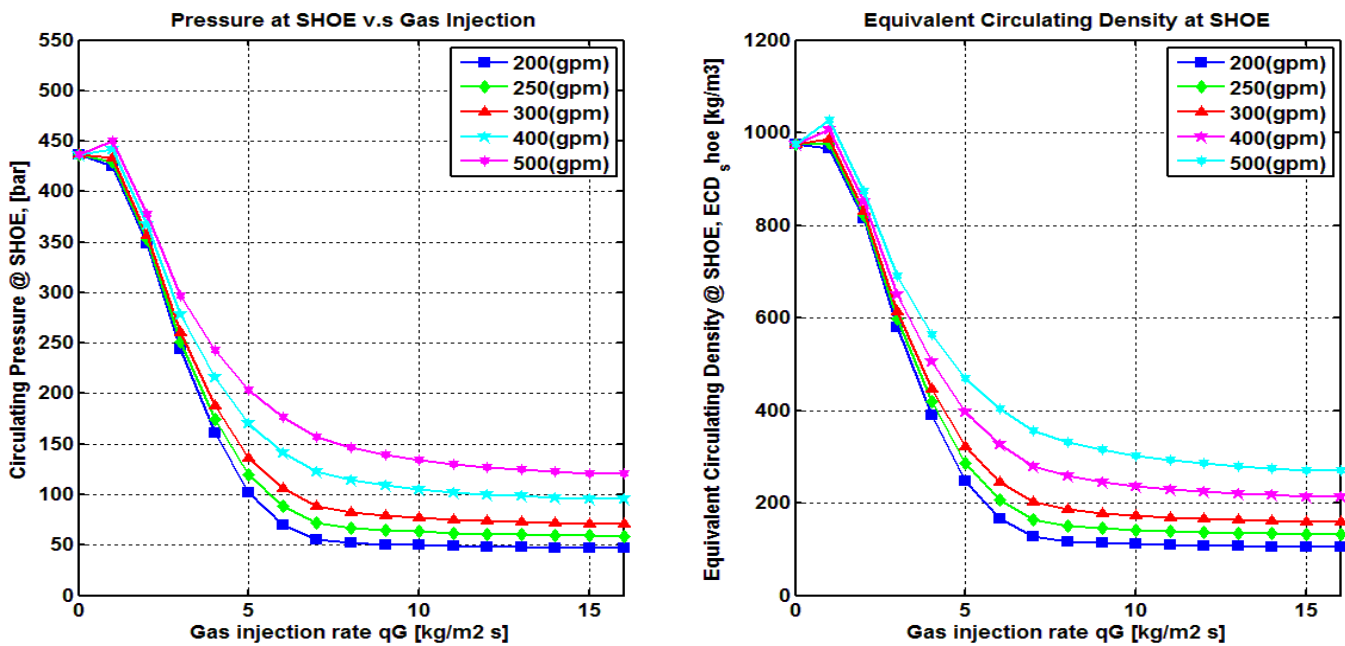


Figure A2.1.7 Sensitivity analysis of gas-liquid injection rate for a vertical well @ shoe, "Injection point x3= 1500 (m)",  $f = 600$

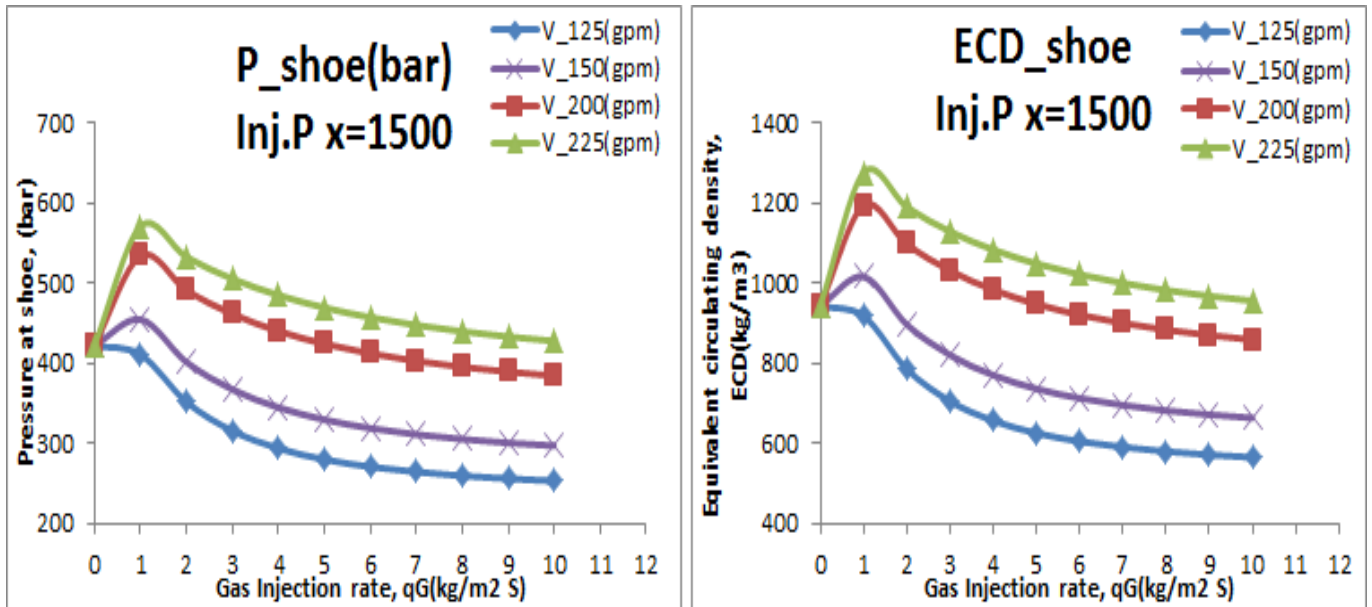


Figure A2.1.8 Sensitivity analysis of gas-liquid injection rate for a vertical well @ shoe, "Injection point x3= 1500 (m)",  $f = 6000$

– Injection point x4 = 2000 (m)

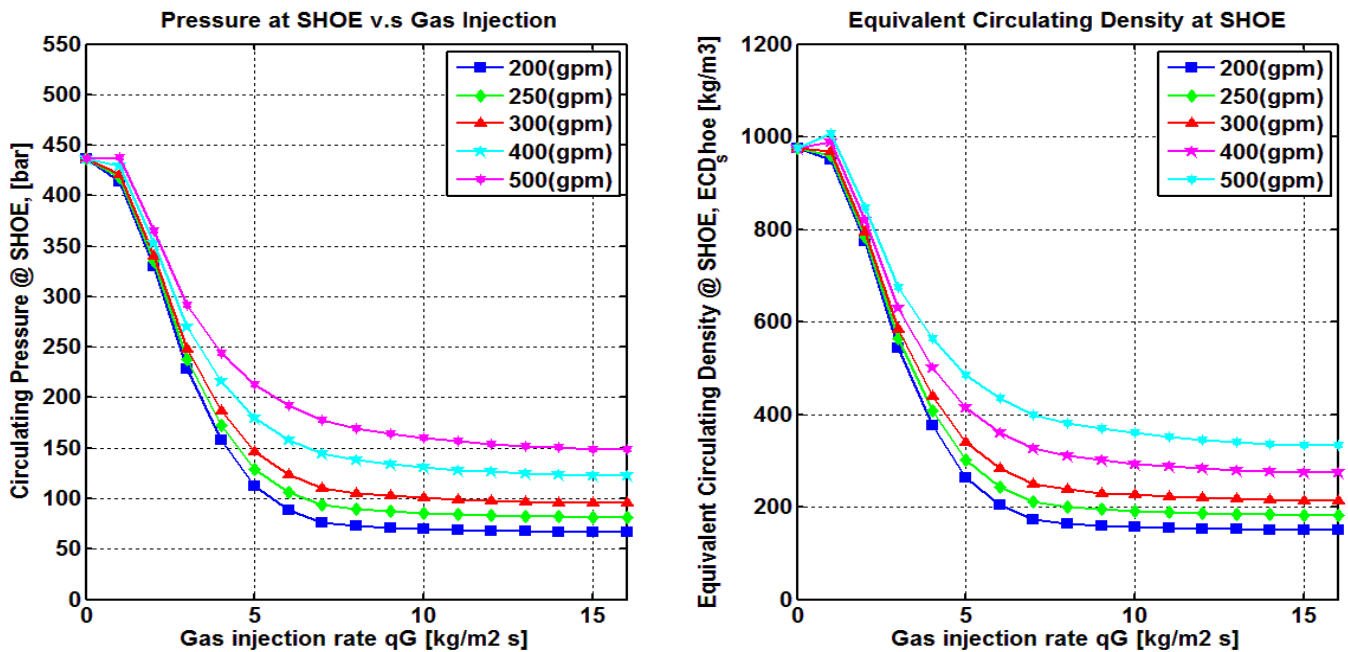


Figure A2.1.9 Sensitivity analysis of gas-liquid injection rate for a vertical well @ shoe, "Injection point x4= 2000 (m)",  $f = 600$

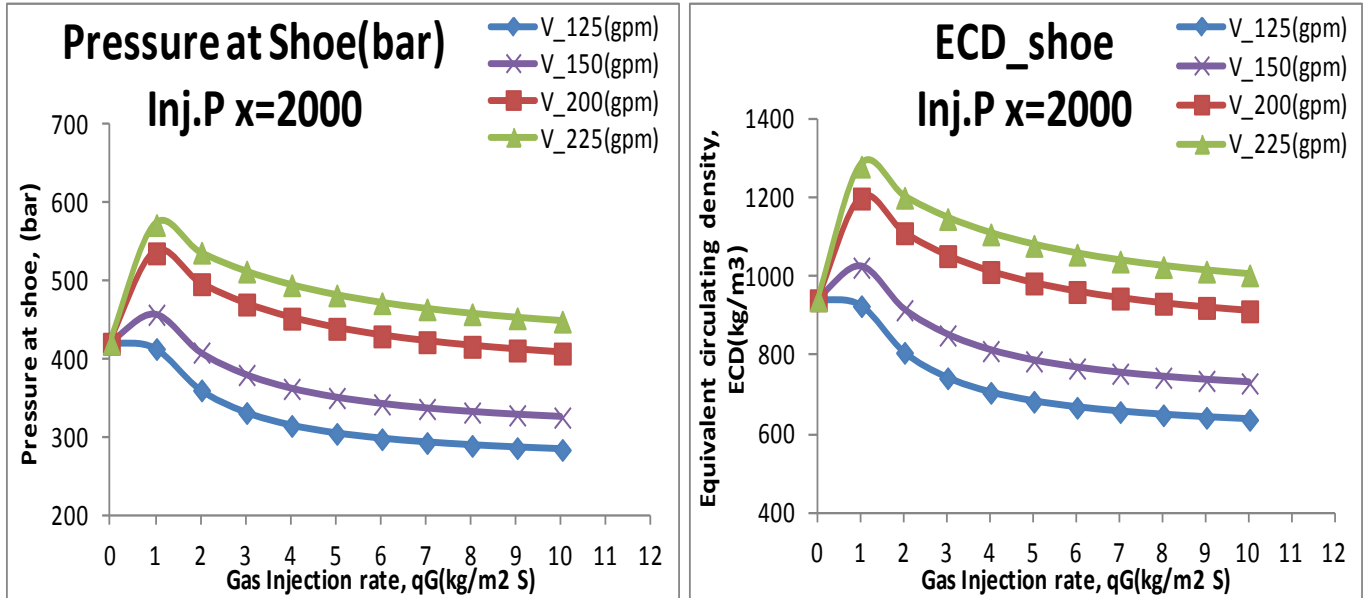


Figure A2.1.10 Sensitivity analysis of gas-liquid injection rate for a vertical well @ shoe, "Injection point x4= 2000 (m)",  $f = 6000$

### A.2.2 Directional well

- Direct nitrogen injection

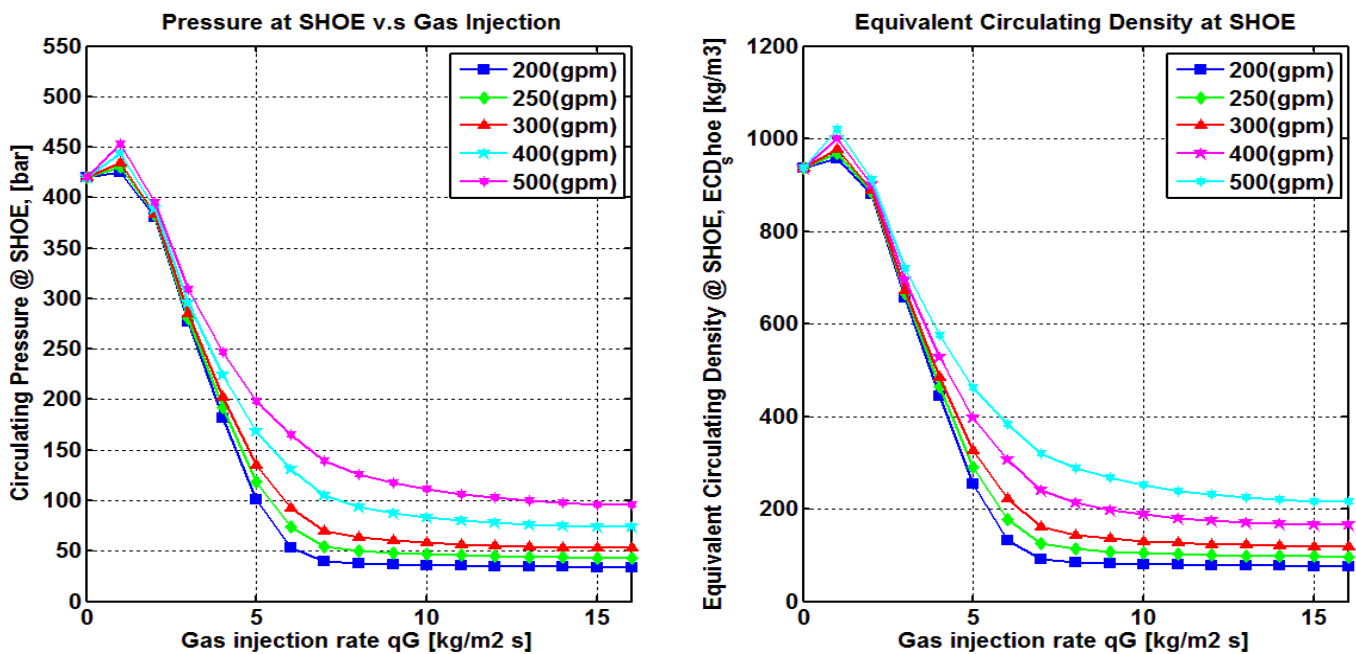


Figure A2.2.1 Sensitivity analysis of gas-liquid injection rate for a horizontal well @ shoe, "Direct Nitrogen Injection",  $f = 600$

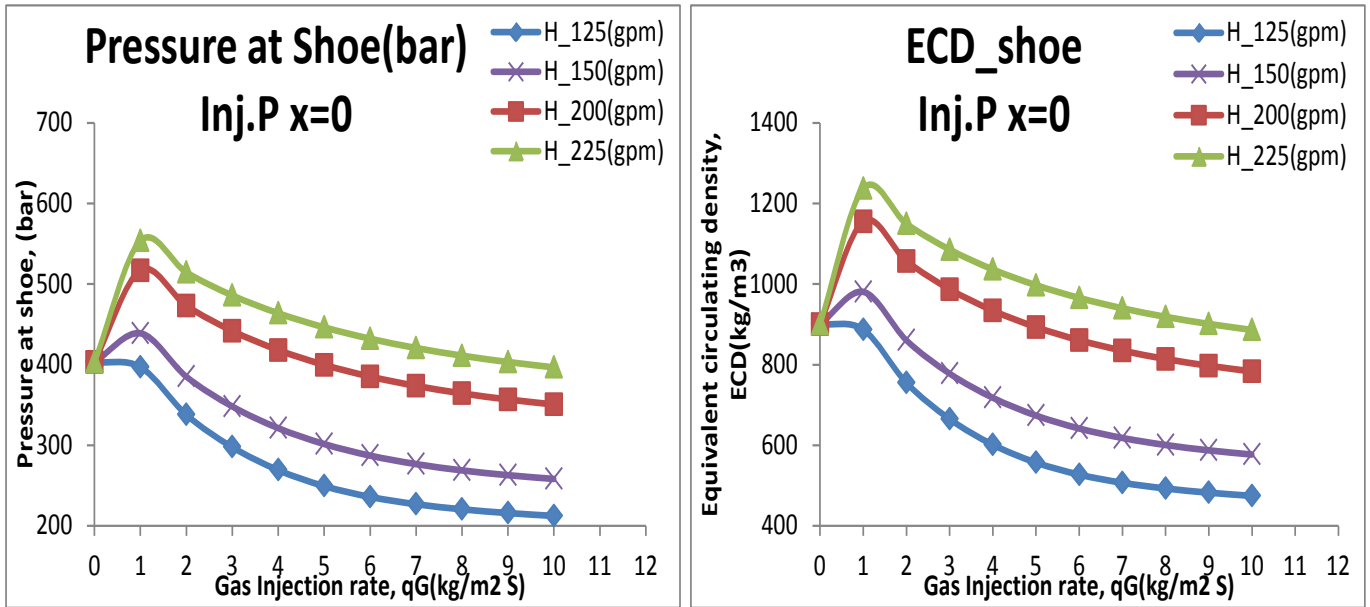


Figure A2.2.2 Sensitivity analysis of gas-liquid injection rate for a horizontal well @ shoe, "Direct Nitrogen Injection",  $f = 6000$

– Injection point x1 = 500 (m)

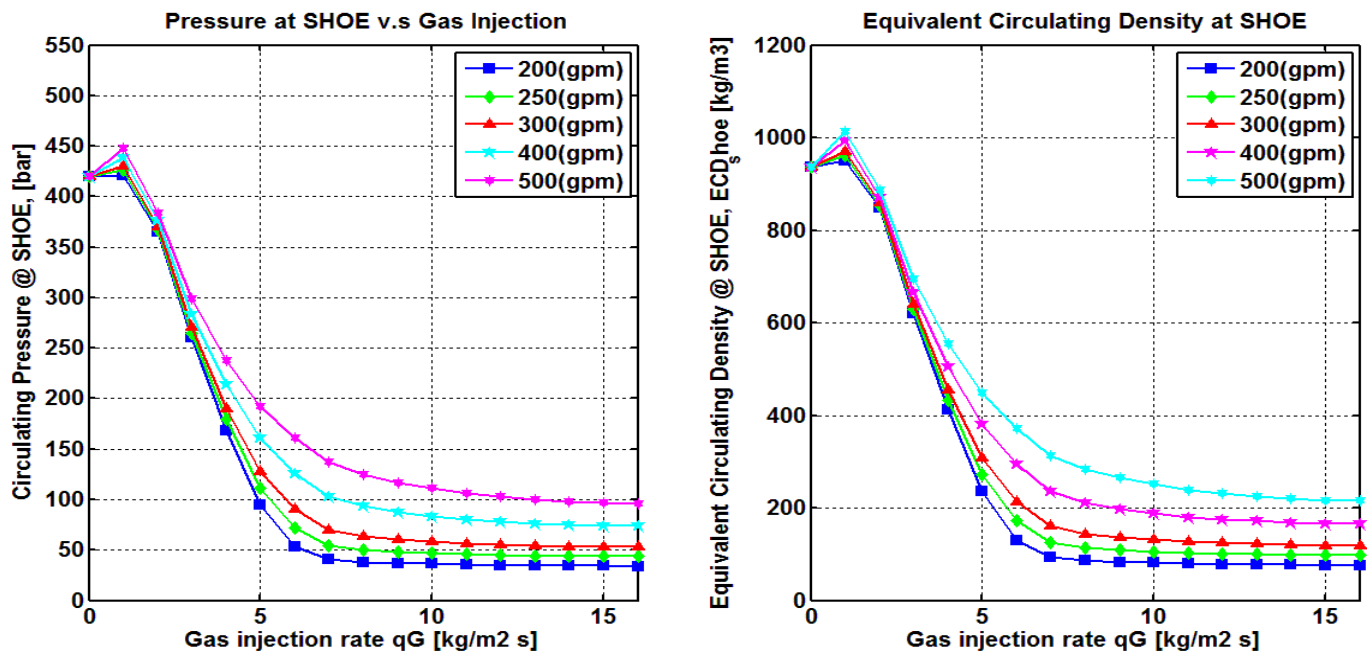


Figure A2.2.3 Sensitivity analysis of gas-liquid injection rate for a vertical well @ shoe, "Injection point x1= 500 (m)",  $f = 600$



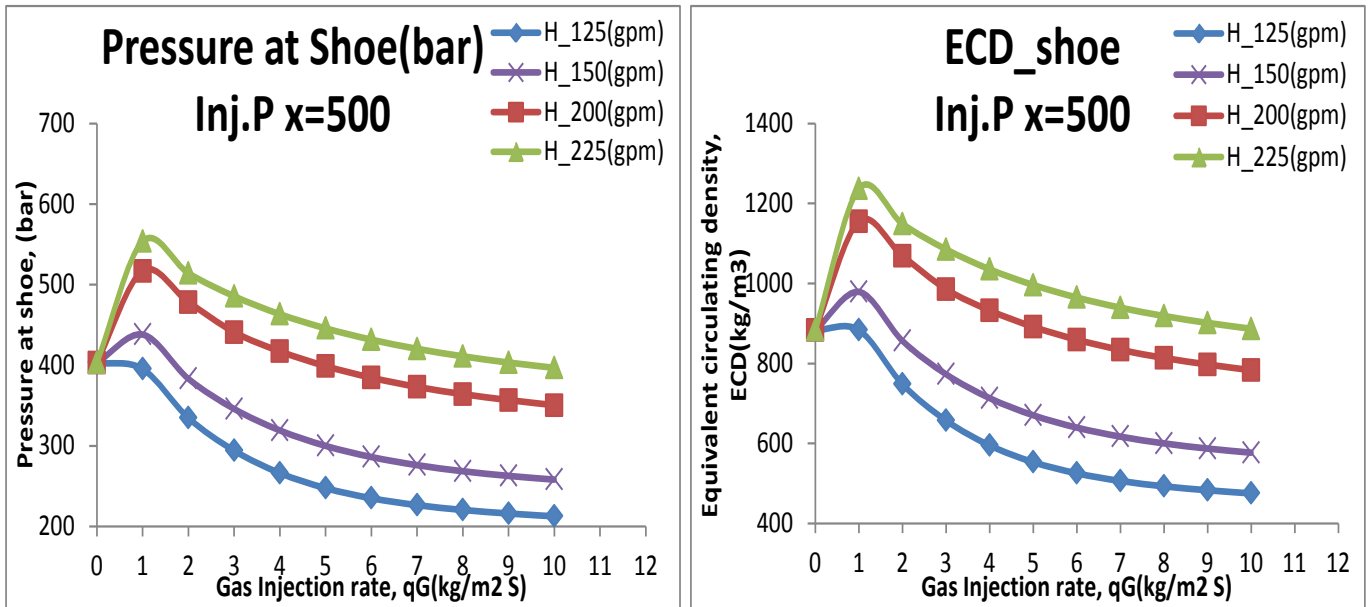


Figure A2.2.4 Sensitivity analysis of gas-liquid injection rate for a vertical well @ shoe, "Injection point x1= 500 (m)",  $f = 6000$

– Injection point x2 = 1000 (m)

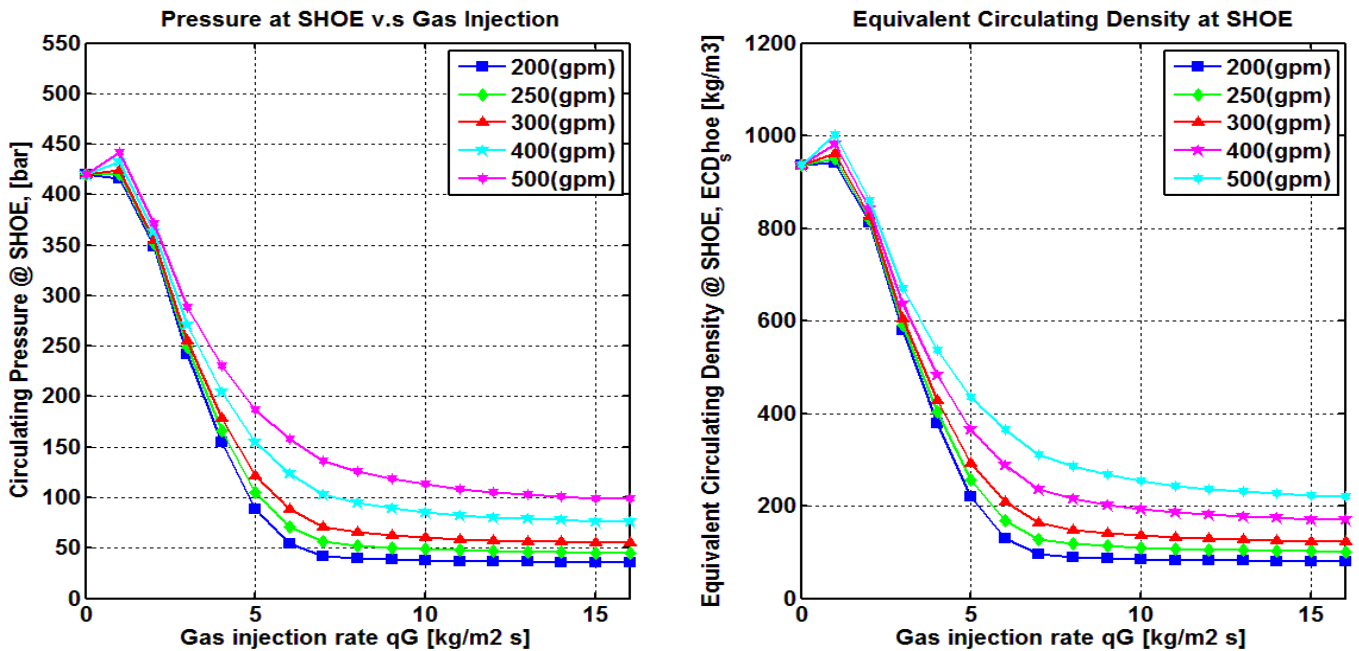


Figure A2.2.5 Sensitivity analysis of gas-liquid injection rate for a horizontal well @ shoe, "Injection point x2= 1000 (m)",  $f = 600$

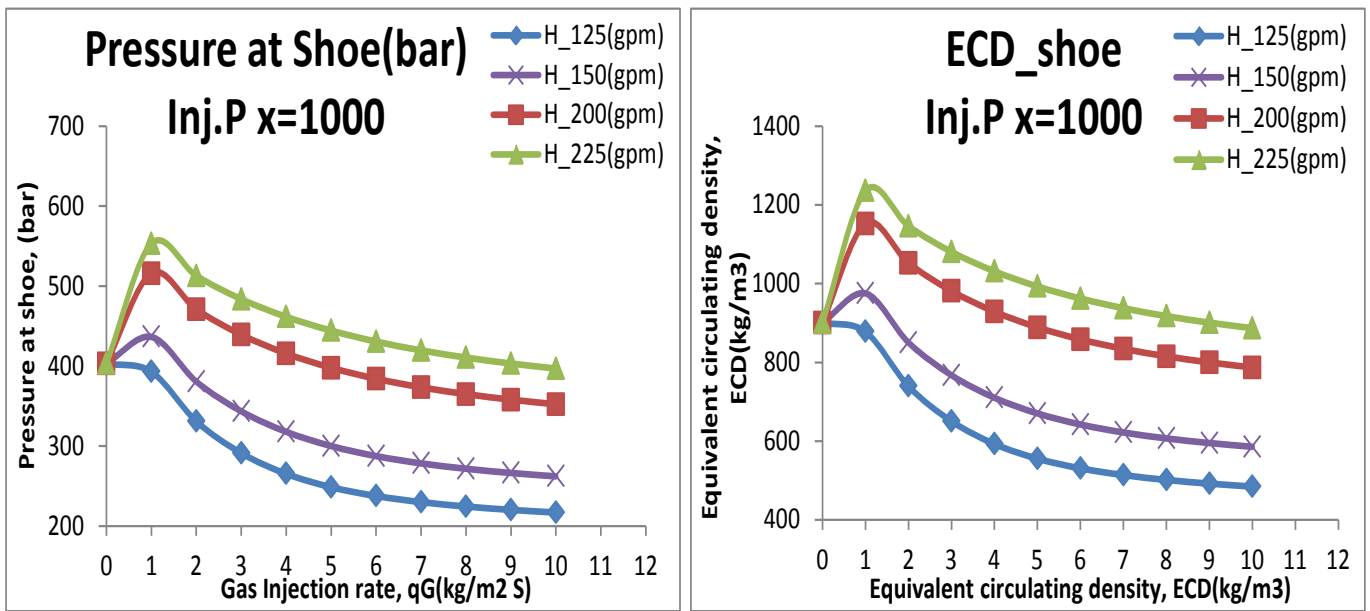


Figure A2.2.6 Sensitivity analysis of gas-liquid injection rate for a horizontal well @ shoe, "Injection point x2= 1000 (m)",  $f = 6000$

– Injection point x3 = 1500 (m)

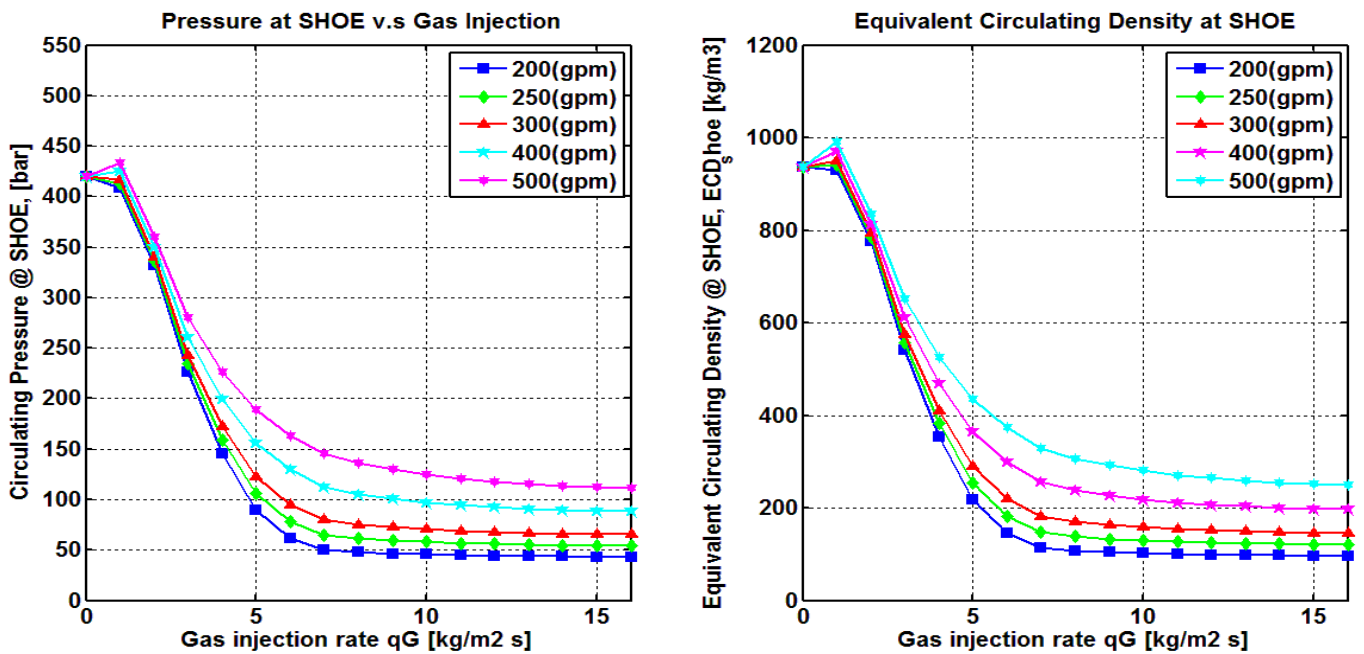


Figure A2.2.7 Sensitivity analysis of gas-liquid injection rate for a horizontal well @ shoe, "Injection point x3= 1500 (m)",  $f = 600$

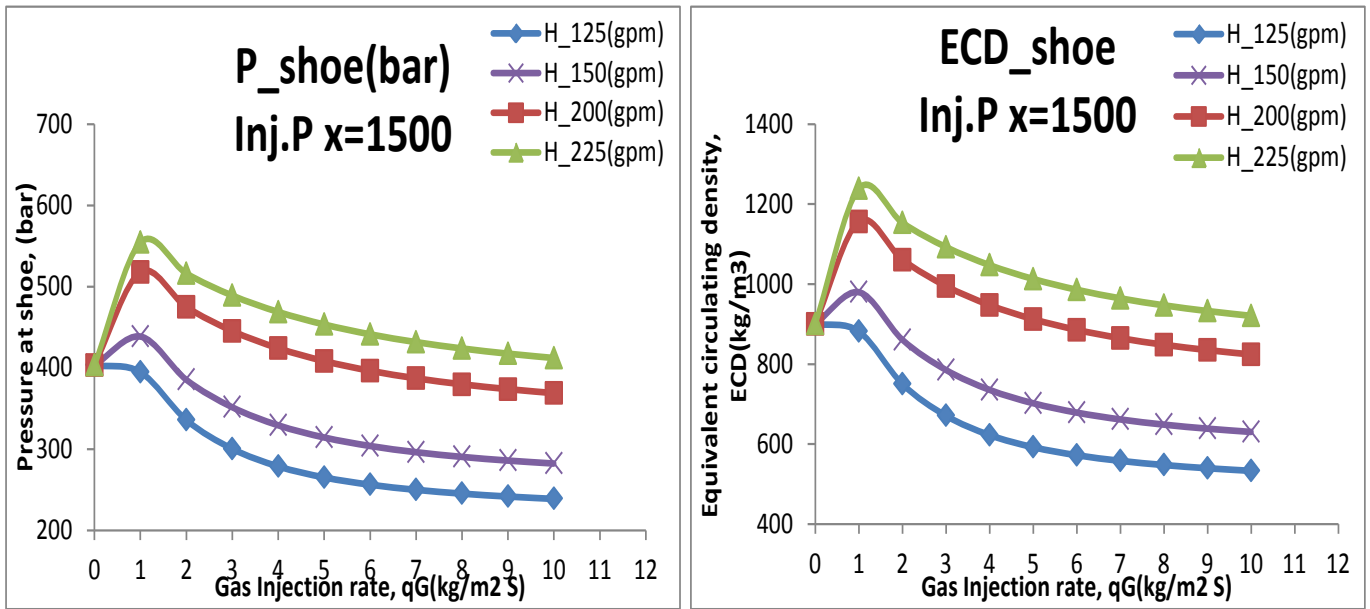


Figure A2.2.8 Sensitivity analysis of gas-liquid injection rate for a horizontal well @ shoe, "Injection point x3= 1500 (m)",  $f = 6000$

– Injection point x4 = 2000 (m)

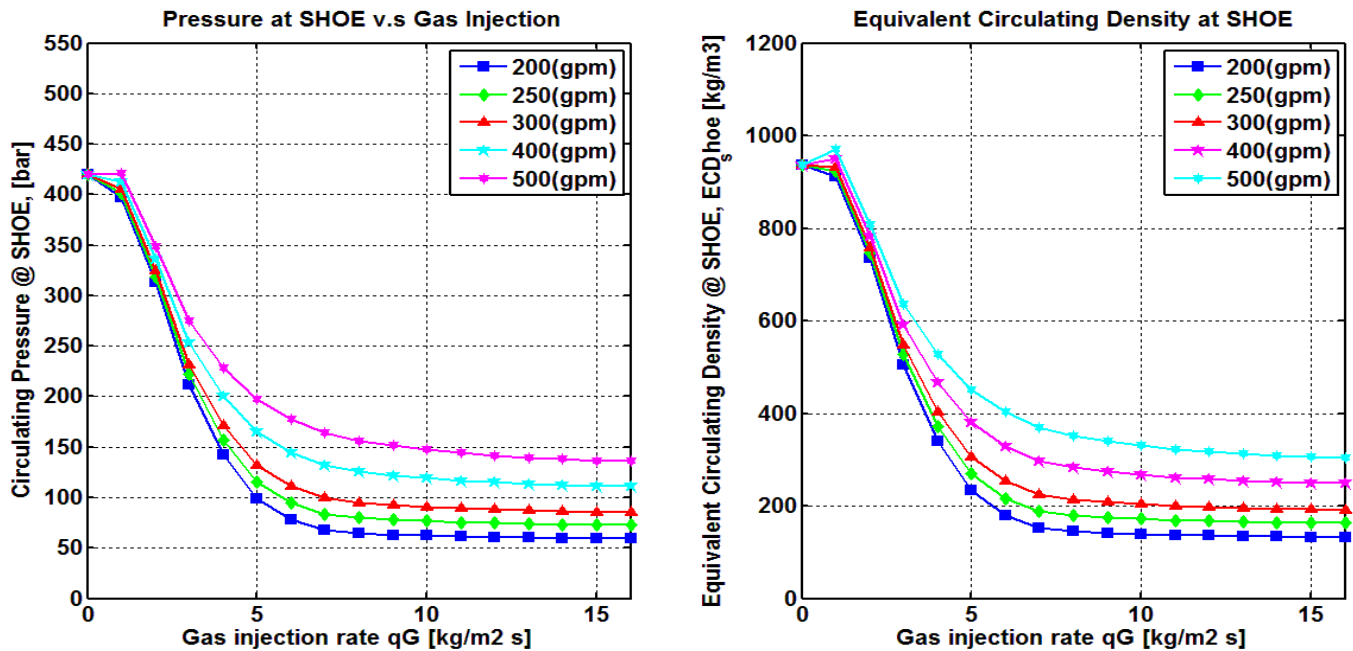


Figure A2.2.9 Sensitivity analysis of gas-liquid injection rate for a horizontal well @ shoe, "Injection point x4= 2000 (m)",  $f = 600$

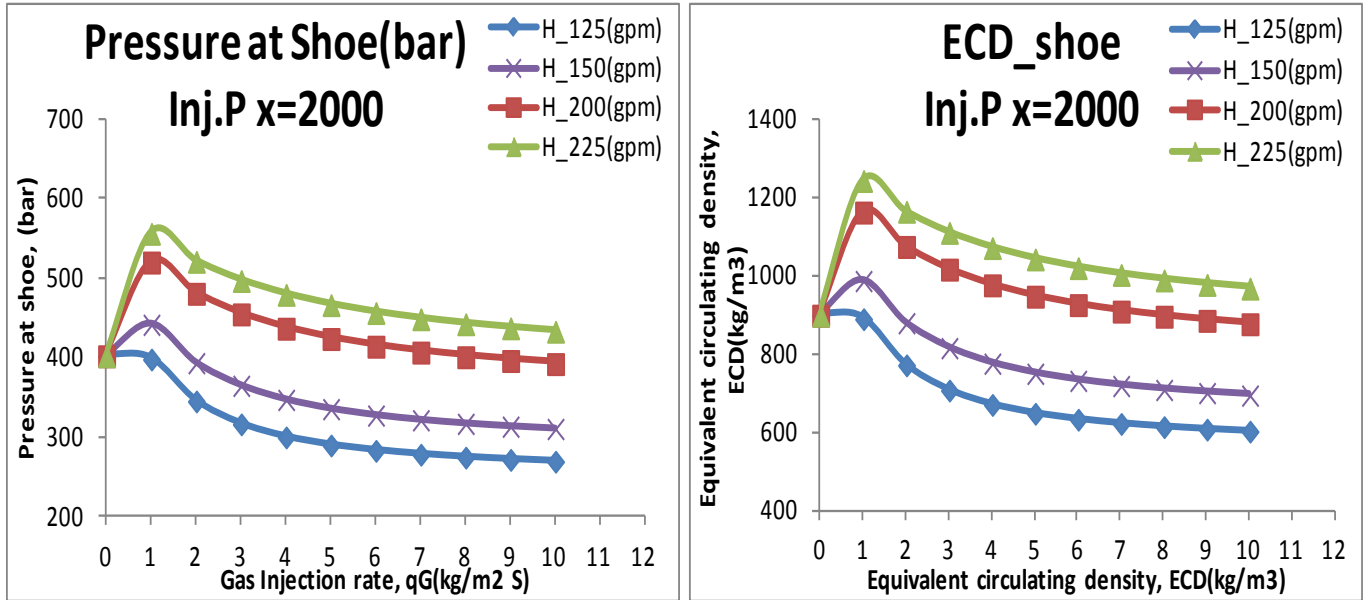


Figure A2.2.10 Sensitivity analysis of gas-liquid injection rate for a horizontal well @ shoe, "Injection point x4= 2000 (m)",  $f = 6000$

### Appendix 3 – Comparison Directional vs Vertical

In this appendix we want to show the reader a simple comparison of the impact that geometry plays in the pressure and equivalent circulating density at bottom and at shoe. The same kind of plots where the gas injection is increased from 1(kg/m2 S) to 10 (kg/m2 S) are presented and the same liquid rates from 125 (gpm) to 225 (gpm) are also used.

- Horizontal wells are depicted by solid lines
- Vertical wells are depicted by dashed lines
- Direct injection

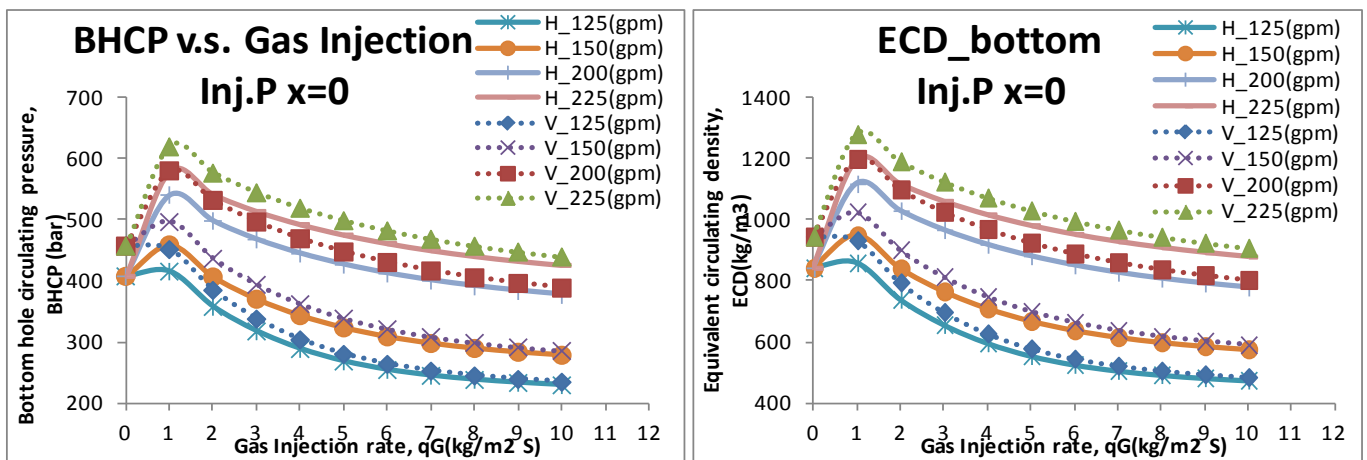


Figure A3.1 Sensitivity analysis of gas-liquid injection rate for a horizontal well @ bottom, "Injection point x1= 0 (m)",  $f = 6000$ , Horizontal "solid line", Vertical "dashed line"

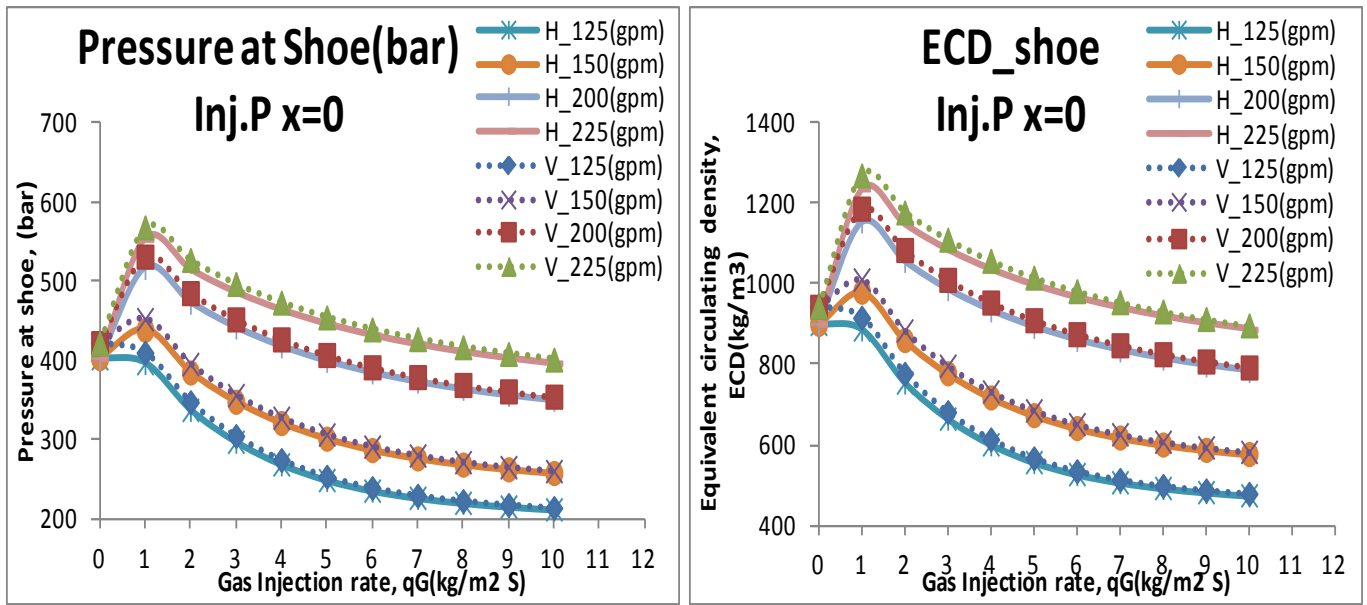


Figure A3.2 Sensitivity analysis of gas-liquid injection rate for a horizontal well @ shoe, "Injection point x1= 0 (m)", Horizontal "solid line", Vertical "dashed line"

– Injection point x1 = 500 (m)

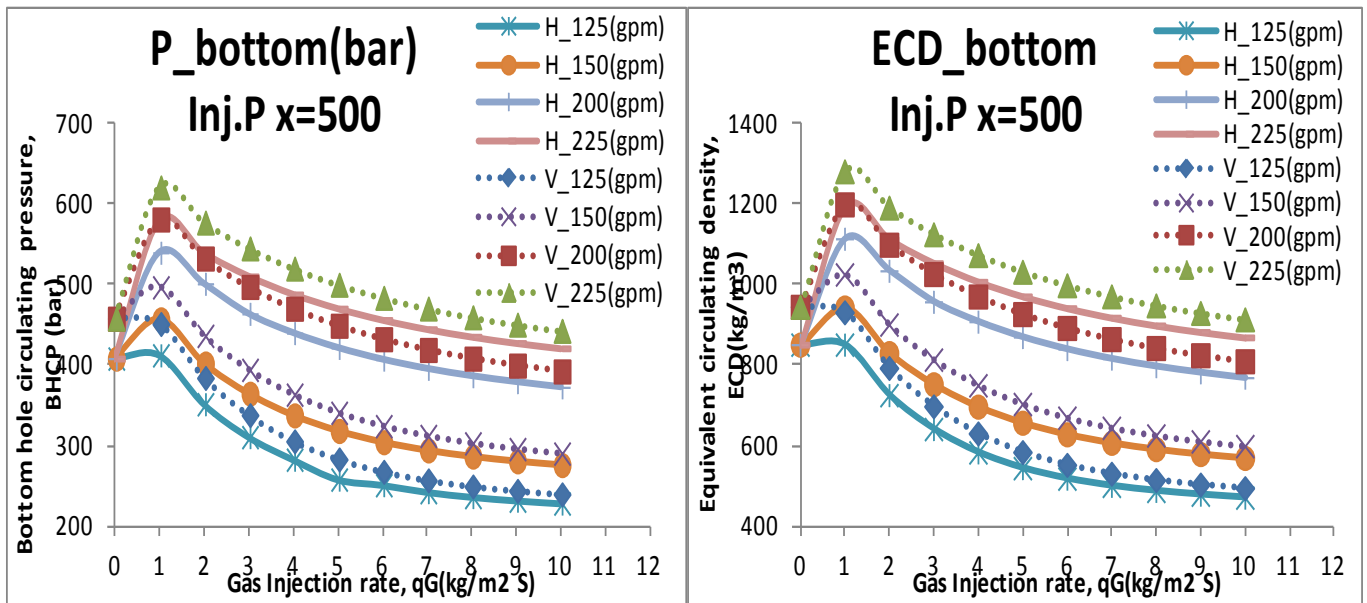


Figure A3.3 Sensitivity analysis of gas-liquid injection rate for a horizontal well @ bottom, "Injection point x1= 500 (m)",  $f = 6000$ , Horizontal "solid line", Vertical "dashed line"

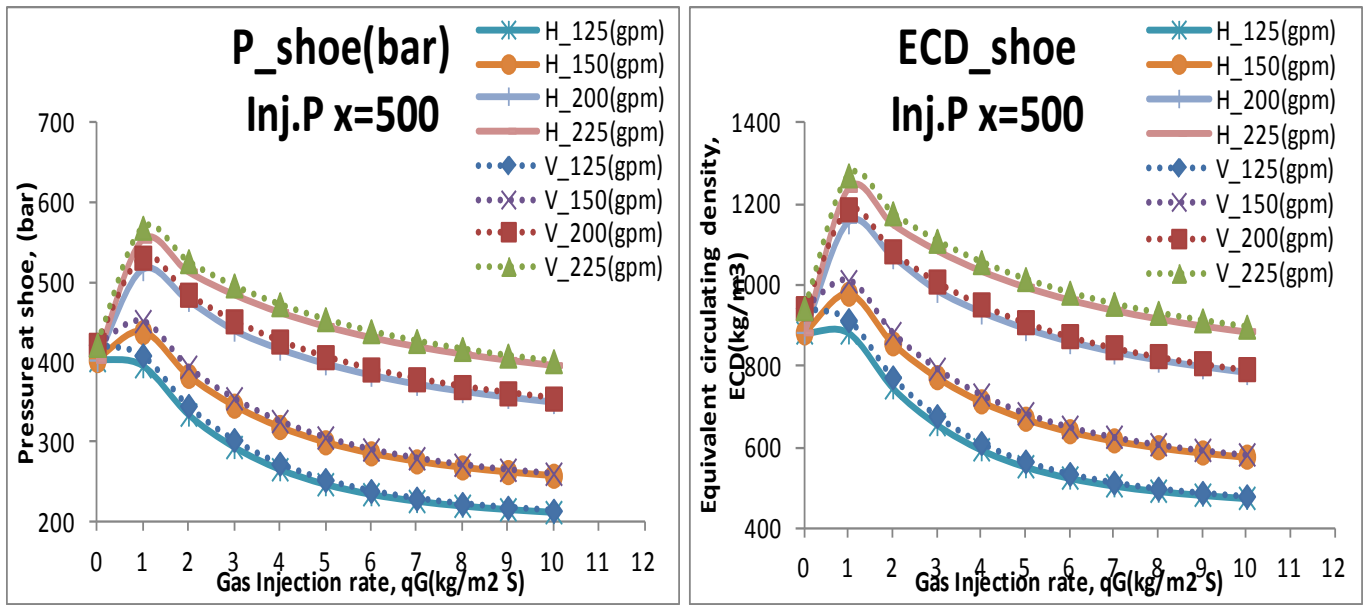


Figure A3.4 Sensitivity analysis of gas-liquid injection rate for a horizontal well @ shoe, "Injection point x1= 500 (m)",  $f = 6000$ , Horizontal "solid line", Vertical "dashed line"

– Injection point x2 = 1000 (m)

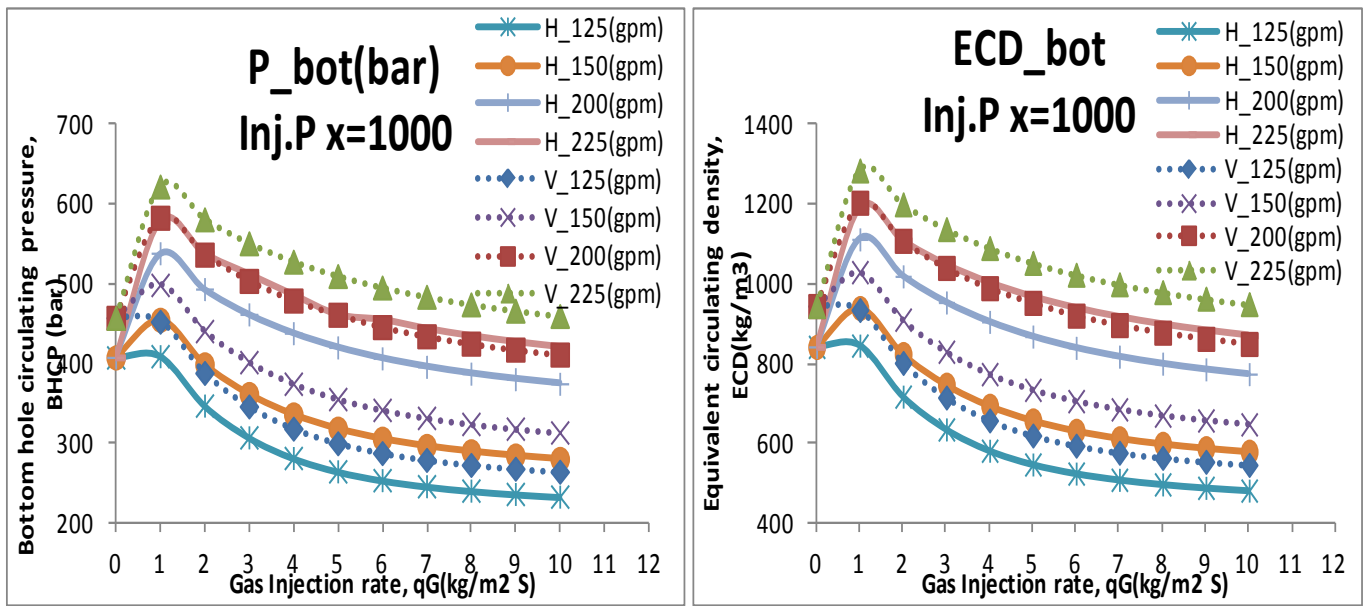


Figure A3.5 Sensitivity analysis of gas-liquid injection rate for a horizontal well @ bottom, "Injection point x1= 1000 (m)",  $f = 6000$ , Horizontal "solid line", Vertical "dashed line"

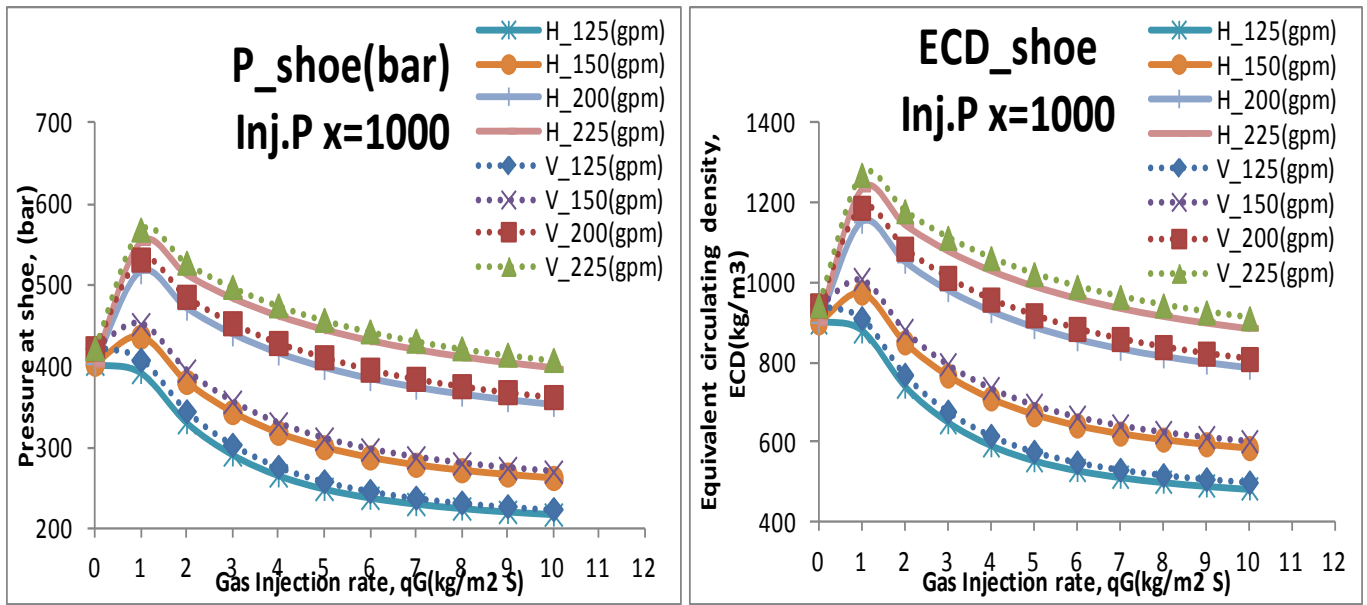


Figure A3.6 Sensitivity analysis of gas-liquid injection rate for a horizontal well @ shoe, "Injection point x1= 1000 (m)",  $f = 6000$ , Horizontal "solid line", Vertical "dashed line"

– Injection point x3 = 1500 (m)

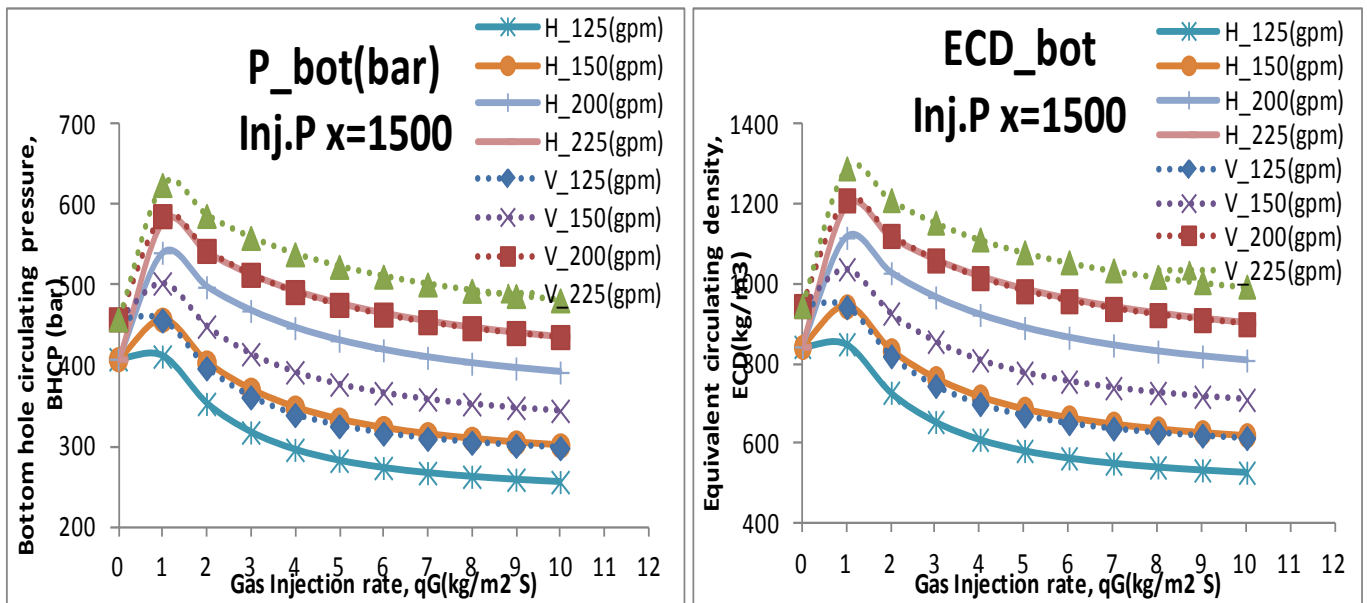


Figure A3.7 Sensitivity analysis of gas-liquid injection rate for a horizontal well @ bottom, "Injection point x1= 1500 (m)",  $f = 6000$ , Horizontal "solid line", Vertical "dashed line"

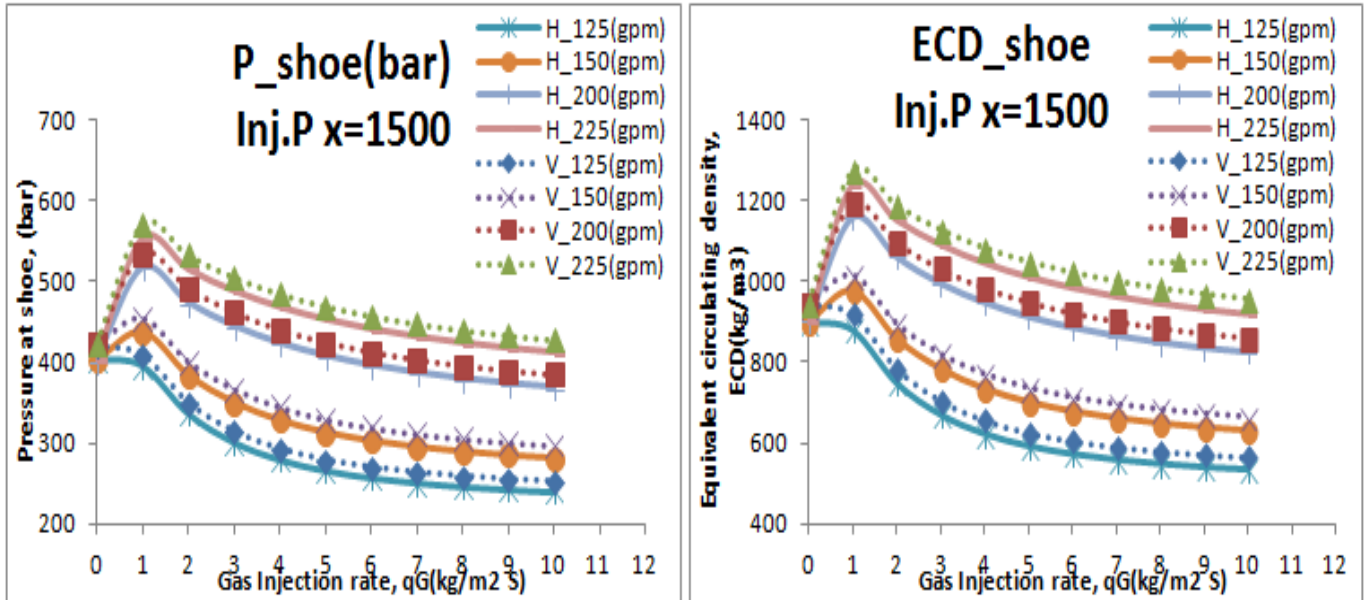


Figure A3.8 Sensitivity analysis of gas-liquid injection rate for a horizontal well @ shoe, "Injection point x1= 1500 (m)",  $f = 6000$ , Horizontal "solid line", Vertical "dashed line"

– Injection point x4 = 2000 (m)

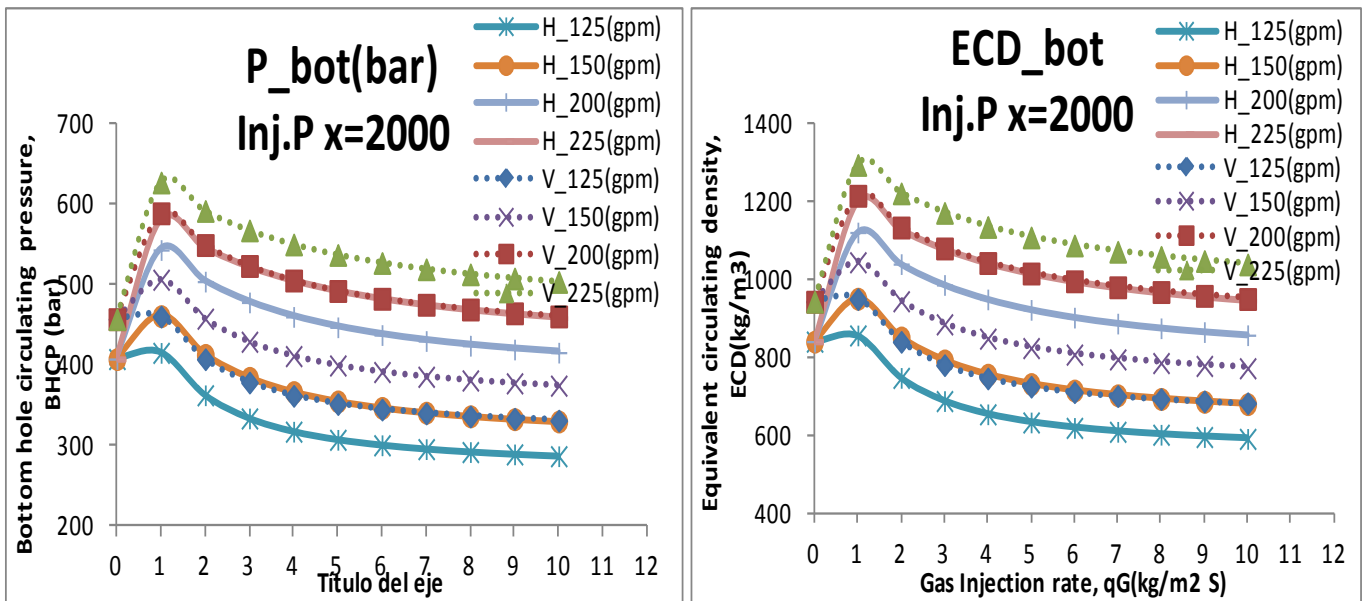


Figure A3.9 Sensitivity analysis of gas-liquid injection rate for a horizontal well @ bottom "Injection point x4= 2000 (m)",  $f = 6000$ , Horizontal "solid line", Vertical "dashed line"



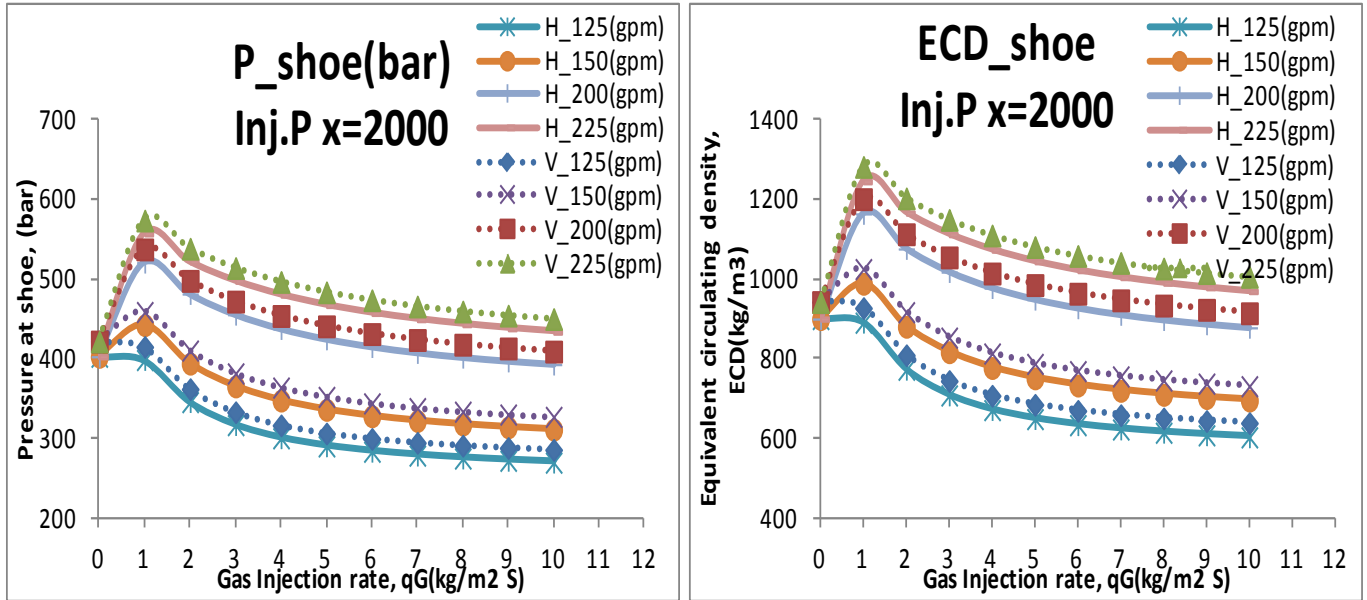


Figure A3.10 Sensitivity analysis of gas-liquid injection rate for a horizontal well @ shoe, "Injection point x4= 2000 (m)",  $f = 6000$ , Horizontal "solid line", Vertical "dashed line"

## REFERENCES

1. Zuber, N. and J. Findlay, *Average volumetric concentration in two-phase flow systems*. Journal of Heat Transfer, 1965. **87**(4): p. 453-468.
2. Evje, S., *A reduced gas-liquid drift-flux model*. University of Stavanger, Norway, 2013: p. 1-16.
3. Tao Zhu, Len Volk, and Hebert Carroll, *Tropical Report-Industry State of the art in Underbalanced drilling*. NIPER/BDM, 1995. **200**: p. 000.
4. Myktyiw, C., P.V. Suryanarayana, and P.R. Brand, *Practical Use of a Multiphase Flow Simulator for Underbalanced Drilling Applications Design - The Tricks of the Trade*. Society of Petroleum Engineers.
5. Steve, N., *Petroleum engineering handbook*, ed. L. Larry W and M. Robert F. Vol. 2 Drilling Engineering. 2006: Society of Petroleum Engineers Richardson, TX. 538-540.
6. Shoham, O., *Mechanistic modeling of gas-liquid two-phase flow in pipes*. 2006: Richardson, TX: Society of Petroleum Engineers.
7. Shi, H., et al., *Drift-flux modeling of two-phase flow in wellbores*. Spe Journal, 2005. **10**(1): p. 24-33.
8. Simoes, S.Q., et al., *The Effect of Tool Joints on ECD While Drilling*. Society of Petroleum Engineers.
9. Bern, P.A., et al., *A New Downhole Tool for ECD Reduction*. Society of Petroleum Engineers.
10. Kolaric, G., et al., *EM MWD Technology Enhances Underbalanced Drilling Efficiency In Mexico*. Offshore Mediterranean Conference.
11. Lage, A.C.V.M., K.K. Fjelde, and R.W. Time, *Underbalanced Drilling Dynamics: Two-Phase Flow Modeling and Experiments*.
12. Time, R.W., *Two phase flow in pipelines, Course compendium with Matlab examples and problems*. Department of Petroleum Engineering, Faculty of Science and Technology, University of Stavanger., 2009.
13. Ishii, M. and T. Hibiki, *Thermo-fluid dynamics of two-phase flow*. 2011: Springer.
14. Shi, H., et al. *Drift-flux modeling of multiphase flow in wellbores*. in *SPE Annual Technical Conference and Exhibition*. 2003.
15. Evje, S. and K.H. Karlsen, *Global existence of weak solutions for a viscous two-phase model*. Journal of Differential Equations, 2008. **245**(9): p. 2660-2703.
16. Evje, S. and K.K. Fjelde, *Hybrid flux-splitting schemes for a two-phase flow model*. Journal of Computational Physics, 2002. **175**(2): p. 674-701.
17. Munkejord, S.T., S. Evje, and T. Flåtten, *The multi-stage centred-scheme approach applied to a drift-flux two-phase flow model*. International Journal for Numerical Methods in Fluids, 2006. **52**(6): p. 679-705.
18. Evje, S. and K.K. Fjelde, *On a rough AUSM scheme for a one-dimensional two-phase model*. Computers & Fluids, 2003. **32**(10): p. 1497-1530.
19. Julia, J.E. and T. Hibiki, *Flow regime transition criteria for two-phase flow in a vertical annulus*. International Journal of Heat and Fluid Flow, 2011. **32**(5): p. 993-1004.
20. Evje, S., *A reduced single-phase model for transient wellbore-reservoir flow dynamics*. University of Stavanger, Norway, 2013: p. 1-13.
21. Lage, A.C.V.M. and R.W. Time, *Mechanistic Model for Upward Two-Phase Flow in Annuli*. Society of Petroleum Engineers.
22. Evje, S., *PVT and reservoir Modeling, Course notes*. Department of Petroleum Engineering, Faculty of Science and Technology, University of Stavanger.
23. Kleppe, H., *Reservoir simulation, Course notes*. University of Stavanger, Norway, 2010.